Sismik Yükler Altında Kazık Duvarlarının Davranışının Sonlu Elemanlar Yöntemiyle Belirlenmesi

Abada Dandachli

YÜKSEK LİSANS TEZİ

İnşaat Mühendisliği Anabilim Dalı

Ağustos 2020

Determination of the Behavior of Pile Walls Under Seismic Loading by Finite Element Method

Abada Dandachli

MASTER OF SCIENCE THESIS

Department of Civil Engineering

August 2020

Determination of the Behavior of Pile Walls Under Seismic Loading by Finite Element Method

A Thesis Submitted to the Eskişehir Osmangazi University
Graduate School of Natural and Applied Sciences in
Partial Fulfillment of the Requirements for the
Degree of Master of Science in Discipline of
Geotechnics of the Department of the
Civil Engineering

by

Abada Dandachli

Supervisor: Ass.Prof.Dr. Kamil Bekir Afacan

August 2020

ETHICAL STATEMENT

I hereby declare that this thesis titled “Determination of the Behavior of Pile Walls Under Seismic Loading by Finite Element Method” has been prepared in accordance with the thesis writing rules of Eskişehir Osmangazi University graduate School of Natural and Applied Sciences under academic consultancy of my supervisor Ass.Prof.Dr. Kamil Bekir Afacan. I hereby declare that the work presented in this thesis is original. I also declare that, I have respected scientific ethical principle and rules in all stages of my thesis study, all information and data presented in this thesis have been obtained within the scope of scientific and academic ethical principle and rules, all materials used in this thesis which are not original to this thesis have been fully cited and referenced, and all knowledge documents and results have been presented in accordance with scientific ethical principle and rules. 06.08.2020

Abada Dandachli

Signature

ÖZET

Dinamik yükler altında zemin ve yapı davranışları değişmektedir ve bu da tasarım parametrelerini etkilemektedir. Dolayısıyla güvenli ve ekonomik bir çözüme ulaşabilmek amacıyla sismik yükler altındaki davranışın çok iyi bir şekilde bilinmesi gerekmektedir. Bu çalışma, arkasında kil zemin yer alan şev üzerine oturmuş kazık duvarların deprem etkisi altındaki sismik davranışını tahmin etmek için sonlu elemanlar yönteminin kullanıldığı bir modellemedir.

Çalışma kapsamında, 12 metrelik istinat duvarları ile desteklenen ve her duvardan 4 metre derinlikte 60 kPa'lık bir düşey yük olan bir şev zemini, sonlu elemanlar programı yardımıyla (PLAXIS 2D) ile analiz edilmiştir. Kullanılan sonlu elemanlar yöntemiyle, duvarların arkasında oluşan toprak basınçları ve eğim oranındaki değişime farklı ivme kayıtları altında dinamik yükler sebebiyle gerilme ve deformasyonlarda oluşabilecek değişimleri modellemek için kullanılmıştır.

Kazık duvarlarda oluşabilecek gerilme ve deformasyonlar, değişen eğim yüzdelerine (1.5:10 - 2:10 - 3:10 - 4.5: 10) ve drenajsız kohezyon değerlerine (C = 75, 100, 125, 150 kpa) dayanan modellerin dinamik yüklemenmeleri sonucu elde edilmişlerdir. Sismik yükler altında elde edilen deformasyon miktarlarını azaltmak amacıyla duvarlar ankrajlı olarak da modellenmiştir. Son olarak seçilen ivme kayıtlarında kullanılan en büyük ivme değerinin önemi gösteren farklı analizler de yapılmıştır. Deformasyon ve yük miktarları farklı frekans içeriğine sahip yükler altında drenajsız kayma dayanımları ve eğim miktarlarında bağlı olarak değişiklik göstermişlerdir.

Bu tez, şev stabilitesi amaçlı modellenen kazık duvarların dinamik yükler altında analizlerinin sonlu elemanlar yöntemleri yardımıyla kapsamlı bir şekilde yapılarak zemin ve yapı elemanlarındaki davranış değişikliğinin saptanmasını amaçlamıştır.

Anahtar kelimeler : Sonlu elemanlar yöntemi, kazık duvarlar, dinamik analiz, drenajsız kayma mukavemeti

SUMMARY

Soil and structure behaviors change under dynamic loads and this affects the design parameters. Therefore, in order to reach a safe and economical solution, the behavior under seismic loads should be well known. This study is a modeling in which the finite element method is used to estimate the seismic behavior of pile walls under the effect of earthquakes, resting on a slope of clayey soil.

Within the scope of the study, a slope supported by 12-meter retaining (pile) walls carrying a vertical load of 60 kPa at a depth of 4 meters was analyzed with the help of finite element method (PLAXIS 2D). It was used to model the changes in stress and deformations due to dynamic loads under different acceleration records at varying undrained shear strentgh and slope ratios that occur behind the walls.

The stress and deformations that may occur behind the pile walls were obtained as a result of dynamic loading of models based on varying slope percentages (1.5: 10 - 2:10 - 3:10 - 4.5: 10) and undrained cohesion values (C = 75, 100, 125, 150 kpa) . The walls are also modeled with anchors in order to reduce the amount of deformation obtained under seismic loads. Finally, different analyses were made showing the importance of the peak acceleration value used in the selected acceleration records. Deformation and load levels varied depending on the undrained shear strength and slope amounts under loads with different frequency content.

This thesis aims to determine the behavior changes in the soil and structural elements by making the analysis of pile walls modeled for slope stability under dynamic loads with the help of finite element methods.

Keywords Finite element method, pile walls, dynamic analysis, undrained shear strength

ACKNOWLEDGEMENTS

I would want to present my genuine and real thanks to my advisor Dr. Kamil Bekir AFACAN for the persistent help of my master study and research, for his understanding inspiration, eagerness, and tremendous information. His direction helped me in all the hour of my research and composing of this thesis.

I want to thank my family too for giving birth to me at the first place and supporting me spiritually throughout my life.

LIST OF CONTENTS

Page

ÖZET ……vi

SUMMARY…… vii

ACKNOWLEDGEMENTS…….viii

LIST OF CONTENTS……..ix

LIST Of FIGURES…….... xii

LIST OF TABLES…….... xvi

LIST OF SYMBOLES AND ABBREVIATIONS……..... xvii

1.INTRODUCTION AND PURPOSE……...1

2. LITERATURE REVIEW…..……..4

2.1 General Description of Slope Stability…….……6

2.2 Slope Failures and Instability Mechanism……...……7

2.2.1 Types of the slope failures…….....7

2.2.2 Causes of slope collapse…….....9

2.2.3 Techniques to improve the slopes stability…….....9

2.3 Important Aspects in Slope Stability Analysis.……...12

2.3.1 FOS and SRF (strength reduction factor) ……..…….…….....12

2.3.2 Model materials properties……...13

2.3.3 Slope Collapse……..…… 13

2.4 Finite Element Method……..……14

2.4.1 Finite element model in plaxis (2D) …….14

2.4.2 Advantages and disadvantages…….…….15

2.5 Limit Equilibrium Method (Slices Methods).……..…….....16

2.5.1Fellenious method….…….…….…17

2.5.2 Bishop method…….…...….19

2.5.3 Janbu method……..……..…….20

2.5.4 Summary of LE method of slices……...…….……20

LIST OF CONTENTS (continued)

Page

2.6 Retaining Wall……..……22

2.6.1 Types of retaining walls……..…..…….23

2.6.1.1 Piled walls……..……..…….23

2.6.1.2 Anchored retaining wall……..……24

2.6.1.3 Cantilever wall……..……...24

2.6.1.4 Gravity wall……....25

2.6.2 Metal strip reinforcement……...……26

2.6.3 Geosynthetic reinforced soil walls……...…….…….26

2.6.4 Comparison of reinforced soil walls and concrete gravity walls…...……27

3- MATERIALS AND METHODS……...…28

3.1 Plaxis Software……29

3.2 Soil Parameters Used in Plaxis……31

3.2.1 Pile (Plate) Model …….…….…….33

3.3 Motions used in the Analysis ……...……...34

3.4 Analysis Program……36

4. RESULTS AND DISCUSSION…….……...…….…41

4.1 Effect of the Slopes on the Lateral Forces and Moments ……..…….…….42

4.1.1 Lateral Moment Behavior …….…….42

4.1.2 Shear force Behavior …….……46

4.1.3 Axial force Behavior …….50

4.1.4 Total displacement Behavior …….……54

4.2 Effect of the Cohesion on the Lateral Forces and Moments …….…….…58

4.2.1 Lateral Moment Behavior …….58

4.2.2 Shear Force Behavior ……...……...……62

4.2.3 Axial Force Behavior …….……..…….66

4.2.4 Total displacement Behavior …….……70

4.3 FEM analysis of Anchored Pile Walls…….……74

LIST OF CONTENTS (continued)

Page

4.3.1 Deterministic analysis of an anchored pile walls…….74
4.3.2 Comparison between Unanchored and Anchored Piles……75
4.4 Calculation of the Reinforcement Capacity of Pile Wall …….……...….78

5. CONCLUSIONS AND SUGGESTIONS ……..……81
5.1 Change in Moment ……...……81
5.2 Change in Shear forces…….……....……83
5.3 Change in Axial forces……...…….……85
5.4 Discussion on the Effect of the Peak Ground Acceleration …….88

REFERENCES……91

LIST Of FIGURES

Figure **Page**

2.1. Translational slide (Chowdhury, 2010)……...…….…….7

2.2. Rotational slide (Chowdhury, 2010)…….…….……..…….8

2.3. (a) Base Failure, (b) Toe Failure, (c) Slope Failure (Duncan, 2005; Chen, 1995) ……8

2.4. Flow slide (Chowdhury, 2010)……..……9

2.5. Improving the stability by retaining wall……...…...10

2.6. Improvement with excavation (Duncan and Wright, 2005) ……...…….…….10

2.7. Improvement by berm …….…….…….…….11

2.8. Improvement slope with vegetation …….11

2.9. Soil nailing detail, (modified after Broms and Wong, 1991) …….……12

2.10 (a) Division of sliding mass into slices (b) Forces acting on a typical slice (Chowdhury, 2010) …….18

2.11. Forces assumed in bishop method(Chowdhury, 2010)……. ….……...……19

2.12. Estimation of the corrective factor f0 ……..20

2.13. Pile retaining wall ……..…23

2.14. Anchored retaining wall…….……24

2.15. Cantilever wall……...…….25

2.16. Gravity wall…….……...25

2.17. Metal strip reinforcement……26

2.18. Geotextile reinforced soil wall……27

3.1. General settings of the model…….……28

3.2. The 15-node triangular element (PLAXIS, 2010) …….……29

3.3. Presentation of the soil materials. …….…….……31

3.4. Parameters and interfaces menu…….……32

3.5. Pile wall model in PLAXIS (16.2°-4.5:10 Slope)…….……...……33

3.6. Properties of the plate ……34

3.7. Duzce earthquake data……35

3.8. Kobe earthquake data…….35

LIST OF FIGURES (continued)

Figure **Page**

3.9. Kocaeli earthquake data…….36
3.10. Loading (16.2° Slope)…….36
3.11 Geometry model with standard earthquake boundary conditions (16.2 degrees Slope). ……...…….....37
3.12. Finite element mesh for the model (16.2 degrees slope) ……..…...…37
3.13. Water pressure level …….……...38
3.14. The phases for analyzing……...…….....39
3.15. Example output of deformed mesh……...40
3.16. Example output of total displacement distribution…….…….40
4.1. Calculation page……...…….……41
4.2. Moment behavior with regard to the slope variation (**Cohesion=75 kPa**)…….…...…42
4.3. Moment behavior with regard to the slope variation (**Cohesion=100 kPa**)…….…43
4.4. Moment behavior with regard to the slope variation (**Cohesion=125 kPa**)…….…….44
4.5. Moment behavior with regard to the slope variation (**Cohesion=150 kPa**)…….…45
4.6. Shear force behavior with regard to the slope variation (**Cohesion=75 kPa**)…….……46
4.7. Shear force behavior with regard to the slope variation (**Cohesion=100 kPa**)…….…47
4.8. Shear force behavior with regard to the slope variation (**Cohesion=125 kPa**)…….……48
4.9. Shear force behavior with regard to the slope variation (**Cohesion=150 kPa**)…….……49
4.10. Axial force behavior with regard to the slope variation (**Cohesion=75 kPa**)…….50
4.11. Axial force behavior with regard to the slope variation (**Cohesion=100 kPa**)…….51
4.12. Axial force behavior with regard to the slope variation (**Cohesion=125 kPa**)…….52
4.13. Axial force behavior with regard to the slope variation (**Cohesion=150 kPa**)…….……53
4.14. Total displacement behavior with regard to the slope variation (**Cohesion=75 kPa**)……...……...54
4.15. Total displacement behavior with regard to the slope variation (**Cohesion=100 kPa**)…….…55
4.16. Total displacement behavior with regard to the slope variation (**Cohesion=125 kPa**)…….56

LIST OF FIGURES (continued)

Figure **Page**

4.17. Total displacement behavior with regard to the slope variation (**Cohesion=150 kPa**)……..…….57

4.18 Moment behavior with regard to the cohesion variation (**Slope 0.15**)……58

4.19 Moment behavior with regard to the cohesion variation (**Slope 0.2**) …….……59

4.20 Moment behavior with regard to the cohesion variation (**Slope 0.3**) …….……60

4.21 Moment behavior with regard to the cohesion variation (**Slope 0.45**) ……...……61

4.22. Shear force behavior with regard to the cohesion variation (**Slope 0.15)** …….…..…62

4.23. Shear force behavior with regard to the cohesion variation (**Slope 0.2)** ……....…63

4.24. Shear force behavior with regard to the cohesion variation (**Slope 0.3)** ……64

4.25. Shear force behavior with regard to the cohesion variation (**Slope 0.45)** ……..….65

4.26. Axial force behavior with regard to the cohesion variation (**Slope 0.15)** ……..…66

4.27. Axial force behavior with regard to the cohesion variation (**Slope 0.2)** ……...67

4.28. Axial force behavior with regard to the cohesion variation (**Slope 0.3)** ……...68

4.29. Axial force behavior with regard to the cohesion variation (**Slope 0.45)** ……..….69

4.30. Total displacement behavior with regard to the cohesion variation (**Slope 0.15**)…...70

4.31. Total displacement behavior with regard to the cohesion variation (**Slope 0.2**)…….71

4.32. Total displacement behavior with regard to the cohesion variation (**Slope 0.3**)…….72

4.33. Total displacement behavior with regard to the cohesion variation (**Slope 0.45**)…...73

4.34. Anchored pile wall model in PLAXIS……74

4.35. Anchor and Geogrid properties……..….75

4.36. difference of total displacement between Unanchored and Anchored Piles…….75

4.37. Difference of moment, shear, and axial forces between unanchored and anchored pile walls…….77

4.38. Charts from Ugur Ersoy Reinforce Concrete……...79

5.1. Variations of maximum moments according the cohesion…….……81

5.2. Variations of maximum moments according the slopes…….…82

5.3. Variations of maximum shear forces according the cohesion…...…….……84

5.4. Variations of maximum shear forces according the slopes…….……85

5.5. Variations of maximum axial forces according the cohesion…….……86

LIST OF FIGURES (continued)

Figure **Page**

5.6. Variations of maximum axial forces according the Slopes……87

5.7. Comparison of total displacement under Duzce (PGA=0.3g) and (PGA=0.46g)…….88

5.8. Comparison of moment, shear, axial forces under Duzce (PGA=0.3g) and (PGA=0.46g)……89

LIST OF TABLES

Table **Page**

2.1. comparison of FE and LE methods……..……..……17

2.2. Features and Limitation for Traditional Equilibrium Methods (Duncan and Wright, 1980). ……..……..……21

3.1. correlation of modulus of elasticity with undrained shear strength…….……..…32

3.2. properties of the soil……..……..……33

LIST OF SYMBOLS

Symbols	Description
t	Shear strength
t_f	Shear stress of sliding surface
c'	Effective unit cohesion
∂'	Effective normal stress
∂	Total normal stress
U	Pore water pressure
ϕ'	Effective internal friction angle
C:	Cohesion
g	Unit weight of soil
y	Dilation angle
E	Young's modulus
n	Poisson's ratio
EA	Normal stiffness
EI	Flexural rigidity
Rinter	Interface strength
Wt	Total weight of the soil slice
T	Shear force due to adjacent slices.
E	Lateral force due to adjacent slices
N	Normal force at base in each slice
F0	Function of the slide geometry and the strength parameters of the soil
Qu	Ultimate bearing capacity of the foundation soil
Qmax	Maximum pressure at the base of the wall
e	Eccentricity of the resultant force at the base
Ac	Area of concrete
fcd	Design compressive strength
fyd	Design yield strength
Ast	Area of steel reinforcement in concrete column design
Astmin	Minimum Area of steel reinforcement in concrete column design

LIST OF SYMBOLS (continued)

Symbols	Description
Astmax	Maximum Area of steel reinforcement in concrete column design
d	Effective depth from the top of a reinforced concrete beam to the centroid the tensile steel
d’	Effective depth from the top of a reinforced concrete beam to the centroid of the compression steel
ρ_{max}	Maximum longitudinal tension reinforcement ratio
ρ_{min}	Minimum longitudinal tension reinforcement ratio

Abbreviation	Description
SRF	Strength reduction factor
FOS	Factor of Safety
LEM	Limit Equilibrium Method
FEM	Finite Element method
FE	Finite Element

1. INTRODUCTION AND PURPOSE

Slope stability analysis is one of the principal applications in geotechnical engineering and transportation engineering therefore there are a lot of researches have been done containing several methods of slope stability analysis which consists of excavations and variations in lateral load or groundwater conditions that can initiate a possible failure. It is very important to get precautions before any structural design in order not to face any casualty or economic loss.

The limit equilibrium method of slices, finite element method, boundary element method and neural network method are the most public methods for slope analyzing. In civil engineering, especially in geotechnical engineering, one of the great computational tools is the Finite Element Method that utilize to model the real condition very well as it increases its power from the facility to simulate physical behaviors. FEM is used for the complicated engineering problems to get correct and credible results. Currently, in engineering new suggested analysis methods, possible failure scenarios can be confirmed using finite element method as a standard so that it could use to analyze the slope's stability using a failure definition by this powerful computational tool.

The main problem with a construction/road near a sloppy soils is a landslide hazard of the slope that can occur due to the static and/or seismic (triggered by an earthquake or explosions nearby) loads on the slope, the condition of the soil materials, and the presence of groundwater. That is why soil reinforcement and soil stabilization may be necessary on the slope. Also, there are many methods of soil stabilization such as using combined method or physical, chemical, mechanical, and biological.

Other than these possible problems, the project sometimes need excavation so the soil behind should be supported. The common solutions are generally used for these situations are the retaining structures that would hold the soil behind the wall under static and dynamic loads.

Retaining walls are one of the geo-engineering structures that can provide the resistance to lateral forces for the mass of land to absorbing a possible lateral movement. These retaining structures should be designed very carefully. There are many types of ground retaining structures are obtainable to bear the earth/water stresses varying on the soil conditions and the distribution of the lateral soil pressure.

PLAXIS is Pieter Vermeer constructed a finite element program in 1974 at the Delft University of Technology to analyze the river dams on the soft soils. Because of the increase in engineering projects mostly related to geotechnical problems, PLAXIS Company was established in 1993 and the first PLAXIS2D was recognized in 1998 for the analyzing and resolving the geotechnical engineering problems in the stability, foundation, tunnels and finding factor of safety (FOS) for slopes.

PLAXIS is one of the finite element programs that has been extended internationally for geotechnical engineering and design as of 2020, PLAXIS is a portion of Bentley Systems, Incorporated, and a US based company expert in software for modelling, designing and to make the infrastructural projects safer.

The objectives of PLAXIS is proposed to run a tool for applied analysis to go towards by geotechnical engineers who they can utilize overall 2D finite element meshes to analysis a big area of geotechnical problems. The program can tool up as an expanded bundle of i) static, ii) elastoplastic, iii) deformation, iv) advanced soil model, v) stability analysis, vi) consolidation, vii) updated mesh and viii) groundwater flow analysis.

This thesis focuses its attention to the slope stability analysis at the best-detailed approach used for evaluating stability problems under dynamic loading. An effort was made to overcome the variations in the consequences of reinforced slope stability analysis obtained from the finite element program (PLAXIS 2D).

In the chapter 2 of this study, review literature on the subject matter is presented which begins with a general description of slope stability such as the types and causes of slope failure followed by the main difference between the best two methods used for slope stability analysis

FEM and LEM methods, and finally description of reinforced soil principles and general information about the retaining walls.

In the third chapter, the methods employed by PLAXIS 2D software, assumptions, methods, and other related items will be discussed and how to extract the results and parameters in the study will be explained.

Chapter 4 describes the analyzing procedure using the FEM software according to slopes variations (0.15 – 0.2 – 0.3 and 0.45) and cohesions variation (75, 100, 125 and 150 kPa). Later in this part, the outcomes of the analysis will be presented in terms of the behavior of moments, shear forces, axial forces, and total displacements under three different earthquakes.

Finally, in the latest part, the change of the maximum moments, shear forces, axial forces and total displacements that formed under three different earthquakes will be discussed widely according to the 1) cohesions and the 2) slope ratio terms. There will be a small discussion part that will compare the results of same model analyzed by two different scaled Duzce earthquake. The accelerations were selected as 0.3g and 0.46g.

2. REVIEW OF LITERATURE

The slope stability analysis in geotechnical engineering is very important for the civil engineering applications especially for road constructions and it has been developed over the years and some of the studies done by researchers are discussed as follows:

Several studies have aimed to do a comparison of the slope stability analysis between LE method and the FE method. A study was published by Carol Matthews et al. in 2014 in England deduced the problems which requires analysis of consolidation seepage, pore water pressure or progressive failure could be better tackled using FE analysis.

Burman et al. in 2015 used the finite element method and the limit equilibrium method to study several slope stability complications and it was noticed that the ordinary slice method supplies the best conservative assessment of safety factor values between the limit equilibrium methods that looked in the research. Consequently, the designs of slopes that are not approved with ordinary slice method is probable not to be on the safe side.

Alex Jacob et al. (2018) investigated the slope stability analysis using PLAXIS 2D was. The results show that any change of rise of water table, would cause in a reduced of FOS, and the slopes which are near the failed slopes are susceptible to collapse because of the similar soil properties.

F. Tschuchnigg et al. (2015) focused on a case study regarding a failing slope that is located in central Europe. They worked on the factor of safety using different approaches in terms of finite element analysis and strength reduction. For similar plasticity of soils, the factor of safety was found very close for two models whereas for non-plasticity the case was observed totally different.

A research has been done after a landslide had occurs in a slope in Lebanon by Ali Fawaz et al. in 2014 and summarized through it that allocation of the nails or piles along the slope can ensure the stability more efficiently knowing that drainage is an effective way to slope stabilization. In the case of fully drained slope, the stability is provided even without any strengthening methods.

As Gupta et al. worked on the similar concept in 2016, it was presented in the work that LE methods predict a higher factor of safety (FOS) compared to the FE method. Another important point is that the stability of slopes does not increase by the expanding of the nail inclination. Nail forces decrease from the top to bottom of the nail. The most stable slope according to finite element and limit equilibrium method were found to be the slope that reinforced with 15º nail inclination with horizontal axes stating an optimum nail slope as 15º.

I Hermanto et al. (2020) states in his work that the value of the factor of increase greatly with the retaining wall in the vertical cohesive soil slope and gives additional force to retain the active pressure. It was also proven that the retaining wall weight has big influence to affect to the displacement value that can occur on the slope.

Paravita Sri Wulandari et al. also studied the finite element analysis on the piles to stabilize a sloppy soil in 2015 and showed that piles can decrease the settlement a certain amount but the addition of it to reach certain number of piles indicates no change in settlement that become constant.

Fei Song et al. (2017) researched the effect of reinforcement layers on the factor of safety of a slope and it was shown that the reinforcement layers' location and their lengths affect the FOS and the critical surface of the reinforced slope. He also concluded that if the vertical spacing between the reinforcement is reduced around 0-H/3, the size of the sliding soil wedge becomes relatively small, and the FOS increases. However, the small length of the reinforcement layers reduces the safety factor and the size of the sliding soil wedge.

Azzam, W.R. 2014 showed that using skirts foundation could control the lateral deformation of a slope and make it safely from failure during earthquakes. Where the behavior of the deformation of a seismic slope in case of foundations without skirts is different. Skirts' thicknesses have an effective role in the decreasing of the slope deformation during earthquakes where the increasing of skirts can increase the subgrade stiffness.

2.1 General Description of Slope Stability

Slope stability is so important to investigate the public safety, economic and ecological necessities to prevent the harmful danger that can occur from a failure like slope slides, falls or toping failure. Generally, slopes have two types:

a) supported slopes (Fredlund, D.G. & Krahn, J., 1977) as nailing, pile wall and gravity wall.

b) unsupported slopes contain the excavation, loading and the natural slopes.

The importance of the embankments comes to change the effective stress and the superfluous pore pressure in underground whereas the excavations reduces the total stress of the soil and can decrease the pore pressure during building because of temporary drainage.

Some important points that summarize the objective of the slope stability analysis:

- Estimation of slope stability under temporary situations and long-term situations.
- Comprehend the shape of geological slopes and the procedures responsible for the different natural topographies.
- Assessment of the risk of landslides that have natural or present engineering slopes.
- Study the landslides that can occur and achieve failure mechanisms and the impact of environmental factors.
- Predicting the probability of the landslides including the natural or existing engineered slopes. Slope failures and slope mechanism
- Analyzing the landslides and realize the failure mechanisms and effect of environmental factors.

2.2 Slope Failures and Instability Mechanism

To make the slope safe and stable, geotechnical engineer must be aware of factors that cause the slope to fail including the soil type, soil layers, groundwater, seepage, and slope geometry.

2.2.1 Types of the slope failures

Three different mechanisms are explained here in order to evaluate the type of the slope failures:

i) *Translational Slide:* The coarse-grained soils are susceptible to this type of failure as a long transport of the sliding mass.

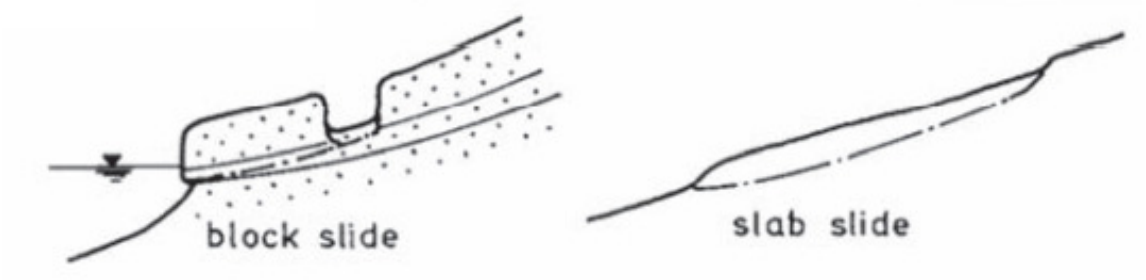


Figure 2.1. Translational slide (Chowdhury, 2010)

Block slide can also be considered in this part. This type of failure occurs whilst smashing of a soil mass along joints, seams, fissures, and vulnerable zones via forces emanating from adjacent soils.

ii) *Rotational slide:* Usually, this type of failure occurs to homogeneous fine-grained soils and include three types of failure:

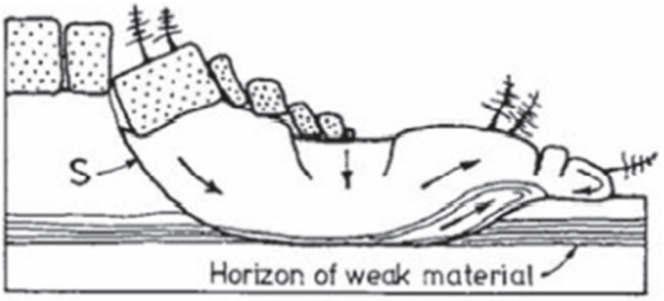


Figure 2.2. Rotational slide (Chowdhury, 2010)

a) Base failure: are common on soft soil layer above stiff soil.
b) Toe failure: the failure surface pass by the toe of the slope.
c) Slope failure: the last type of the rotational slide is that the failure surface passes across the slope.

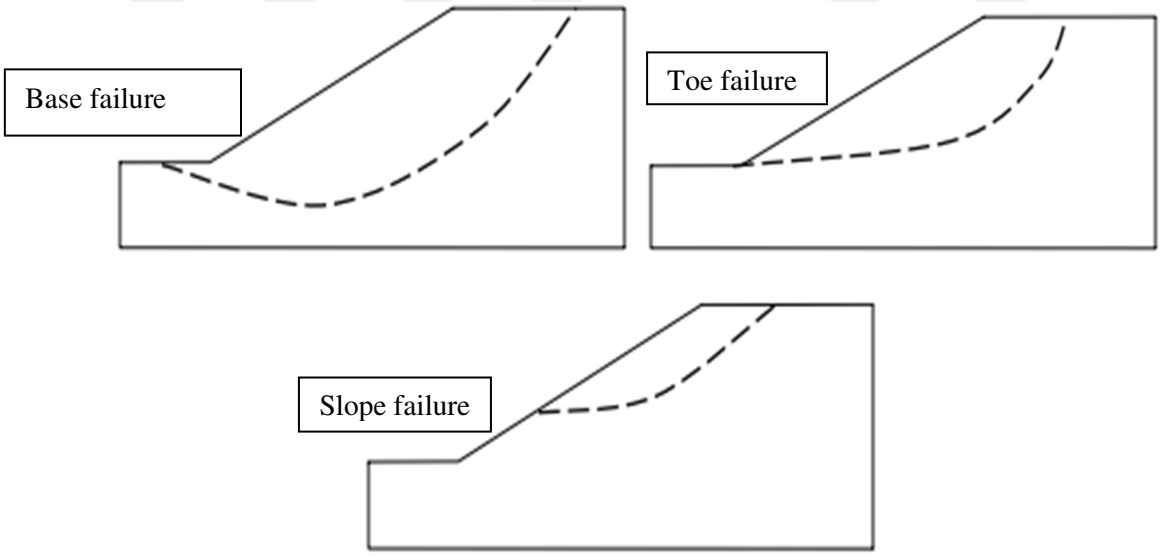


Figure 2.3 (a) Base Failure, (b) Toe Failure, (c) Slope Failure (Duncan, 2005; Chen, 1995).

iii) *Flow slide:* When a soil becomes as a fluid and flow out in many directions by inner and outside forces the slide called flow slide. Usually happen in wet and dry soils.

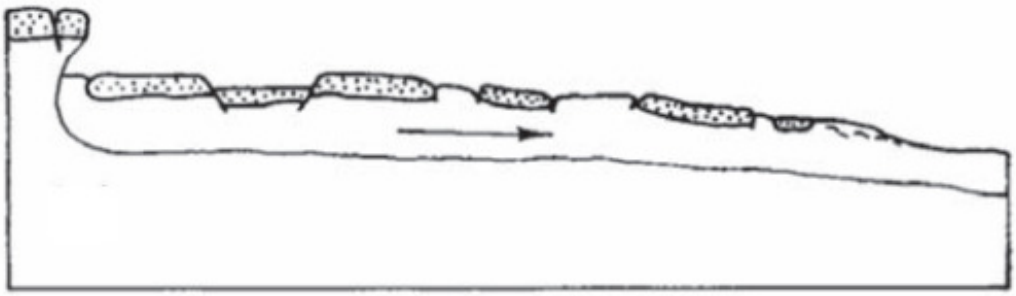


Figure 2.4. Flow slide (Chowdhury, 2010)

2.2.2 Causes of slope collapse:

Generally, the main reason of the most slope collapse is the environmental features and conditions such as the unexpected loads and the natural forces. Below there are a few major factors that causes slope failures:

1. Rainfall: heavy rainfall saturates and erode the soil and may weaken underlying soil layers heading to slope collapse.
2. Earthquake: under earthquakes the shear strength and the stiffness of the soil decreases as the pore water pressure could increase to a high value in the ground by the dynamic forces and cause the viscous fluid.
3. External loading: such as construction or highway which placed at the top of the slope causes the collapse not like the Berm load which puts at the toe of the slope that can increase the stability of the slope.
4. Excavation or by erosion.

2.2.3 Techniques to improve the slopes stability

Duncan and Wright, 2005 informed the major techniques available to improve the slope stability such as:

1) Increasing the stability by offering the lateral support as reinforcement and retaining walls as seen in Figure 2.5.

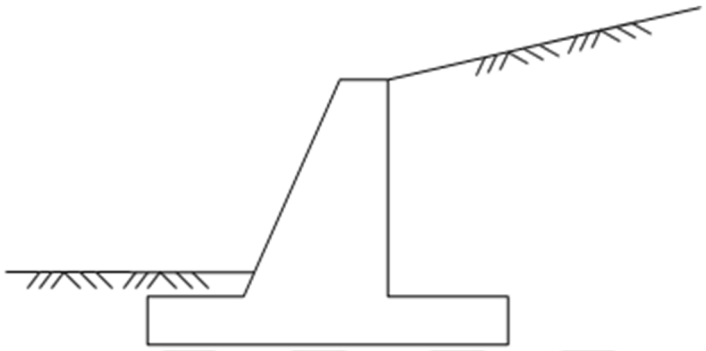


Figure 2.5. Improving the stability by retaining wall

2) Excavations the top, bench and flatten slope and consequently unloading will be occur in the weight of mass that it tends to slide (Figure 2.6).

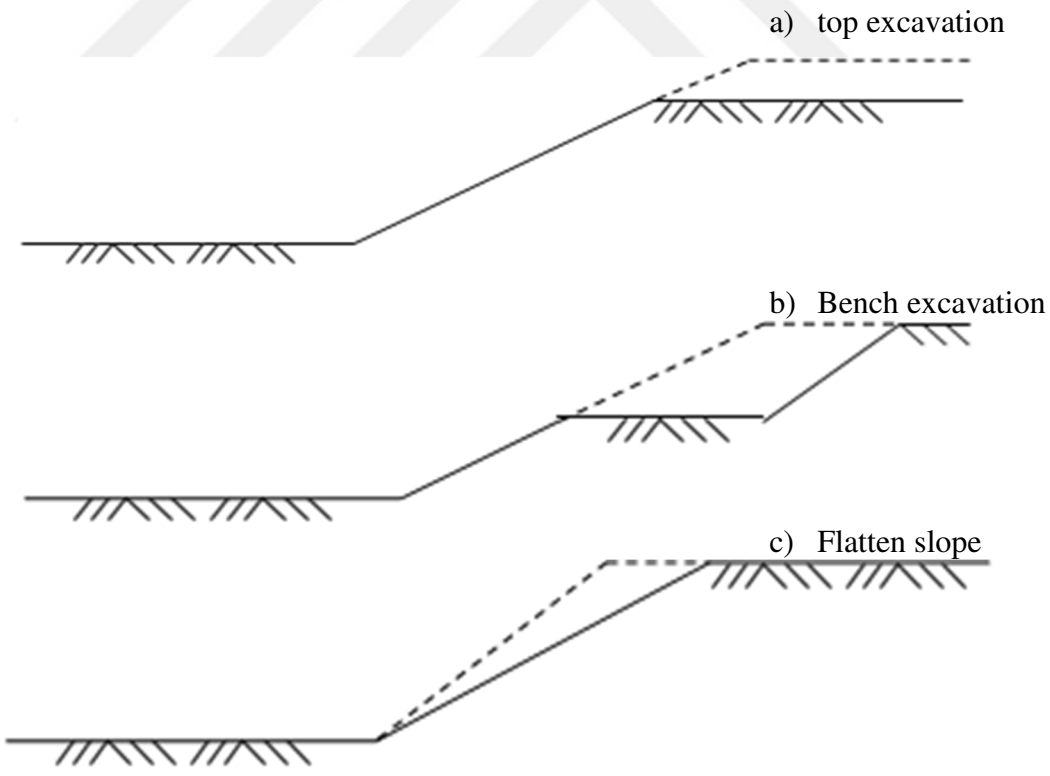


Figure 2.6. Improvement with excavation (Duncan and Wright, 2005)

3) Increasing resisting forces by inserting a berm (as shown in Figure 2.7) on the toe of the slope whereas, this method is suitable when base failure is expected.

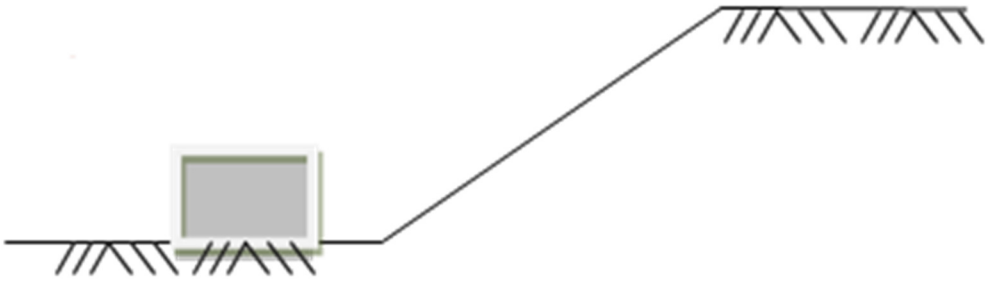


Figure 2.7. Improvement by berm

4) Improvement the stability by drainage that can reduce the seepage forces, thus the groundwater pressure be dropped, and the permeation of the surface water is banned.

5) Reducing the runoff risks on the slope by vegetation as seen Figure 2.8, which can help the objection of rainfall, especially providing the surface stability within the root area.

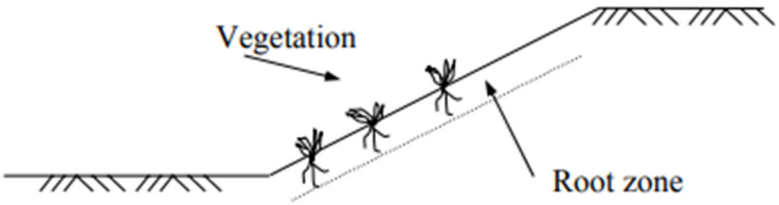


Figure 2.8. Improvement slope with vegetation

6) Soil nailing is one of the most important rapid techniques recently adopted in engineering to stabilize the soil which can increase the shear strength and reduce the displacements by installing and pushing nails into pre-drilled holes using plaster inside the ground. That depends on the concrete facades on the surface of the structure as shown in Figure 2.9 (Broms and Wong, 1991).

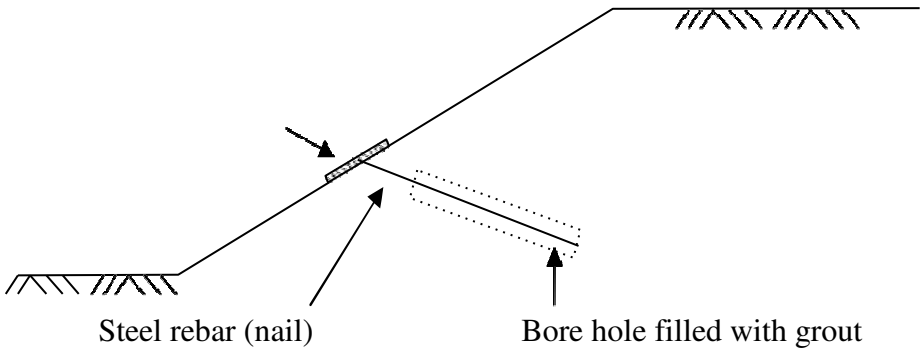


Figure 2.9. Soil nailing detail, (modified after Broms and Wong, 1991).

2.3 Important Aspects in Slope Stability Analysis

Slope stability analysis can affect with many aspects in terms of the FOS calculation and its influence on slope stability, the material properties of the slope's model and the possible type of the slope failure.

2.3.1 FOS (Factor of safety) and SRF (Strength reduction factor):

When the FOS of a slope is bigger than 1 it can be said that slope is stable. The material shear strength is responsible to slope fails once it is not enough to resist the actual shear stress. The formula of the FOS against slope failure accordance to the shear failure can be derived as in Equation 2.1-2.5:

$$FOS = \frac{\tau_F}{\tau} \tag{2.1}$$

$$\tau = c' + \sigma_n{}' \cdot \tan \phi' \tag{2.2}$$

$$\tau_F = c_F{}' + \sigma_n{}' \cdot \tan \phi_F{}' \tag{2.3}$$

$$c_F{}' = \frac{c'}{SRF} \tag{2.4}$$

$$\phi_F{}' = \tan^{-1}\left[\frac{\tan\phi'}{SRF}\right] \quad (2.5)$$

Where

τ is the shear strength

τ_f is the shear stress of sliding surface (failing surface)

c' is the cohesion

σ' is the effective normal stress

ϕ' is the effective internal friction angle

2.3.2 Model materials properties

The Mohr Coulomb material type is mostly used in slope stability analysis and the properties that required for the Mohr-coulomb material model are grouped in six factors, 1) friction angle (ϕ), 2) cohesion (c), 3) unit weight of soil (γ) (in order to estimate the normal and effective stress), 4) dilation angle (ψ), 5) Young's modulus € and 6) Poisson's ratio (ν).

The Mohr-Coulomb criterion relays on the shear strength to the cohesion (c), normal stress (σ) and angle of internal friction (ϕ) of the material. Poisson's ratio and the Young's modulus have little impact on the foretell the safety factor in slope stability analysis; however, they have a deep effect on the calculated deformations before slope failure. The details about these parameters used in this study will be explained in Chapter 3.

2.3.3 Slope collapse

Indicator of slope collapse in finite detail software is due to mon-junctions within the number of iterations. This simply means that no pressure distribution may be executed to fulfill both of the Mohr-Coulomb criterion and the global equilibrium. Commonly, value of the maximum nodal displacement simply after slope failure has a large jump as compared to the only before failure.

2.4 Finite Element Method

The finite element method was established in the 1940s by Alexander Hrennikoff (1941) and Richard Courant (1942)., and through it the concept of simulation, defined as the analysis of finite elements as digital techniques, was found to find approximate solutions to the marginal value problems of partial differential equations and reduce the expected errors.

In geotechnical engineering, the Finite element method (FEM) 'can also be called Finite element analysis (FEA)' continues to be the most broadly used and probable the most flexible approach for analyzing boundary value issues as FEM is one of the numerical methods which is based on differential equations for fixing problems of engineering with mechanical behavior of solids. Additionally, the FE method is used to analyze the failure area and the staged production impact to predict the real site conditions like the displacements, pressures, and the water pressures. The calculation of factor of protection using finite element is likewise feasible by the usage of the strength reduction method. (Hrennikoff, A. (1941)

2.4.1 Material models in PLAXIS (2D)

Mohr-Coulomb Model: the easy model to characterize the soil behavior is the Mohr-Coulomb model and can be considered as an elastic plastic soil model. The parameters contained in this model are cohesion, angle of Friction, dilatancy angle, Young's modulus, and Poisson's ratio. Since most of them are easy to estimate from the static laboratory tests, it is one of the mostly used compared to others.

Linear Elastic Model: This model is centered on Hooke's law. This model contains just with two parameters: Young's modulus and Poisson's ratio and is applied to analysis the structural basics in soil for example footing, pile or rock.

Hardening soil model (isotropic hardening): Soft soils and stiff soils are the types that can simulate by this advanced model. The compression and shear hardening are the two main types of this model, where there are used to model irreversible plastic strain respectively due to primary compression in oedometer loading and primary deviatoric loading. The primary characteristics of hardening soil model are as follows:

Input parameter m

Input parameter E^{ref}_{50}

Input parameter E^{ref}_{oed}

Input parameters E^{ref}_{ur}, v_{ur}

2.4.2 Advantages and disadvantages

Advantages and disadvantages generally appear in 2D and 3D analyzes but the disadvantages are particularly evident in 3D analyzes and are less applicable to 2D models. The major advantages are shortened below:

- It has the ability to predict in detail the places of bending and failure of the structure by displacing and distributing pressures on the facility, and the software applications of this tool have a different set of simulation options for modeling and analysis.
- Helps reduce costs and materials, and reduces weight in producing perceptions, rigidity, and strength in structural alignment.
- FEM has important feature, such as better insight into the speed of critical designs and increasing their accuracy at the lowest possible cost, and this makes productivity and decrease in project budget.
- FEM has modern algorithms that have been developed throughout the engineering history that contribute to raising engineering standards and greatly improving the design process.

The main disadvantages of the Finite element method as it is explained above evident in 3D analyzes more than the 2D model, including:

- Make efforts before and after treatment if the entire analyzed domain size is not determined.
- Constituent models always need sophisticated algorithms.
- Depending on the general structure and algorithms applied for the FE. Code run and the disk storage demands are excessive due to large equation systems.

2.5 Limit Equilibrium Methods (Slices Methods)

Recently, the limit equilibrium analysis has been used by many engineers to analyze the slope stability due to its high accuracy, which in turn assumes that the failure was caused by a sliding block on a sliding surface i.e. the balance between a solid object and a sliding surface where these methods are formed from cutting the slope to accurate slats and then calculating shear pressure (τ) then the safety of factor be calculated according to the Mohr-Coulomb failure criterion. It is also easy to assess the factor of safety and there are so many free-applications to run these kinds of analysis.

Limit equilibrium method derives its reputation from its relative simplicity and skill in assessing slope stability of various input parameters and an accurate calculation of the safety factor. Among the most famous methods of LE analysis are (Bishop and Fellenius), as the difference between their results is somewhat similar and does not exceed 6%, as informed by (Duncan 1996). The main differences between the FE and LE methods are explained in Table 2.1. One is more practical/applicable but needs complex stress-strain models, whereas the other is easy to conduct but may not be that accurate in terms of slip surfaces.

	Finite element method	Limit equilibrium method
1	Counting displacement	Can not counting displacement
2	Based on computer performance that upgraded application of FE in engineering analysis.	The stability analysis includes due to greatest simplicity and accuracy
3	Need complete stress strain model for soil.	Only Mohr-coulomb soil model required
4	Modelling progressive failure	Cannot Modelling progressive failure
5	For very high realism model slopes and better calculation of the displacement of soil	It cannot visualize the deformation of the soil due to is based on simply only summation moment, vertical forces, and horizontal forces
6	By the software, the critical surface can find automatically	Critical surface can find out using geometry not automatically

Table 2.1. Comparison of FE and LE methods

The methods of slices involve braking up the sliding mass into a series of slide mass into n smaller slices and the safety factor considered constant along the failure surface. It can be investigated under total or effective stress conditions, at any geometry or loading, any pressure pore state and any rock or soil layering.

2.5.1 Fellenius Method

Fellenius (1936) introduced the first method that is the most simplest methods of slices and known also as Ordinary and Swedish method which applied for circular slip surface, only moment equilibrium condition; except no-consideration of the inter-slice forces E_i and X_i .

It is supposed that side forced T and E may be neglected, and the normal force N may

be determined simply by resolving the weight of the slice in a direction normal to the arc at the mid-point of the slice.

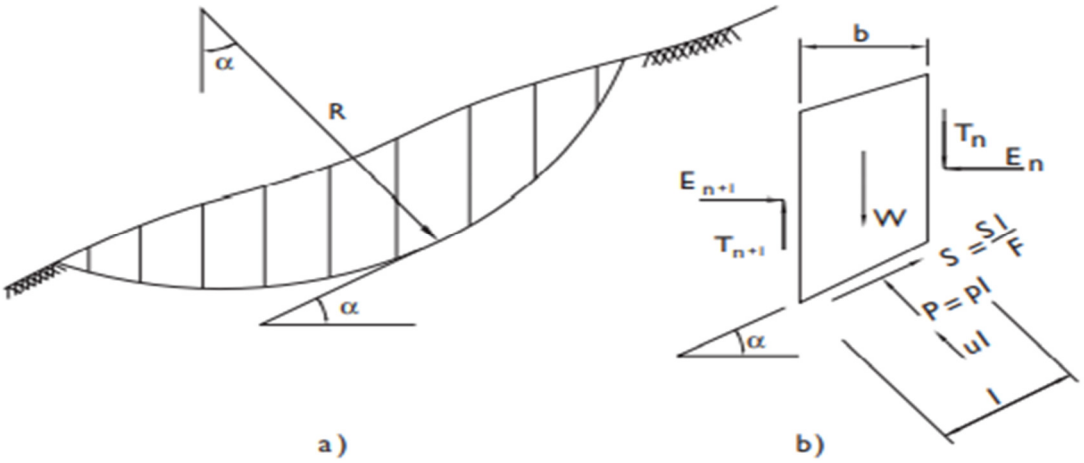


Figure 2.10. (a) Division of sliding mass into slices (b) Forces acting on a typical slice. (Chowdhury, 2010)

W is the total weight of the soil slice, including the weight of water if the slope is saturated and the external loads on the slop surface.

T and E forces on the vertical boundaries of the slice are shear and lateral force due to adjacent slices.

P is the normal force at base in each slice.

The details to get the factor of safety formulation will not be covered here since it is easy to find it in the literature but the final outcome shown in Equation 2.6 and 2.7 will be presented for the sake of the see the differences between the approaches.

$$FOS = \frac{\text{sum of moment maximum resisting forces}}{\text{sum of moment of moving force}} \tag{2.6}$$

$$FOS = \frac{\Sigma c' \cdot b \cdot \sec\alpha + (W\cos\alpha - u \cdot b \cdot \sec\alpha)\tan\phi}{\Sigma W \cdot \sin\alpha} \tag{2.7}$$

The advantage of fellenius method is that the equation does not require iteration process in solving the factor of safety.

2.5.2 Bishop Method

Bishop approach of slope stability analysis is very well known. Its premises are circular surfaces of failure; only the equilibrium of the moment is satisfied; it neglects the shear force and involves normal forces between slices.

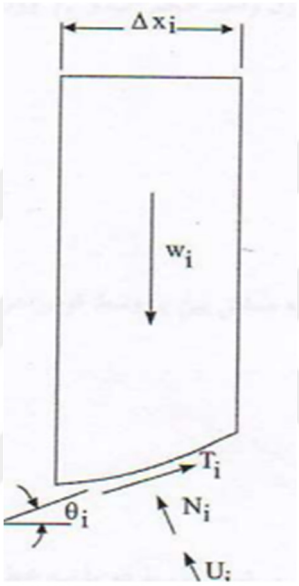


Figure 2.11. Forces assumed in Bishop Method (Chowdhury, 2010)

To resolve the problem of conventional method the equations are: $\Sigma F_y=0$ and $\Sigma M_0=0$.

$$FOS = \frac{\Sigma \frac{1}{m_a} (c' \cdot b + (W - u \cdot b) \cdot \tan\phi)}{\Sigma W \cdot \sin\theta_i} \tag{2.8}$$

The resolution of the Bishop's method is found with an iterative procedure:

1) Assume an initial value of $F \rightarrow F_0$
2) Calculate m_a, i with F_0 for each slice
3) Determine F using m_a, i (if $F = F_0$ the procedure is complete, otherwise the iteration procedure continues).

2.5.3 Janbu Method:

The hypotheses of this method consider the inter-slice forces, neglects inter-slice shear forces, satisfies only horizontal force equilibrium and for any type of failure surface. Janbu proposed a correction factor (F0) which should be greater than that which should be added to the previously determined FS in order to obtain the final value of the safety factor. F0 is a function of the soil's slide geometry and force parameters as shown in Figure 2.12.

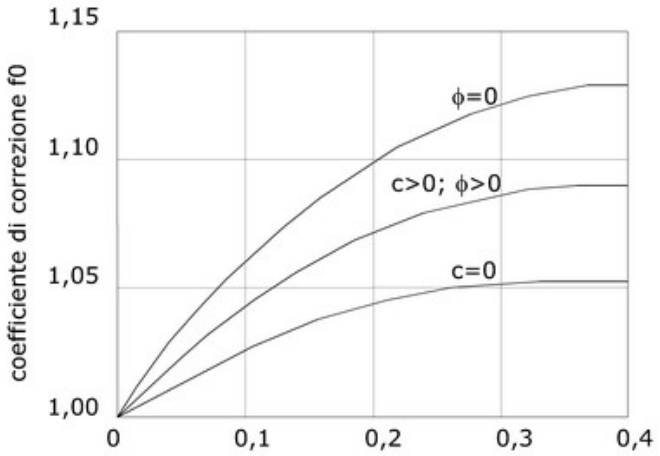


Figure 2.12. Estimation of the corrective factor F_0

The factor of safety in Janbu method is equal to :

$$F = \frac{\Sigma \frac{sec.a}{ma}\{c' \cdot b + W(1-ru) \cdot \tan\phi\}}{\Sigma W \tan.a} \qquad (2.8)$$

2.5.4 Summary of LE Method of Slices

The Fellenius method is the simpler method, and its FOS can be obtained simply without any iterative dimension calculation and can be solved by hand calculation or spreadsheet. Since sometimes presenting findings may be 20-30 percent higher than those obtained from other approaches, because it is considered to be conservative. This is not, however, commonly used in practice.

Method	Features and Limitation
Slope Stability Charts (Janbu, 1968, Duncan et al, 1987)	- Accurate enough for many purposes. - Faster than detailed computer analysis.
Ordinary Method of Slices (Fellenius, 1927)	- Only for circular slip surfaces. - Satisfies moment equilibrium. - Does not satisfy horizontal or vertical force equilibrium.
Bishop's Modified Method (Bishop, 1955)	- Only for circular slip surfaces. - Satisfies moment equilibrium – Satisfies vertical force equilibrium. -Does not satisfy horizontal force equilibrium.
Force Equilibrium Methods (e.g. Lowe and Karafiath, 1960, Army Corps of Engineers, 1970)	- Any shape of slip surfaces. -Does not satisfy moment equilibrium. -Satisfies both vertical and horizontal force equilibrium
Janbu's Generalized Procedure of Slices (Janbu, 1968)	-Any shape of slip surfaces. -Satisfies all conditions of equilibrium. - Permit side force locations to be varied. - More frequent numerical problems than some other methods.
Morgenstern and Price's Method (Morgenstern and Price, 1965)	- Any shape of slip surfaces. -Satisfies all conditions of equilibrium. - Permit side force orientations to be varied.
Spencer's Method (Spencer, 1967)	- Any shape of slip surfaces. - Satisfies all conditions of equilibrium. - Side forces are assumed parallel.

Table 2.2. Features and Limitation for Traditional Equilibrium Methods (Duncan and Wright, 1980).

The Bishop's method is widely used methods although its use has been suggested only for surfaces with circular failure (Abramson et al., 2002), but its analysis is easy for hand calculation and the convergence is quick. Janbu 's simplified approach has few convergence problems and can be used for all types of fault surfaces typically seen in sandy soils. The Janbu method suggested a correction factor but the methods for measuring this factor are based on minimal case searches, so the engineers are asked to use these factors when applied to complicated non-homogeneous slopes of the soil. The features and limitations for the traditional equilibrium methods are discussed and compared in bullets in Table 2.2.

2.6 Retaining Walls

Retaining walls is one of the techniques applied to the ground to hold the soil that provides a tensile restraining force and consequently the possible deformations on slope reduce which may be produced from the lateral stress and compressing under different loads. This structure is designed to improve the soil in unnatural slopes to prevent the failure and retain the mass of soil that can tend down, and slope can occur from gravity and stresses stand-in the soil. Generally, the retaining walls dividing into two classifications:

- Internally stabilized walls that aim to carry tensile loads and stabilize the soil mass through artificial reinforcements laid in the soil.
- Externally settled walls and their function is to resist the movement of the soil through heavy materials outside the soil mass. (Khan and Sikder, 2004).

Deeply embedded piled supporting systems are also used to stabilize landslide slopes. Such structures, which penetrate into the stable rock through the entire landslide mass, mechanically secure the unstable slope and then encourage it to be very successful. Nonetheless, to use ordinary retaining walls on a natural base or on a stacked foundation is cheaper in some situations. While retaining walls are widely used on landslide slopes, they effectively stabilize unstable soil masses, particularly in conjunction with other facilities (for example, counter benches).

Since ordinary retaining walls are easier to shape than deeply embedded anti-landslide

retaining structures, it is recommended that slopes that are stabilized by retaining walls when the site and project conditions are acceptable. Should existing retaining walls within the slope begin to loosen stability or to deteriorate, there is not any need to hurry to form new any landslide facilities; methods of reinforcing the available retaining walls should be investigated. Designing retaining walls and their reinforcement on landslide sites is carried out in conformance with the requirements of this area, since such retaining walls, in addition to the pressure exerted by the soil failure prism determined by the coulomb theory, are subjected to the landslide pressure.

2.6.1 Types of retaining walls

The developments in technical of engineering and especially in geotechnical engineering, various types of retaining walls systems have been promoted in recent decades. Among the most prominent of these types are piled walls, anchored walls, cantilever, and gravity walls.

2.6.1.1 Pile walls

They provide a high stiffness as retaining elements that can prevent the lateral pressure in depth excavation without any distribution in the structure, but it cannot bear very high pressure. Piles are useful to retain the sliding slopes, support deep excavation and cuts in slope in seismic areas where structural components transfer forces to the ground by shearing and bending, depending on the static system and the dimensions.



Figure 2.13. Pile retaining wall

2.6.1.2 Anchored retaining wall

The features of the anchored retaining wall are that a high wall can be built whereas the anchors prevent occurring a sliding pressure, overturning. Deeping cable rods into the ground build it then the ends are poured with concrete to provide anchor. This type of walls suitable for loose soil and they are used when the wall is thin, and the space is limited. (Figure 2.14).

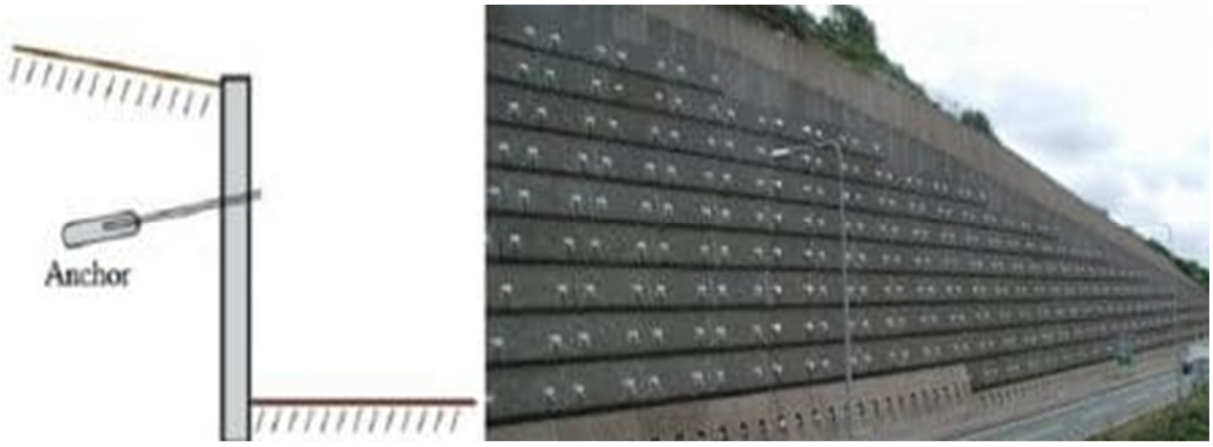


Figure 2.14. Anchored retaining wall

2.6.1.3 Cantilever wall

This wall is one of the most used type in retaining walls, economical until 10m high as a smaller quantity required of concrete comparing with the other walls. This type of wall consists with stem and base slab and it can be constructed on site or by precast concrete. Heel is a term of the part of the base slab under backfill material and toe is the other part as shown in Figure 2.15. There are stability checks that consists of sliding, overturning, and the bearing pressure and they all must be satisfied during its design.

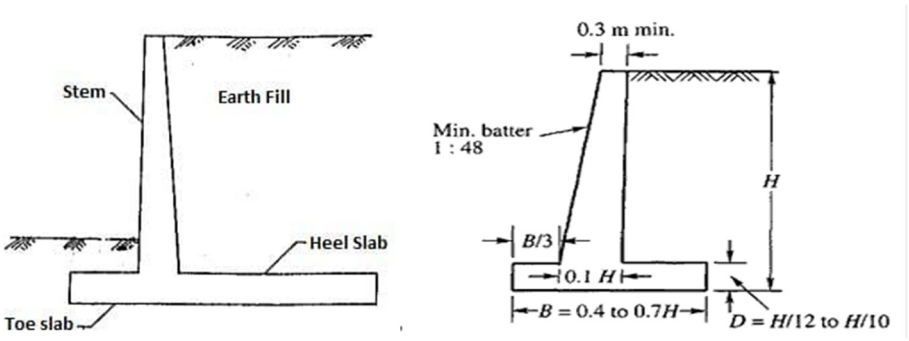


Figure 2.15. Cantilever wall (Clayton, 2014).

2.6.1.4 Gravity wall

Gravity walls have many types such gabions, bin, and crib walls. This type of retaining wall resists the lateral ground pressure depending only on its weight; therefore, the cross-section of the wall should be huge compared to the cantilever walls just to bear the lateral acting loads.

The materials that the gravity wall constructed in are concrete or stone and it is only economical up to a limit of height (around 6 m). An example of a gravity wall is presented in Figure 2.16. Same as the cantilever wall; sliding, overturning and the bearing forces must take into consideration when it is designed.

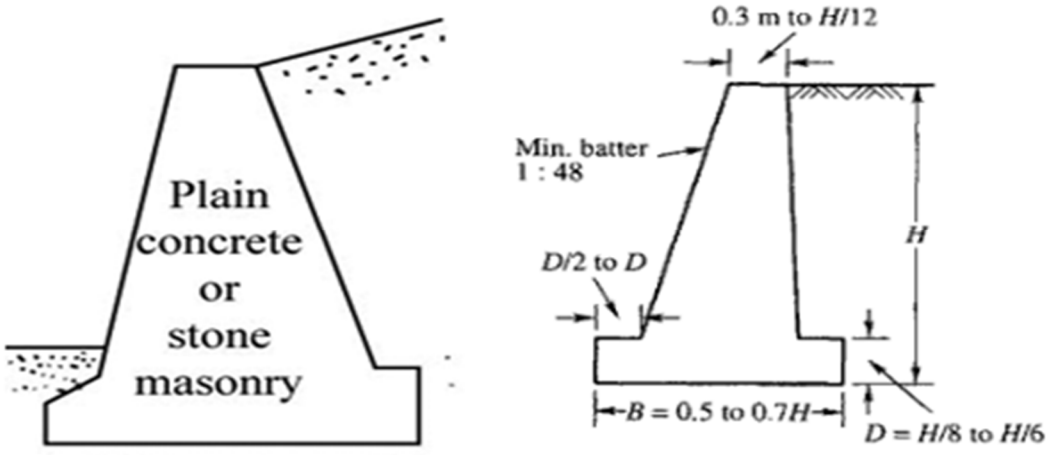


Figure 2.16. Gravity wall (Clayton, 2014).

2.6.2 Metal strip reinforcement

Metal strip reinforcement (MSR) is one of the internally stabilized walls that aim to stabilize the soil mass through reinforcements. It can be defined as layers of reinforcement in the backfill soil such as metallic, geo-synthetics, strips, grids, and sheets. Granular soil is the best type of soil that will be retained fill soils for the Mechanically Stabilized Earth (Elias et al, 2001).

The reinforcements can prevent the deformations under probably stresses by adding tensile strength to the soil through the reinforcement's tieback the solid face to elements behind the wall. They are located horizontally in the retained fill to tieback the stiff face and recompense for the soil's lack of tensile strength. The strength may be better meaningfully when inserting tensile reinforcements in the soil.

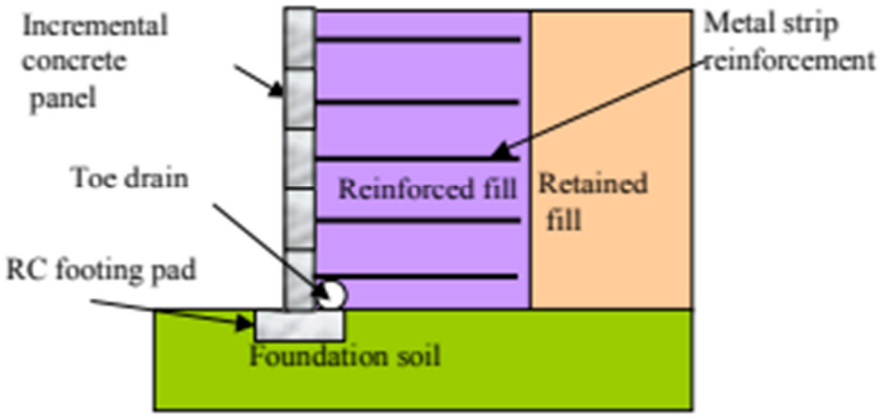


Figure 2.17. Metal strip reinforcement (Rowshon, Jadid. 2016)

2.6.3 Geo-synthetic reinforced soil walls

The geotextile sheets place horizontally with the long dimension parallel to the centerline. Each of MSE and geo-synthetic reinforced soil (GRS) walls uses compacted drainage good granular in the backfill soil but the difference between them are in design and construction. The geotextile fabric can surround each layer of compacted soil and prevent movement of soil particles.

Reinforcements in geo-synthetic reinforced soil walls internally stabilize the soil with carrying tensile loads (Vanbuskirk, 2010).

Generally, geo-synthetic reinforcements are used in GRS walls that are permeable, polymeric large fabrics mats that are designed especially for soil. The tensile strength should be at least 28.5 kN/m as it is recommended in Landslide Solutions Inc. (2008). The spacing of the reinforcement has big importance for performance of GRS more than MSE walls. (Bradley and VanBuskirk, 2009). Figure 2.20 shows an example of geotextile reinforced soil wall referenced from Rowshon Jadid (2016).

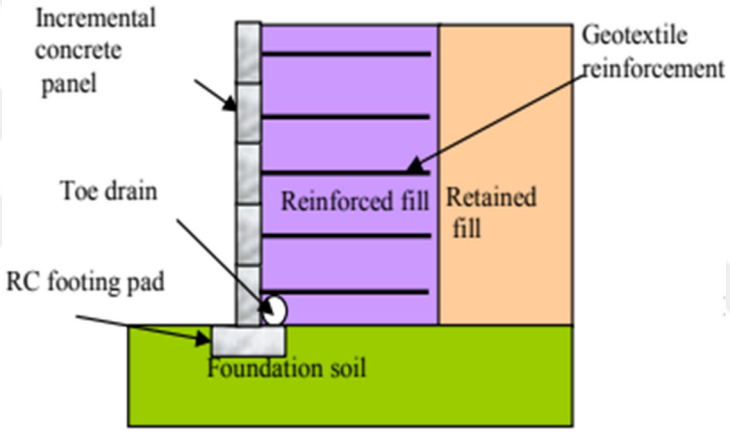


Figure 2.18. Geotextile reinforced soil wall (Rowshon Jadid. 2016)

2.6.4 Comparison of reinforced soil walls and concrete gravity walls

The advantages of the reinforced soil retaining walls are more than the concrete gravity walls, the most prominent are that:

- Building without rigid foundation support according of its tolerant to deformations.
- Rapid construction and simple procedure that do not require a lot of big construction equipment thus less cost.
- They are feasible to height up for 25m as technically.
- For internal and external stability, a big space required behind both types of walls to obtain enough width of wall.

3- MATERIALS AND METHODS

A model has been studied with the help of PLAXIS software 2D for a slope needing support due to the gradual structures. The study itself was arisen from a problematic case study that consists of three blocks to be constructed on a slope soil with different elevations to be able get the sea view in Yalova Province, Çınarcık District.

This research's objectives are to study the behavior of soil properties related to slopes ratios in terms of how undrained strength and the slopes ratio can affect the pile-supported system in static and dynamic state and the behavior of the piles under different soil parameters and variations in the slope's ratio. Finally, it is aimed to get out the differences in consequences of reinforced slope stability analysis obtained from FE based.

The slopes ratios that had studied are 1.5:10, 2:10, 3:10 and 4.5:10, the inclined degrees are 8°, 11.3°, 16.2° and 22.2° respectively and the undrained strengths are 75, 100, 125 and 150 kPa. The plain strain model was chosen, which can suppose that the displacements and strains in z-direction 0; however, the normal stresses in this direction should be taken into consideration. The element was taken on 15-node triangular elements as it is produces very high-quality stress result for hard problems.

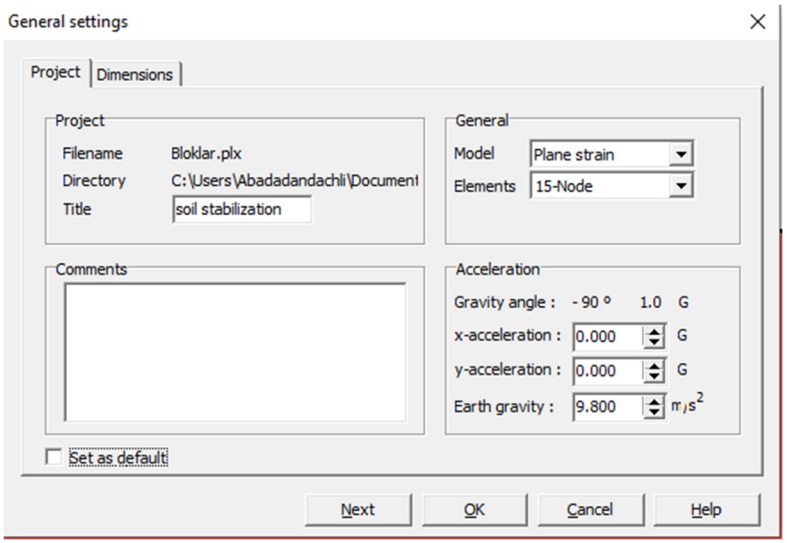


Figure 3.1. General settings of the model

3.1 PLAXIS Software

PLAXIS is one of FE programs that extended international for geotechnical engineering and used to analyze a big area of problems and predict the deformations which can occurs. The geometry model is the first step should be done to analyze any project in PLAXIS that mean a type of a real 2D problem; it includes soil layers and structure elements. The results of the analyzing can obtain after planning the steps in phases section. The general aspects of the model are as follows:

i. *Points*: determine the starting and the end lines, as well as it can fix the strength, the position of springs, and the local mesh elements are cleaned locally.

ii. *Lines*: are utilized to explain the physical boundaries of geometry, structural alignment lines, and discontinuities in geometry that includes partitions or pylons or excavation areas.

iii. *Elements*: for the duration of the mesh creation, 15-triangular nodes have consisted in the work surface generated via the 2-dimensional mesh construction (Figure 3.2).

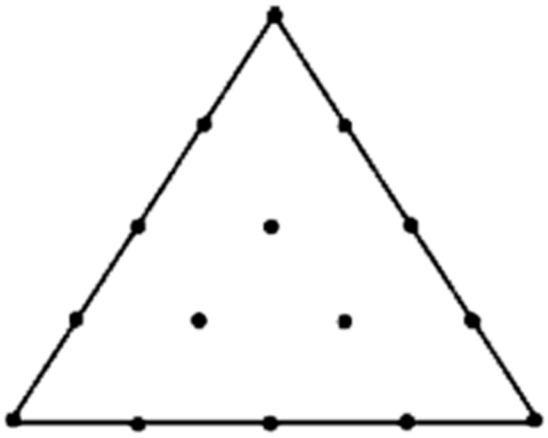


Figure 3.2. The 15-node triangular element (PLAXIS, 2010)

iv. *Clusters*: the areas surrounded by lines are called clusters. PLAXIS can automatically detect conglomerates based on the entered engineering lines since all properties are homogeneous within the mass. Create a two-dimensional racial grid based on a set of clusters and lines within the engineering model

An outline of the basic features of PLAXIS program is given underneath:

1. Graphical input of geometry models: CAD drawing procedures can allow the modeling of the geometry more detailed that < the input soil data ,the construction phases and limit cases > depend on it which they makes the finite element mesh more easily to generated .
2. Automatic mesh generation: PLAXIS permits for computerized technology of unstructured finite detail meshes with alternatives for global and local mesh refinement.
3. Mohr-Coulomb model: the greatest applied conditions of this strong non-linear model is the soil parameters whereas this model can be used to calculate the collapse loads of footings, bearing capacities and the FOS (factor of safety) by" phi-c "reduction method.
4. High-order elements: the PLAXIS 2D have 6-node and 15-node triangular elements to analysis the displacement and the pressures in the soil as for the PLAXIS 3D have 10-node elements.
5. Plates: Their conduct can be elastic or non-linear elastoplastic whereas is can be accustomed to model slim constitutions in the field with a knowing bending stiffness while the plates are soil plates, walls and tunnel linings are this module's ordinary applications.
6. Dynamic analysis: the study of the vibrations and the robust movements in the ground can be calculated with the dynamic module, it is also can analysis the deformation and stability of the soil under earthquake loading states.
7. Interfaces: Joint elements are obtainable to model soil-structure interaction and the Values of interface friction attitude and cohesion are normally now not like the friction attitude and cohesion of the local soil.

3.2 Soil Parameters Used in PLAXIS

Soil types is chosen from the material part. The model material to estimate the failure is selected as Mohr-Coulomb. In this study, the soil type is soft sensitive clays (undrained) where its specifications are divided into three different sections: general, parameters and interfaces as it is shown in (Figure 3.3 and 3.4). The unit weight of the soil is taken 18 kN/m³ in all the analysis, but the cohesion of the soil is increased during the different models as 75 kPa, 100 kPa, 125 kPa and 150 kPa.

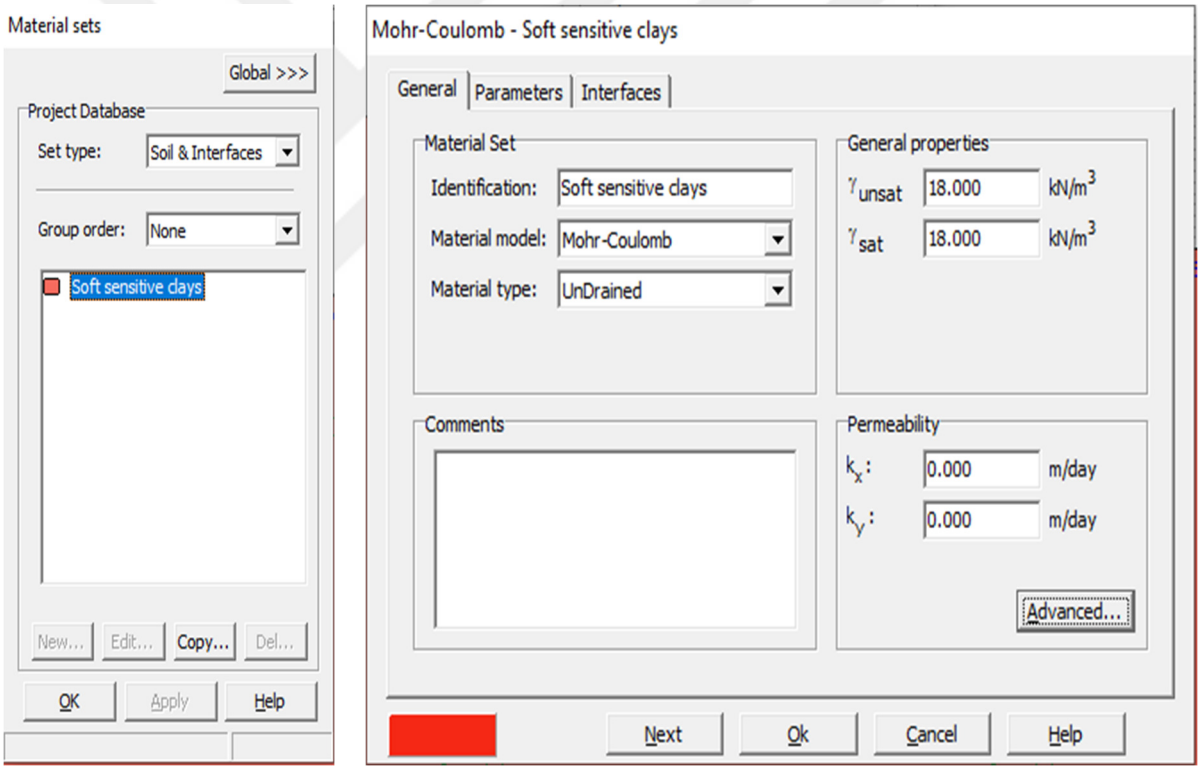


Figure 3.3. Presentation of the soil materials.

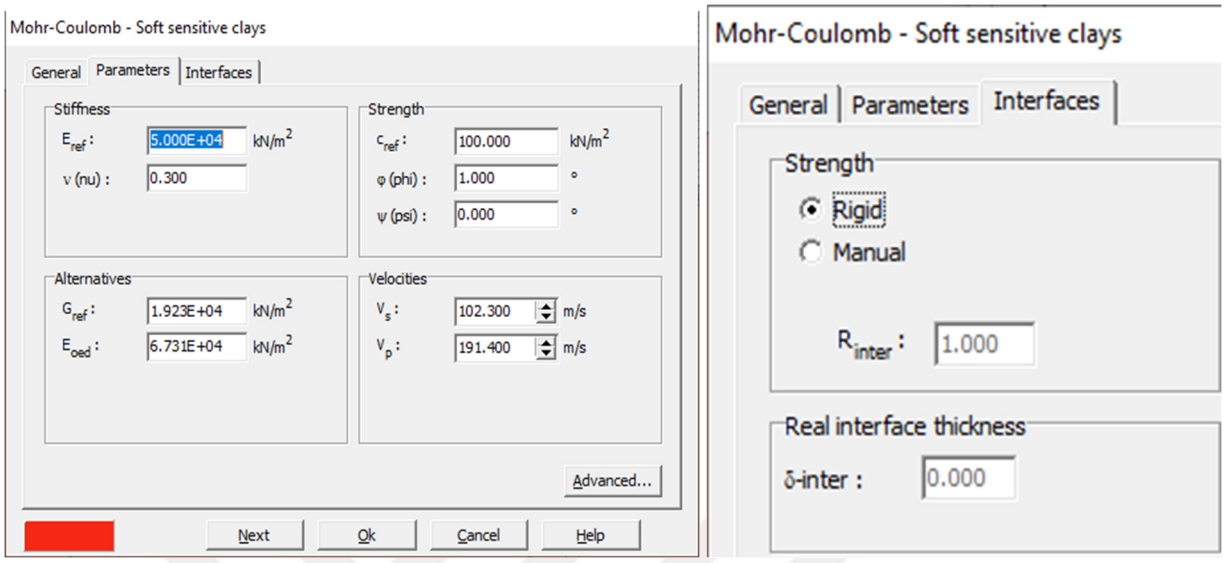


Figure 3.4. Parameters and interfaces menu

The elasticity modulus was calculated from the correlation of modulus of elasticity with undrained shear strength as it is shown in Table 3.1.

Soil type	Relationship	Reference
Clay	E= (500 to 1500) Cu	Bjerrum
Soft sensitive clay	**E= 500 Cu**	**NRC of Canada**
Fine to stiff clay	E= 1000 Cu	NRC of Canada
Very stiff clay	E= 1500 Cu	NRC of Canada

Table 3.1. Correlation of modulus of elasticity with undrained shear strength

The material properties that were used for different models are presented in Table 3.2. In order not to count on the effect of the Poisson ratio, it is kept constant as 0.3. Another important point is that although the study focused on the undrained behavior of clays, the friction angle is taken as 1° for the calculations to have NaN matrices.

Cohesion (kPA)	Unit weight (γ) (kN/m^3)	Angle of internal friction (ϕ^o)	Young's modulus (E) (kPa)	Poisson's ratio(ν)	Rinter
75	18.0	1	**37500**	0.3	1
100	18.0	1	**50000**	0.3	1
125	18.0	1	**62500**	0.3	1
150	18.0	1	**75000**	0.3	1

Table 3.2. Properties of the soil

3.2.1 Pile (Plate) Model

The model of piles walls is centered on the stability of the system and the moment of resistance to the moving soil. In this study, the slope is supported by three different pile systems modeled as plastic plates; each pile's height is 12 meters with the thickness of 1m. Standard fixities were set as boundary condition for the geometry model. Total fixities were set at the bottom of the piles as presented in Figure 3.5.

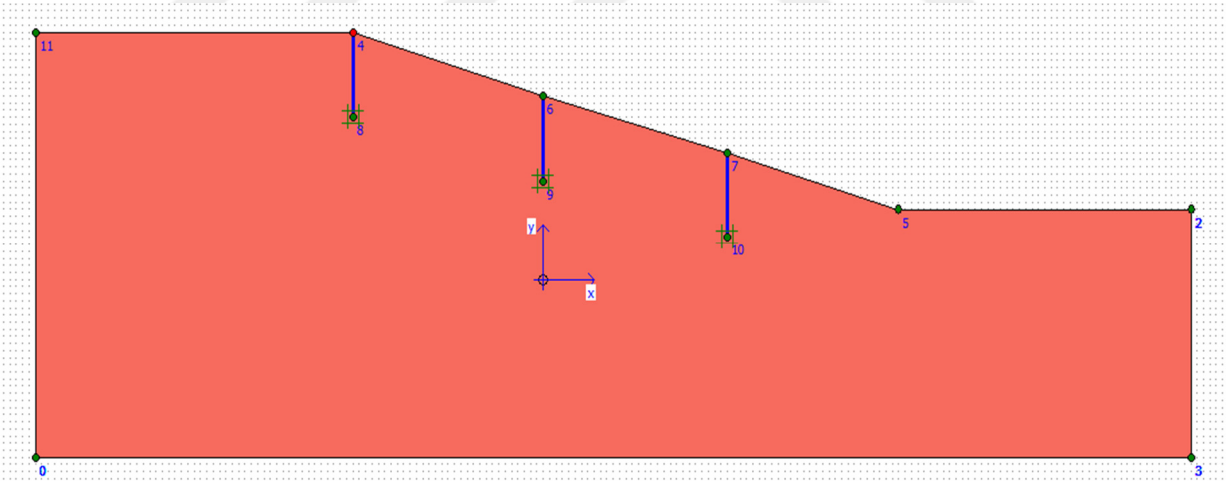


Figure 3.5. Pile wall model in PLAXIS (16.2°-4.5:10 Slope)

Figure 3.6 shows the properties of the plate material. Material type is selected to be elastic since there is no information about the plastic behavior.

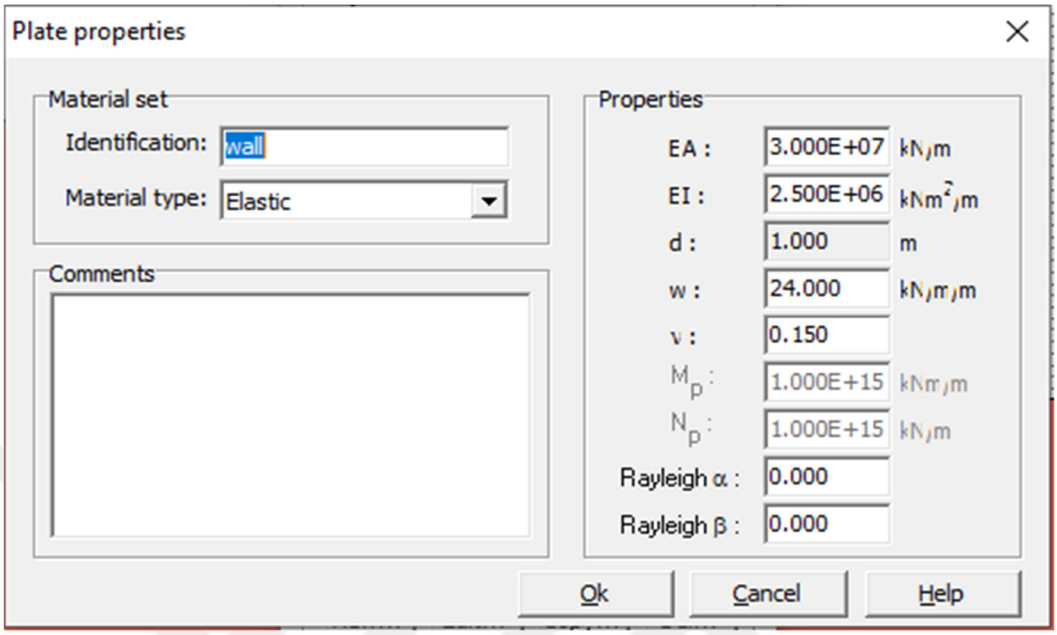


Figure 3.6. Properties of the plate

3.3 Motions used in the Analysis

In this thesis, three different real earthquake data is used for the dynamic analysis. These motions are taken from the Pacific Earthquake Engineering Research (PEER) data repository and they are Kocaeli Earthquake (1999), Duzce Earthquake (1999) and Kobe Earthquake (1995). These real data has different properties in terms of duration and frequency content.

All the motions were scaled to the 0.46g since the new Turkish Building Code (2018) suggests this specific peak ground acceleration for the specific location of construction to be built and they are presented in Figure 3.7 (Duzce Eq.), 3.8 (Kocaeli Eq.) and 3.9 (Kobe Eq.). The analysis lie on two main sections: 1) Construction and constitutive loading and 2) Dynamic loading. The displacement is reset to zero after the forming the model to the site conditions.

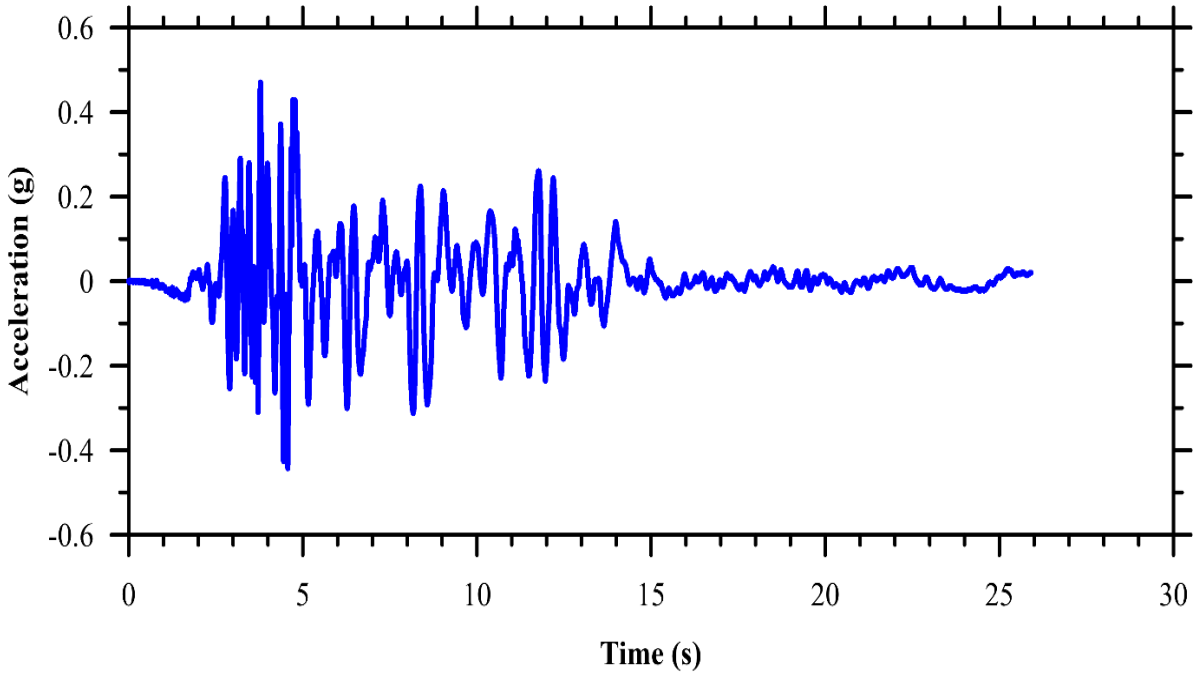


Figure 3.7. Duzce earthquake data

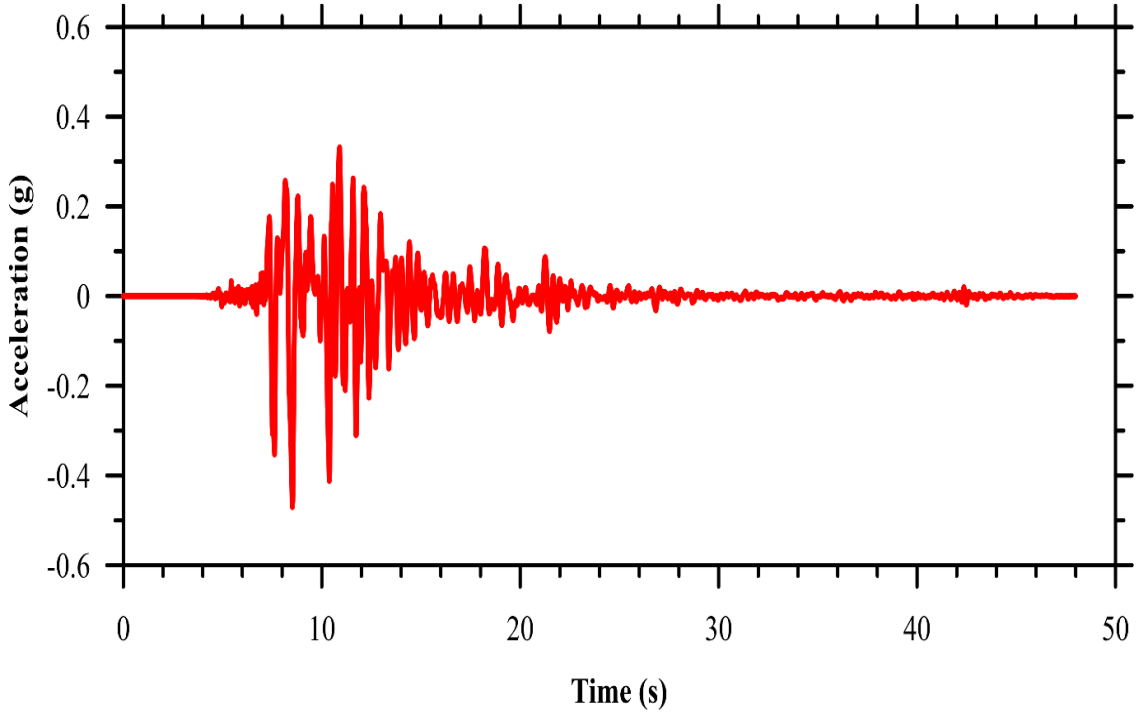


Figure 3.8. Kobe earthquake data

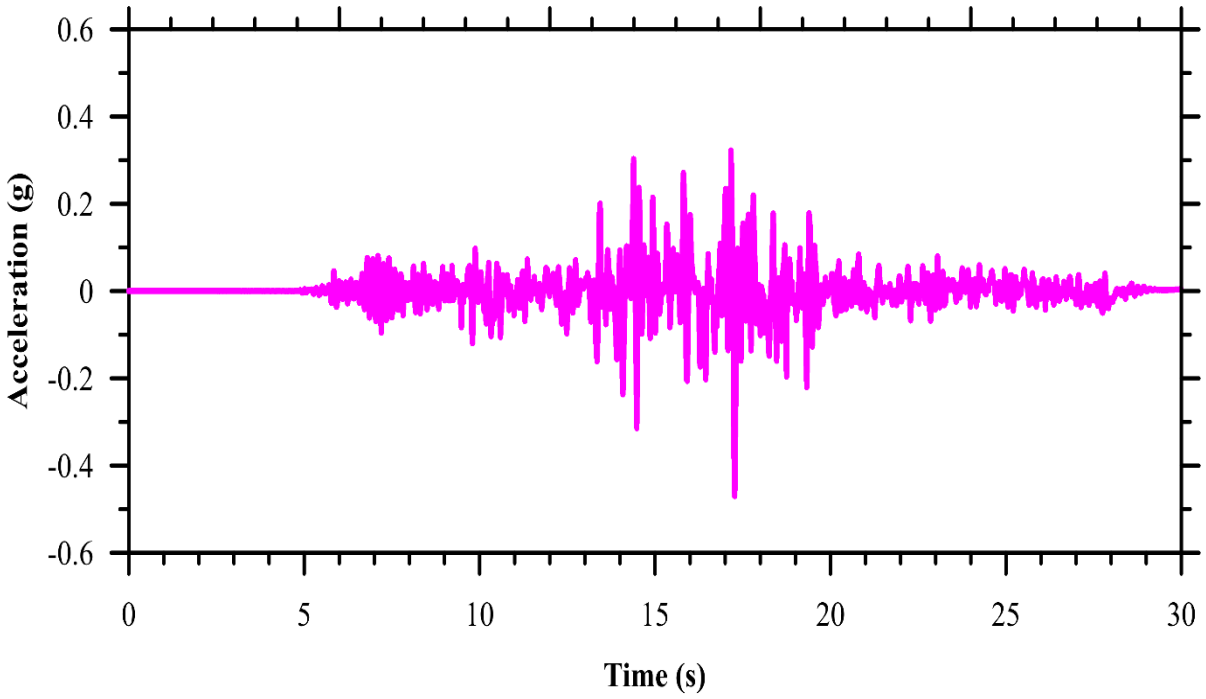


Figure 3.9. Kocaeli earthquake data

3.4 Analysis Program

After reinforcing the slope by pile-wall, it was assumed that there is a static load with 60 kPa at depth of 4 m from each wall as it is shown in Figure 3.10. The buildings to be constructed in this area have three stores and it was considered that each store might exert as much as 20 kPa.

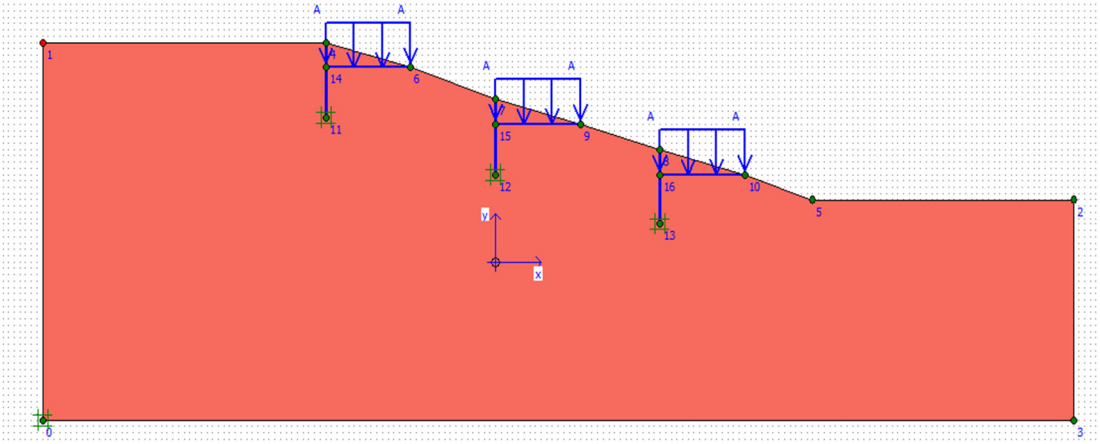


Figure 3.10. Loading (16.2° Slope)

Model boundaries must be far enough to avoid the direct effects of boundary conditions therefore at least 40 m of distance were modeled from the construction side. The total distance on the x-direction is around 180 m whereas it is 60 m in y-direction. Figure 3.11 shows the standard absorbing boundaries were used at the bottom and at the right-hand boundaries to avoid spurious reflections.

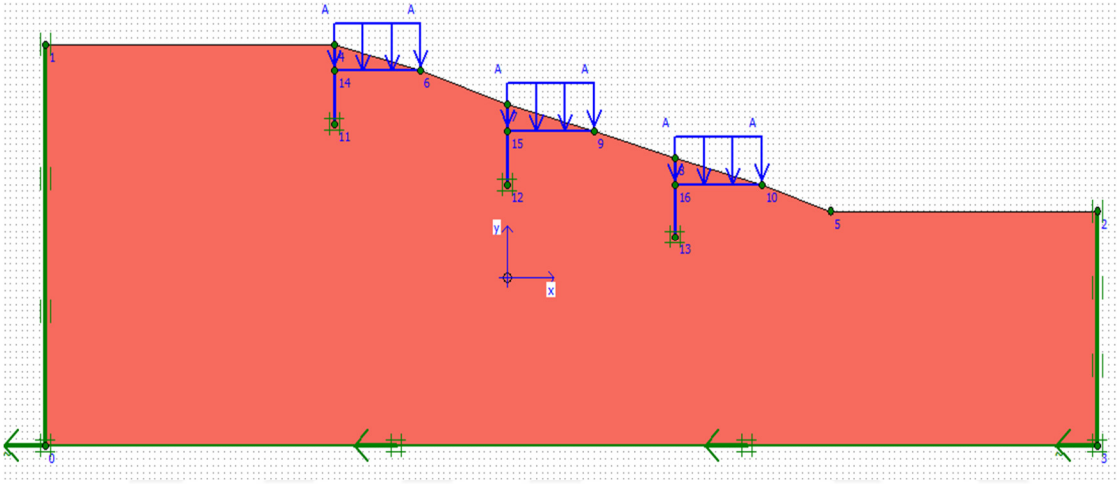


Figure 3.11. Geometry model with standard earthquake boundary conditions (16.2°Slope).

The mesh generation were set as medium; also, a refinement was done for the piles. Standard fixities were set as boundary condition for the geometry model. The result of the mesh generation is presented in Figure 3.12.

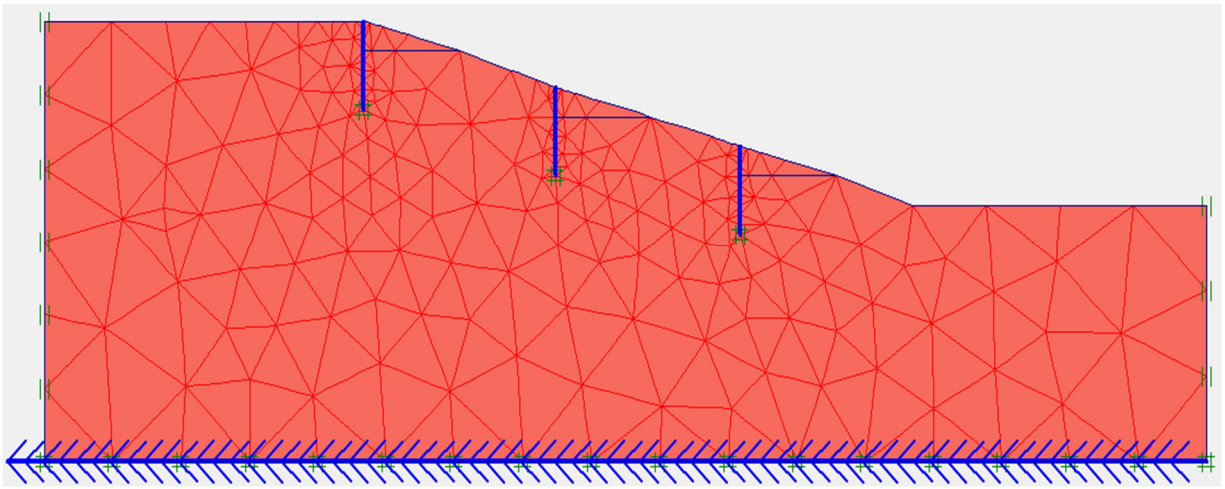


Figure 3.12. Finite element mesh for the model (16.2 degrees slope)

The local site conditions state that there is no water table for at least 50 m boring; therefore, the water table was not considered, groundwater level was chosen at the bottom of the ground surface as seen in Figure 3.13.

The direction of the dynamic loading was chosen after several calibration models and it was observed that the maximum deformations and stresses were recorded when the direction was selected as right to left. The other important point for the model is that all the walls were fixed at their base since they would not hold the soil if not fixed.

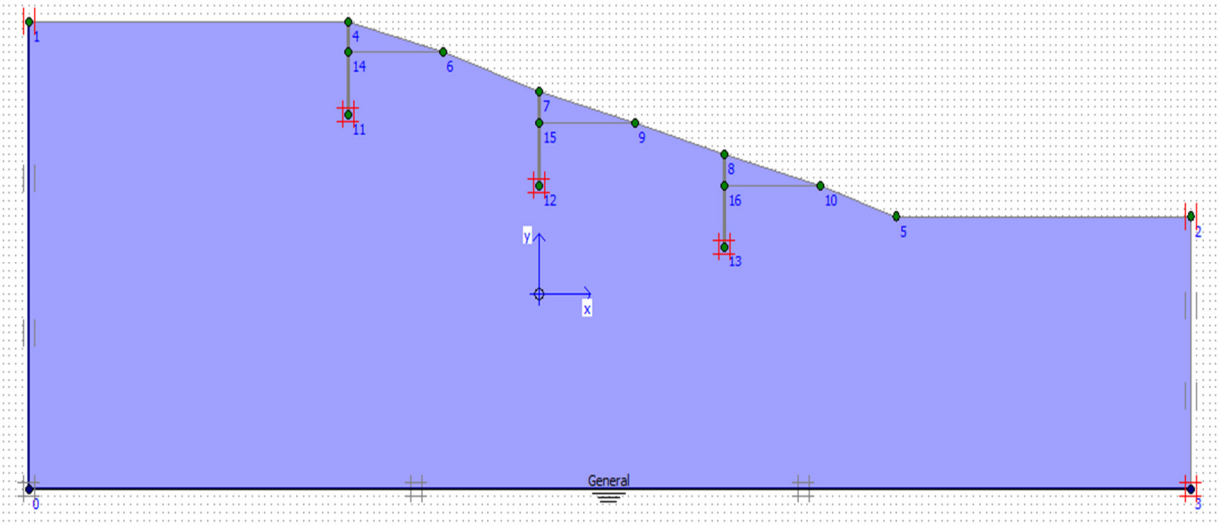


Figure 3.13. Water pressure level

The analysis of this research contains 11 calculation phases. The first 10 phases, plastic calculation was selected in the general tab sheet in order to constitute the site conditions and the construction phases. Phase 11 is the seismic phase when it can calculate by select dynamic analysis in the general tab sheet.

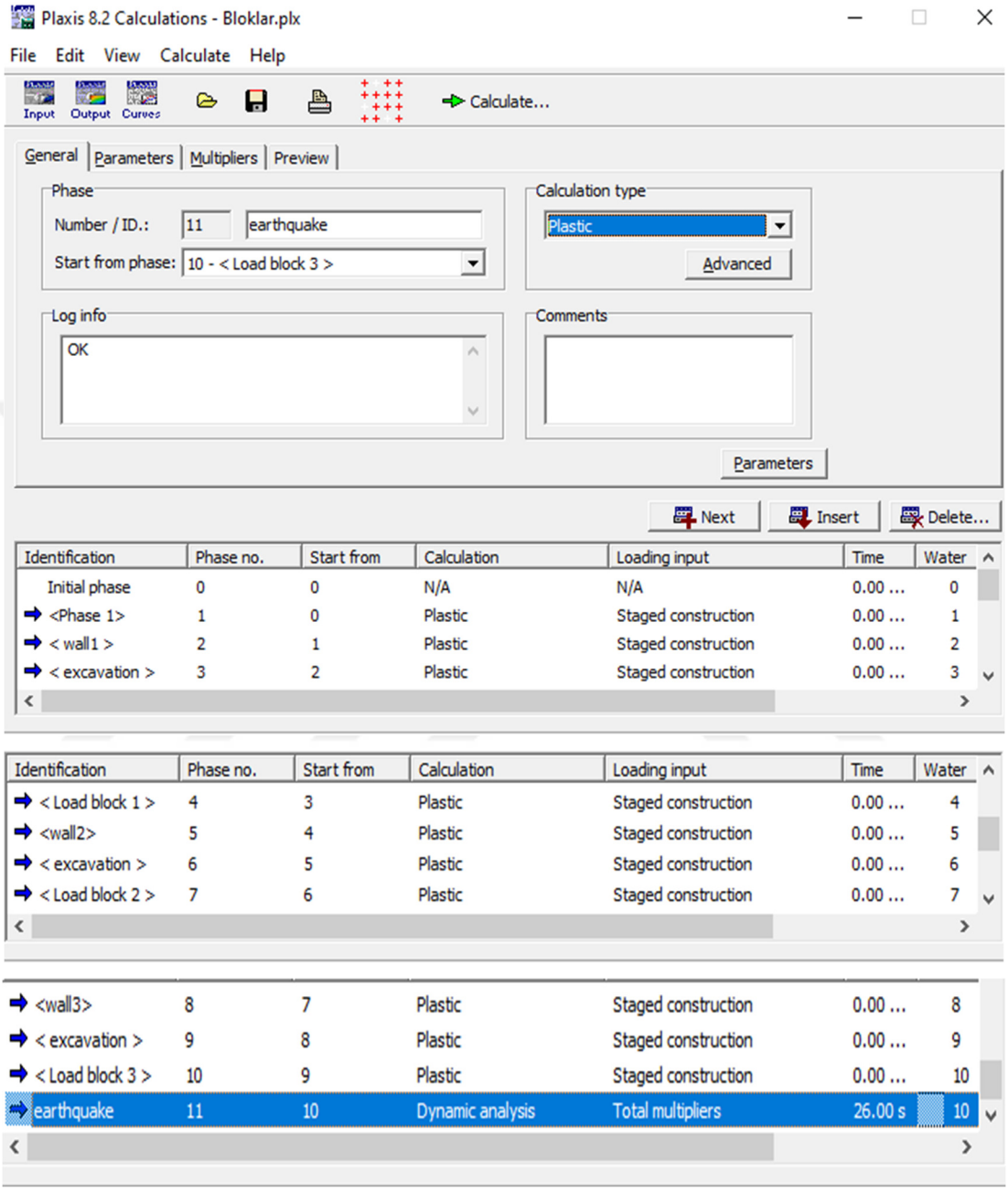


Figure 3.14. The phases for analyzing

Figure 3.14 details all the phases: In the first phase, nothing was defined. The second phase, the pile is created (Wall 1). In the third one, a 4m excavation was done (excavation 1) to define the load of the block 1 in the phase 5 (Load block 1). The procedure of the phases is repeated respectively as (wall 2 – 4m excavation - Load block 2; wall 3 – 4m excavation - Load block 3).

Outcomes were distracted with the help of output program after finishing the model analysis. In this partition, we are able to see the results of the FE analysis such as the displacements and the stresses. In addition, the results can be observed as graphical or tabular form. Example outputs of deformed mesh and total displacement distributions are sorted in Figure 3.15 and 3.16

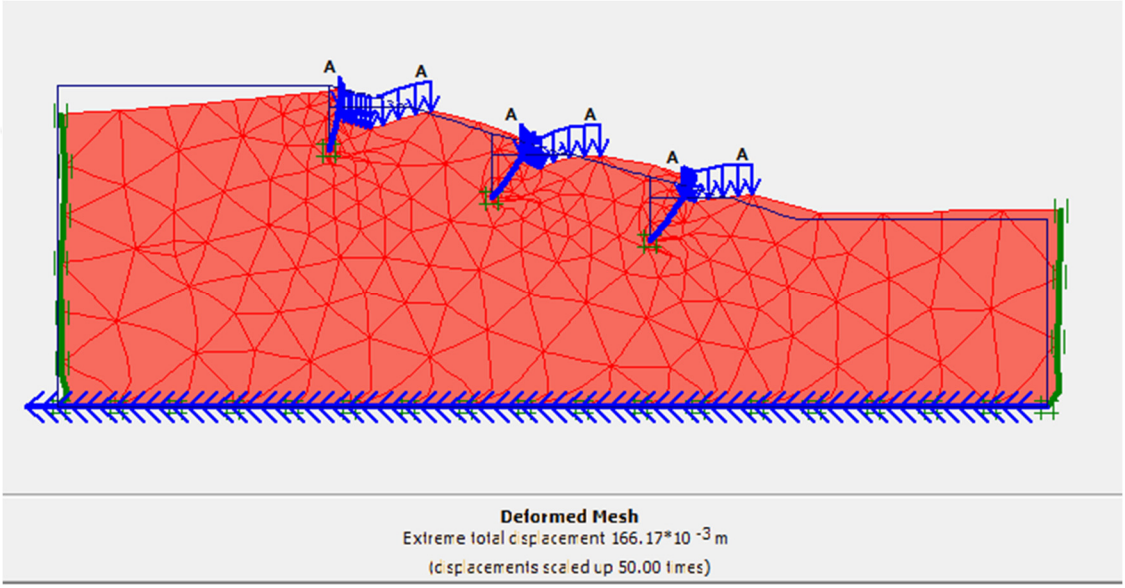


Figure 3.15. Example output of deformed mesh

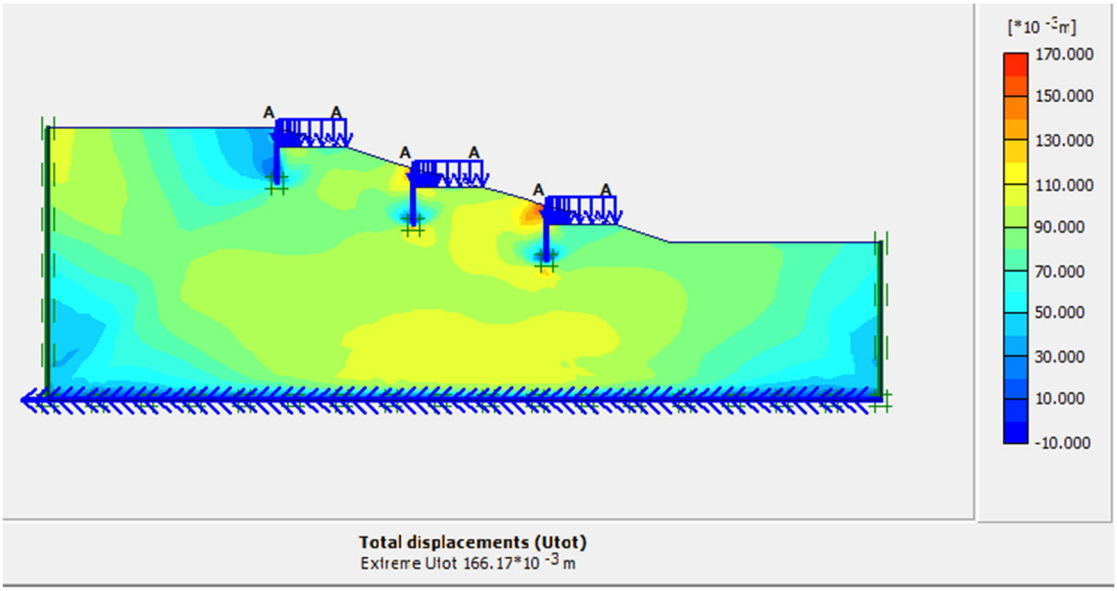


Figure 3.16. Example output of total displacement distribution

4. RESULTS AND DISCUSSION

With the help of FEM software, the analysis results of the model will be presented in this chapter according to slope and cohesion variation. The calculation has been done inserting a simulation of the loading after the definition of the model geometry and material parameters. Discussion of the outcomes are reported herein.

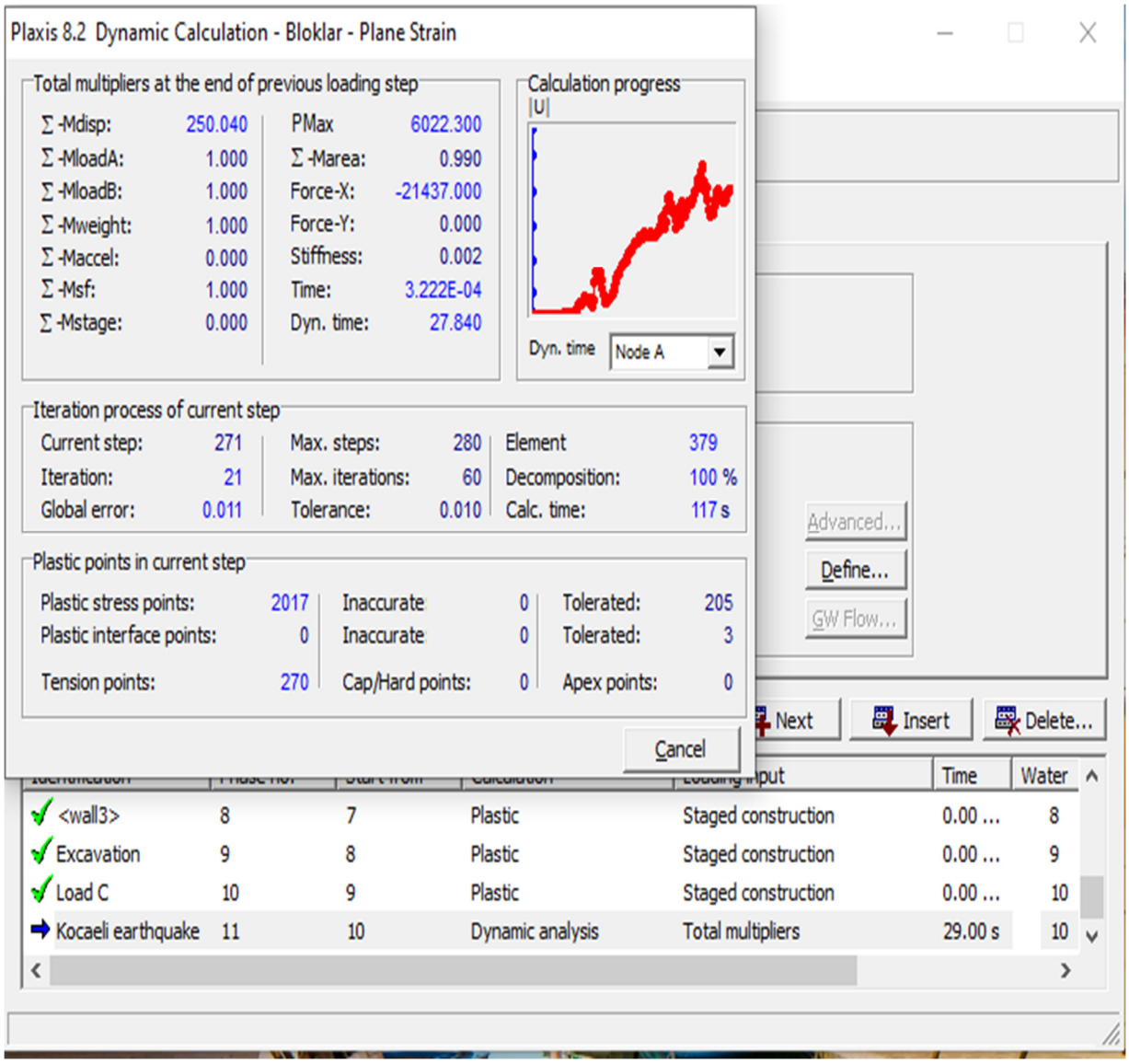


Figure 4.1. Calculation page

4.1 Effect of the Slopes on the Lateral Forces and Moments

In this part, the outcomes of the analysis in terms of moments, shear forces, axial forces and total displacement of the Wall 1,Wall 2 and Wall 3 under three different earthquakes (Duzce, Kocaeli and Kobe) and in static state were studied according to slopes variation (0.15 – 0.2 – 0.3 and 0.45). The variation of the cohesion will be covered later, and the main focus will be the slope itself.

Note: in case of cohesion75 Kpa, the slope 0.45 had collapsed.

4.1.1 Lateral Moment Behavior

The moment results of the Wall 1, Wall 2, and Wall 3 in static state and dynamic loading of Duzce, Kocaeli, Kobe earthquakes are presented in Figure 4.2 to Figure 4.5.

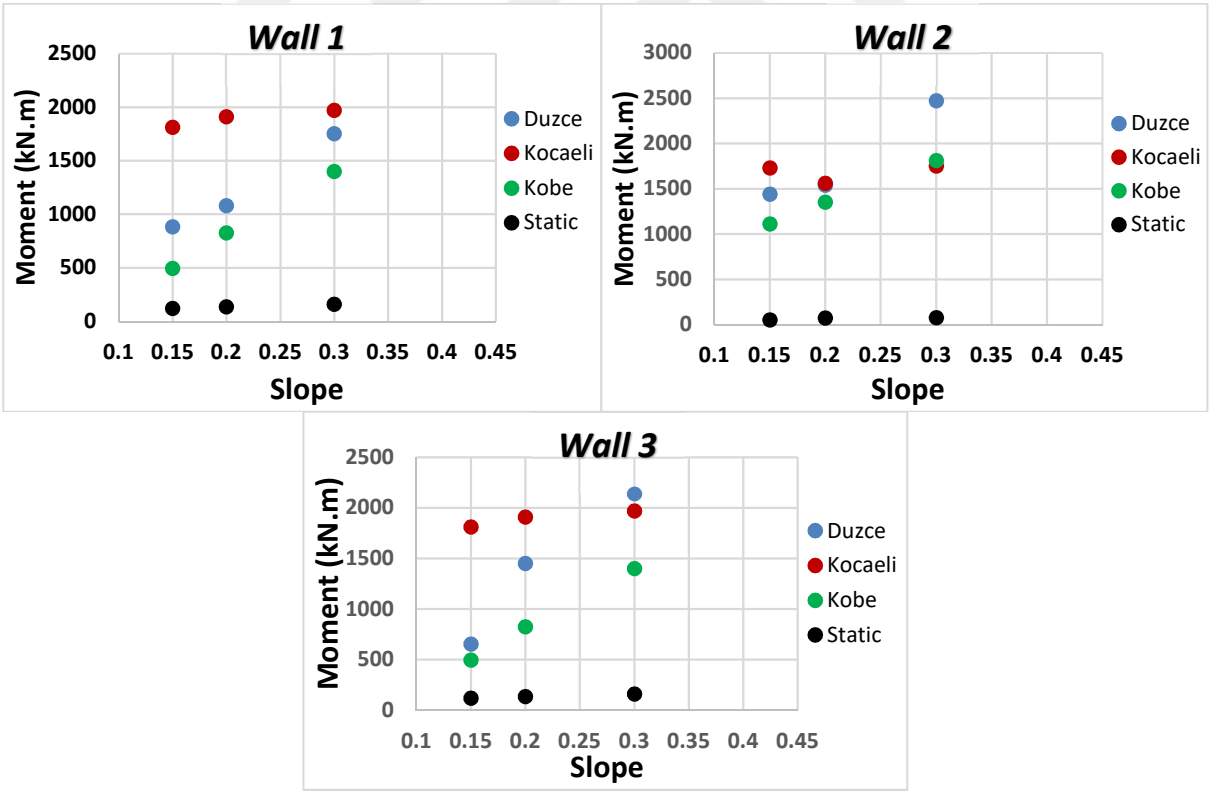


Figure 4.2. Moment behavior with regard to the slope variation (**Cohesion=75 kPa**)

It can be seen form the Figure 4.2 that in all the walls the moments formed under static state are much smaller compared with the dynamic state. In addition, they were amplified

compared to the static state under Kocaeli earthquake more than the other earthquakes especially at 0.15 and 0.2 slopes. Whereas the highest moment was observed at the slope 0.3 by Duzce earthquake on the Wall 2 that is to be constructed in the middle. The slope is collapsed at 0.45 ratio in the case of cohesion 75 kPa meaning soil/walls are not capable of carrying the dynamic load under this circumstance.

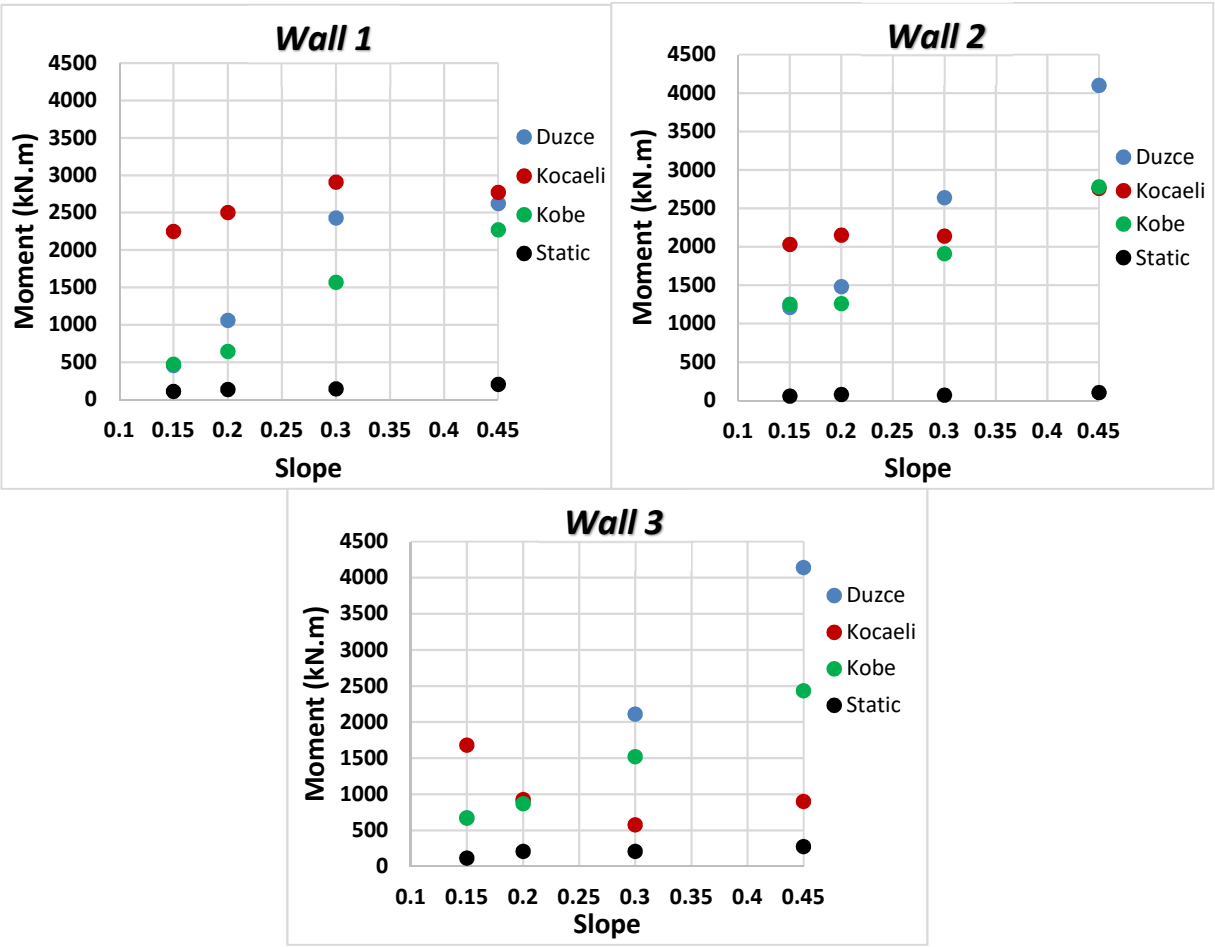


Figure 4.3. Moment behavior with regard to the slope variation (**Cohesion=100 kPa**)

Moving to Figure 4.3 to the case when the undrained strength was 100 kPa, it was observed that the highest value of the moment was recorded as 4140 kN.m on the Wall 3 at a slope of 0.45 under Duzce Earthquake loading. It was also seen that the moments increased with the rise of the slope ratio in the Wall 1 and 2, but the Wall 3 was affected inversely by Kocaeli Earthquake where the biggest value occurred was at the slope 0.15.

The frequency content of the loading has a big influence on the stress transmission between the soil and plate material.

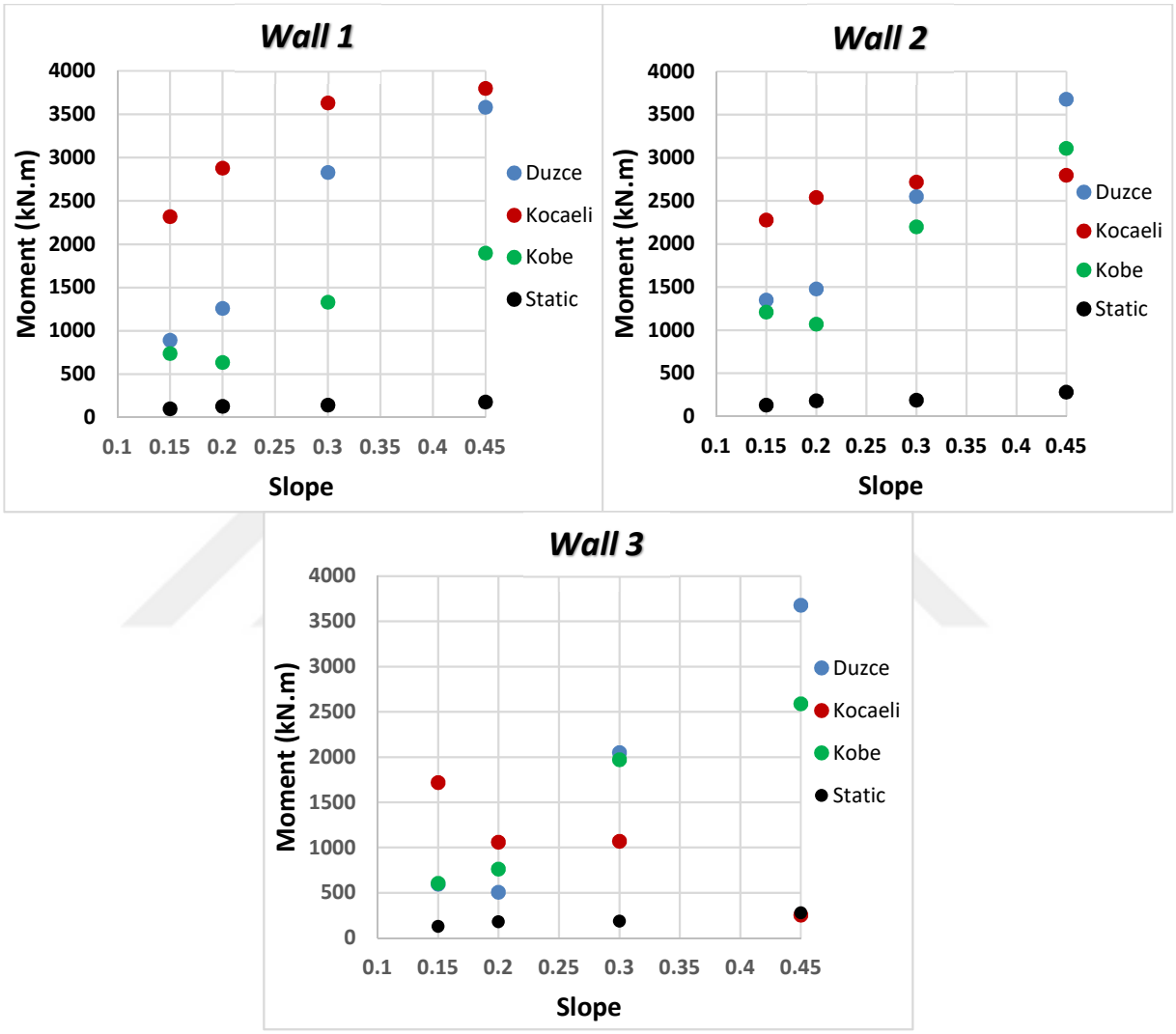


Figure 4.4. Moment behavior with regard to the slope variation (**Cohesion=125 kPa**)

There is a raising trend of the moment values respectively with the slopes under Kocaeli, Duzce and Kobe Earthquakes in the Wall 1. The Kobe earthquake had a lower impact in terms of moment compared to other earthquakes on the walls at 0.15 and 0.2 slopes. But in Wall 3, the moment which was produced by Kobe is the biggest with regard to the others at 0.45 slope.

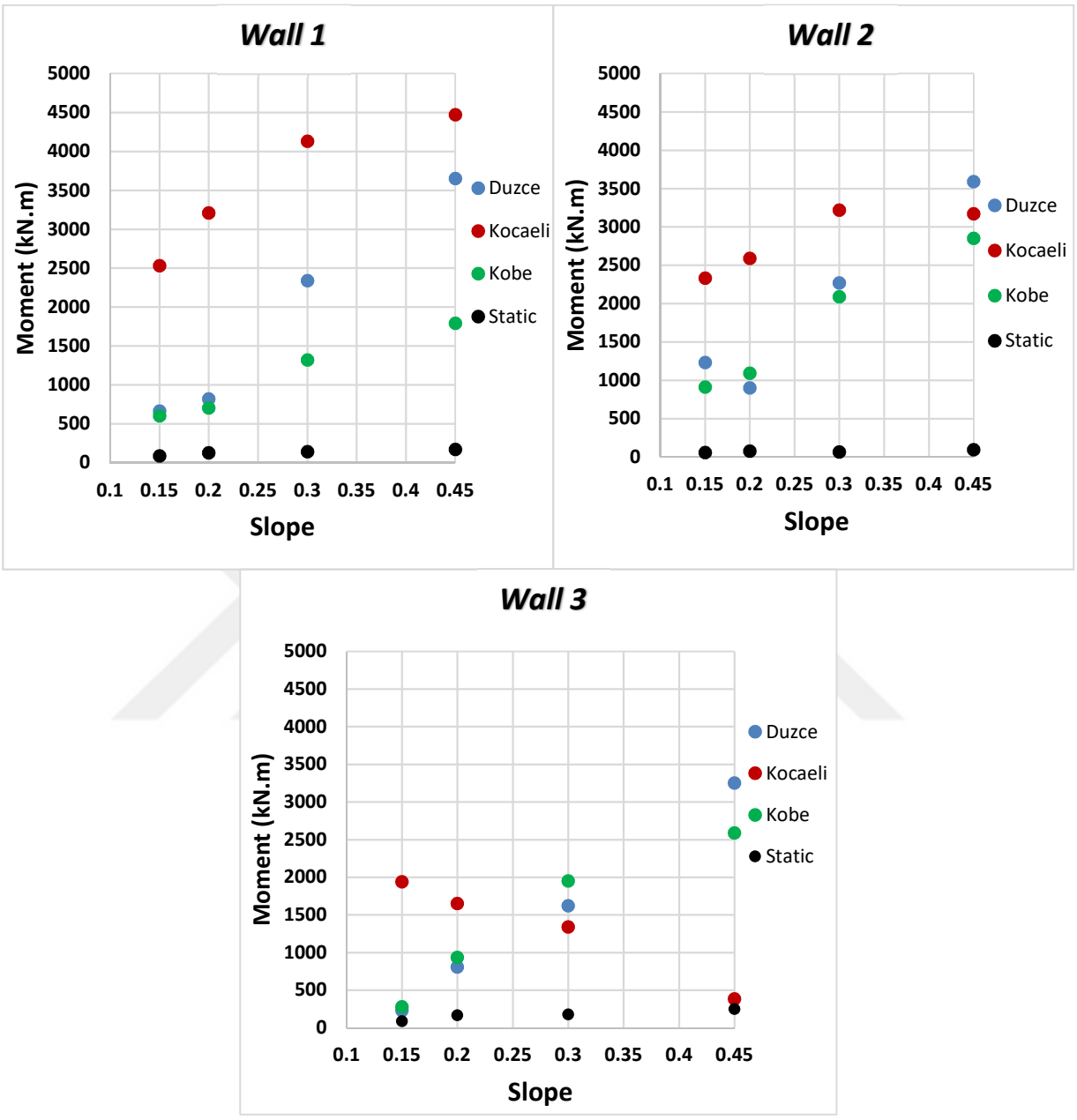


Figure 4.5. Moment behavior with regard to the slope variation (**Cohesion=150 kPa**)

The final comparison of the behavior will be at the undrained shear strength of 150 kPa and the behavior is presented in Figure 4.5. The maximum moment between the cohesion cases has been occurred when the cohesion was 150 kPa, in the first wall at slope 0.45 (4470 kN.m). Correspondingly, it can be seen that there is a reduction of the moments in Wall 2 and 3 in all the slopes compared with Wall 1.

4.1.2 Shear Force Behavior

The results of the shear force analysis are shown in following figures (from 4.6 to 4.9) for all three walls with the variation of cohesion in Static state and dynamic state for the Duzce, Kocaeli and Kobe earthquakes.

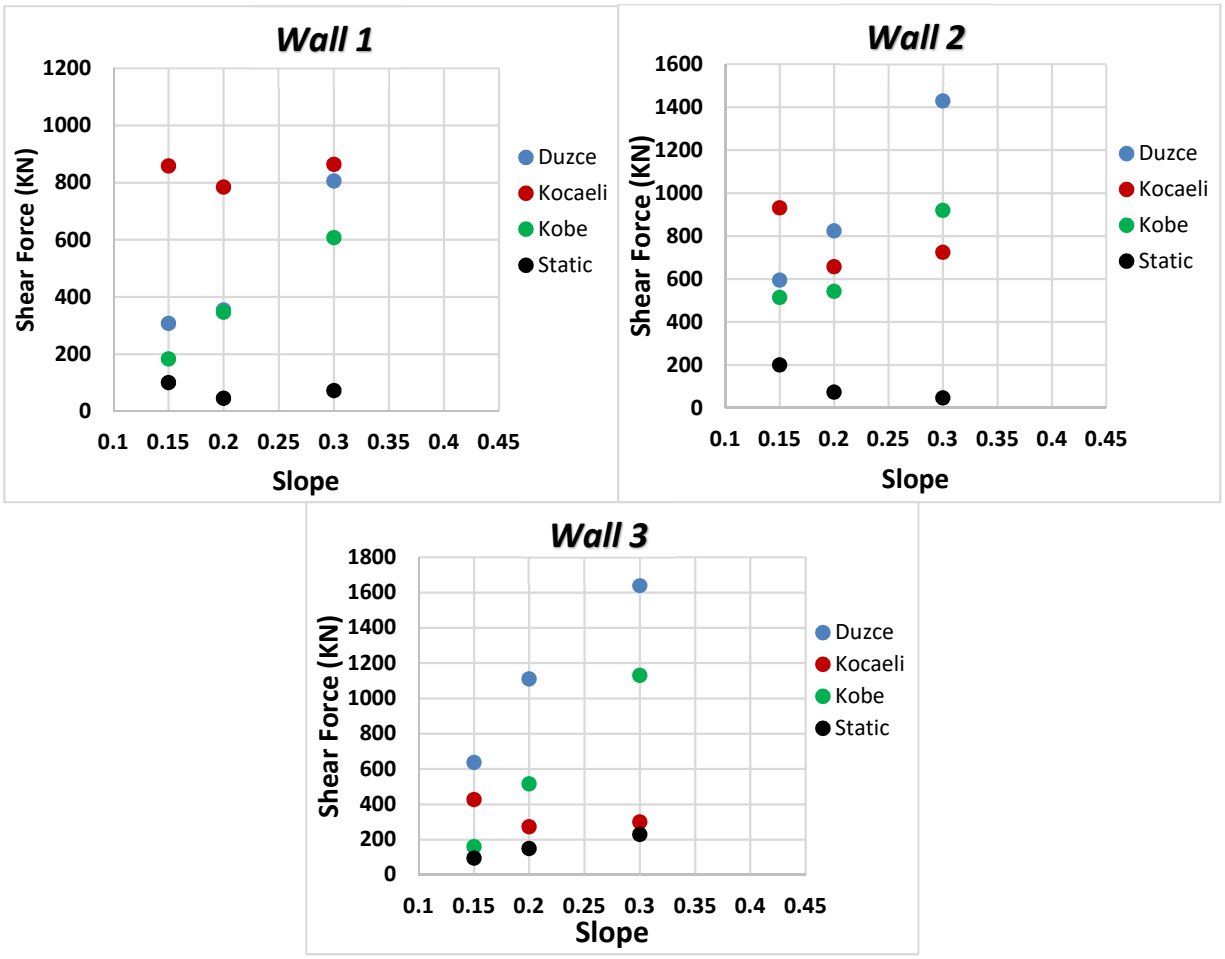


Figure 4.6. Shear force behavior with regard to the slope variation (**Cohesion=75 kPa**)

In case of the cohesion of 75 kPa, the maximum shear force was occurred at slope 0.3 in the third wall as 1640 KN under Duzce earthquake. In the static state, the Wall 2 observed a reduction of the shear force when the slope raises from 0.15 to 0.3; however, in the Wall 3 there is an increasing tendency of shear force in the static state as the slope increases.

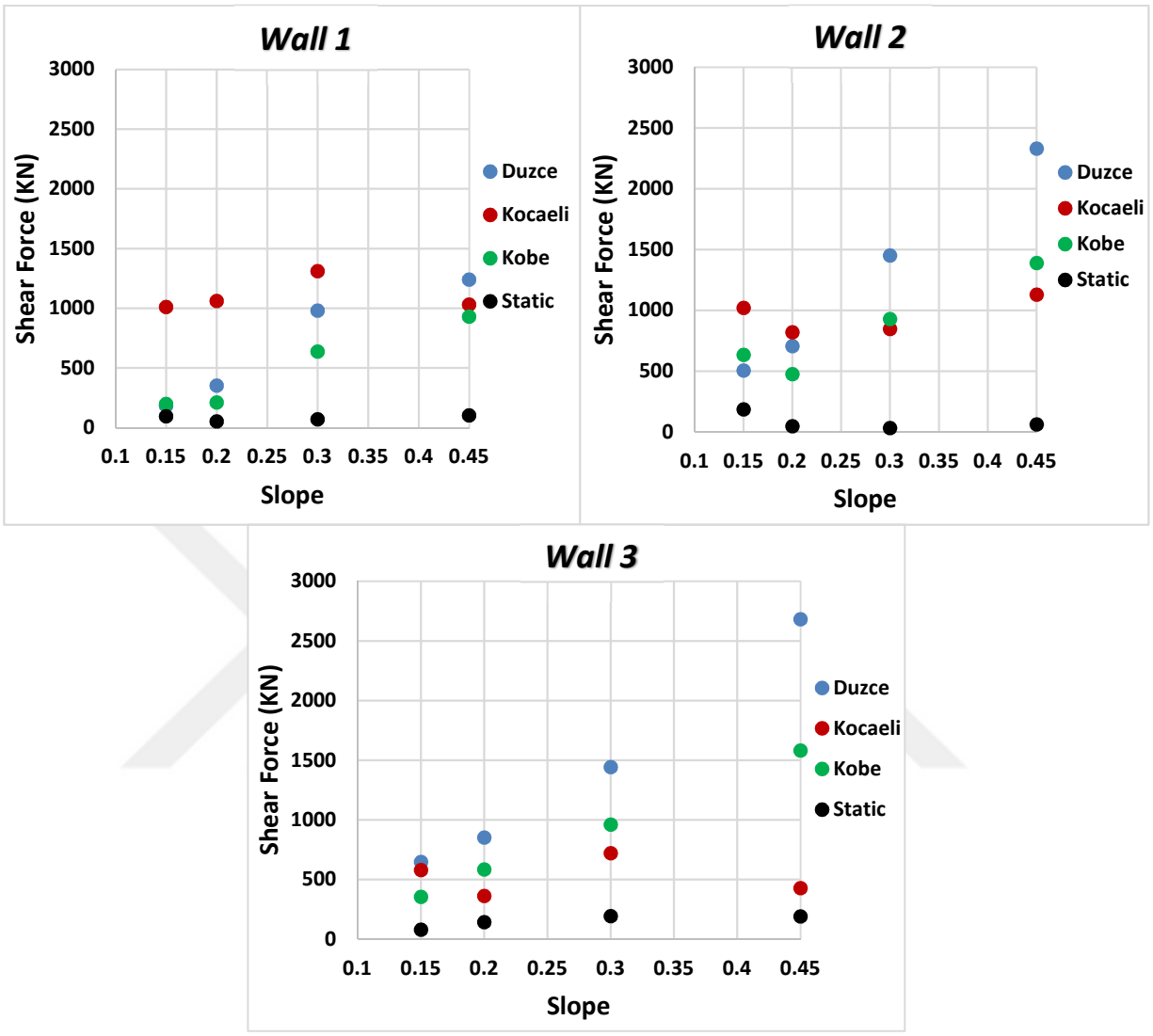


Figure 4.7. Shear force behavior with regard to the slope variation (**Cohesion=100 kPa**)

Figure 4.7 presents the shear force behavior compared to the slope variation at 100 kPa of cohesion. At the slope 0.15 and 0.2, a big difference between the shear force values were composed under Kocaeli and Duzce Earthquakes in the Wall 1 and the values were recorded 1010-1060 kN and 182-350 kN, respectively.

Slope of 0.45 produced the maximum shear force values in the three walls under Duzce Earthquake as 2680 kN. Another point here to mention is that the shear force values increased when the slope ratio raises for the Kobe Earthquake loading, excepting the Wall 2 with a slope of 0.2.

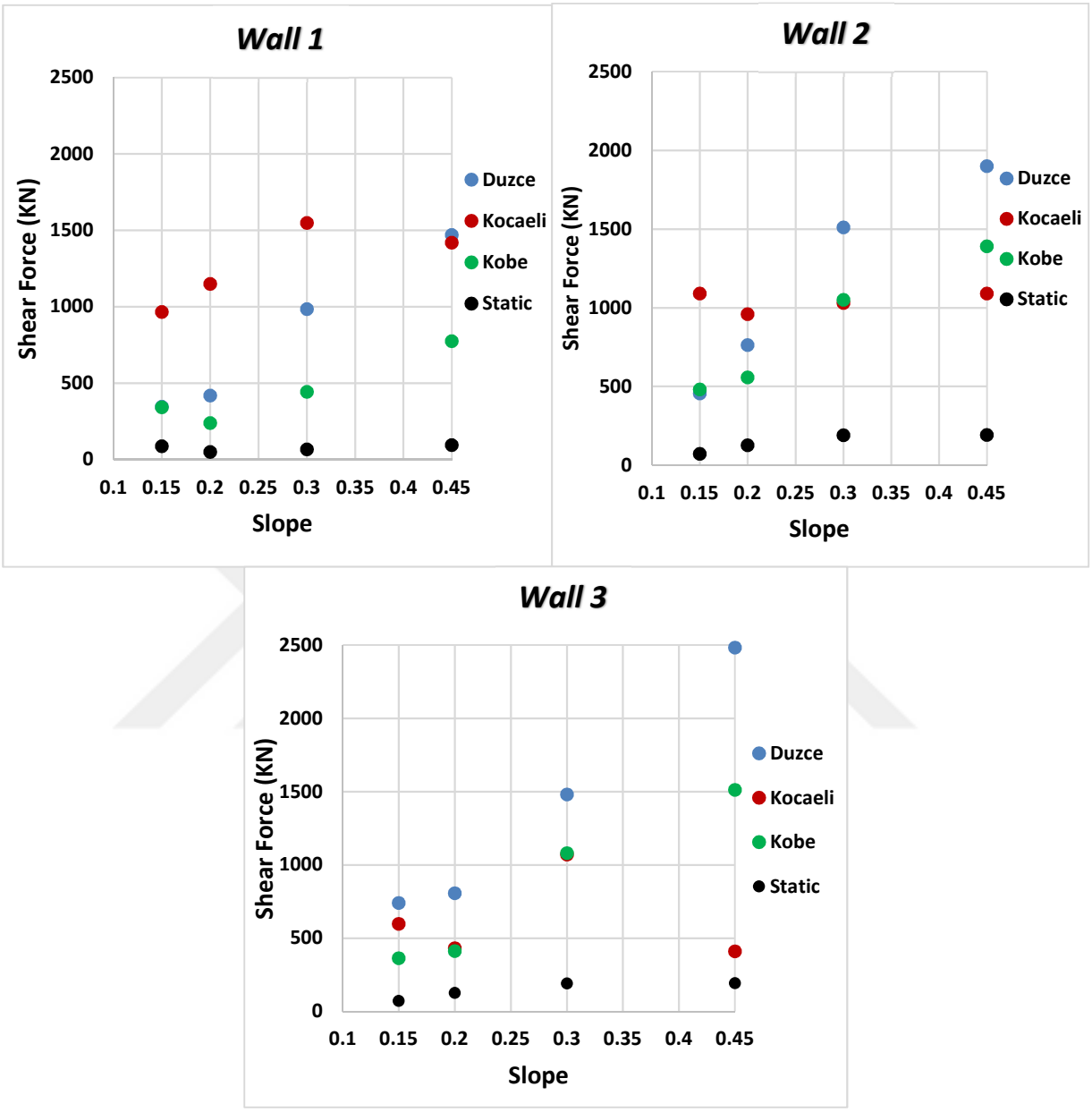


Figure 4.8. Shear force behavior with regard to the slope variation (**Cohesion=125 kPa**)

In the three walls there is an escalation occurred under Duzce and Kobe earthquakes when the slope increased from 0.2 to 0.45 slopes as seen in Figure 4.8. Moreover, Duzce earthquake impacted more on the Wall 3 than the others at the slope of 0.45 where the biggest shear force value was occurred as 1530 kN.

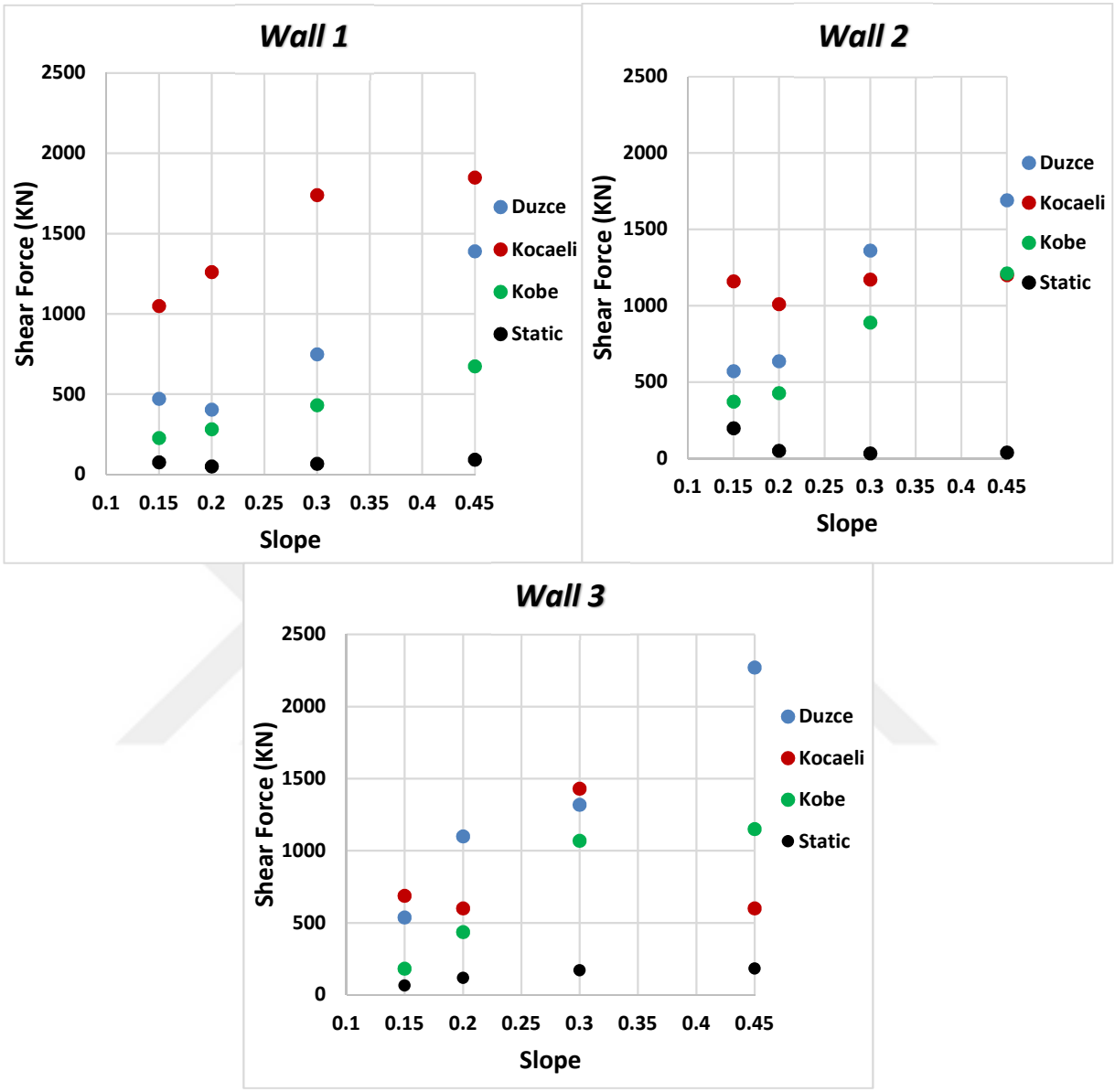


Figure 4.9. Shear force behavior with regard to the slope variation (**Cohesion=150 kPa**)

Moving to the final case of 150 kPa of shear strength, the shear force values were formed the highest under Duzce earthquake on the Wall 2 and 3 at the slope of 0.45. It can also be seen that the values of shear forces were composed the lowest under Kobe Earthquake shaking in all the walls and all the slopes. In addition, the minimum value of shear forces between the cohesion cases was observed in the third wall at slope 0.15 by the excitation of Kobe Earthquake as 184 KN.

4.1.3 Axial Force Behavior

Axial forces were noted as a result of the analysis for the variation of slope at different shear strengths under static and dynamic loads and they are presented below.

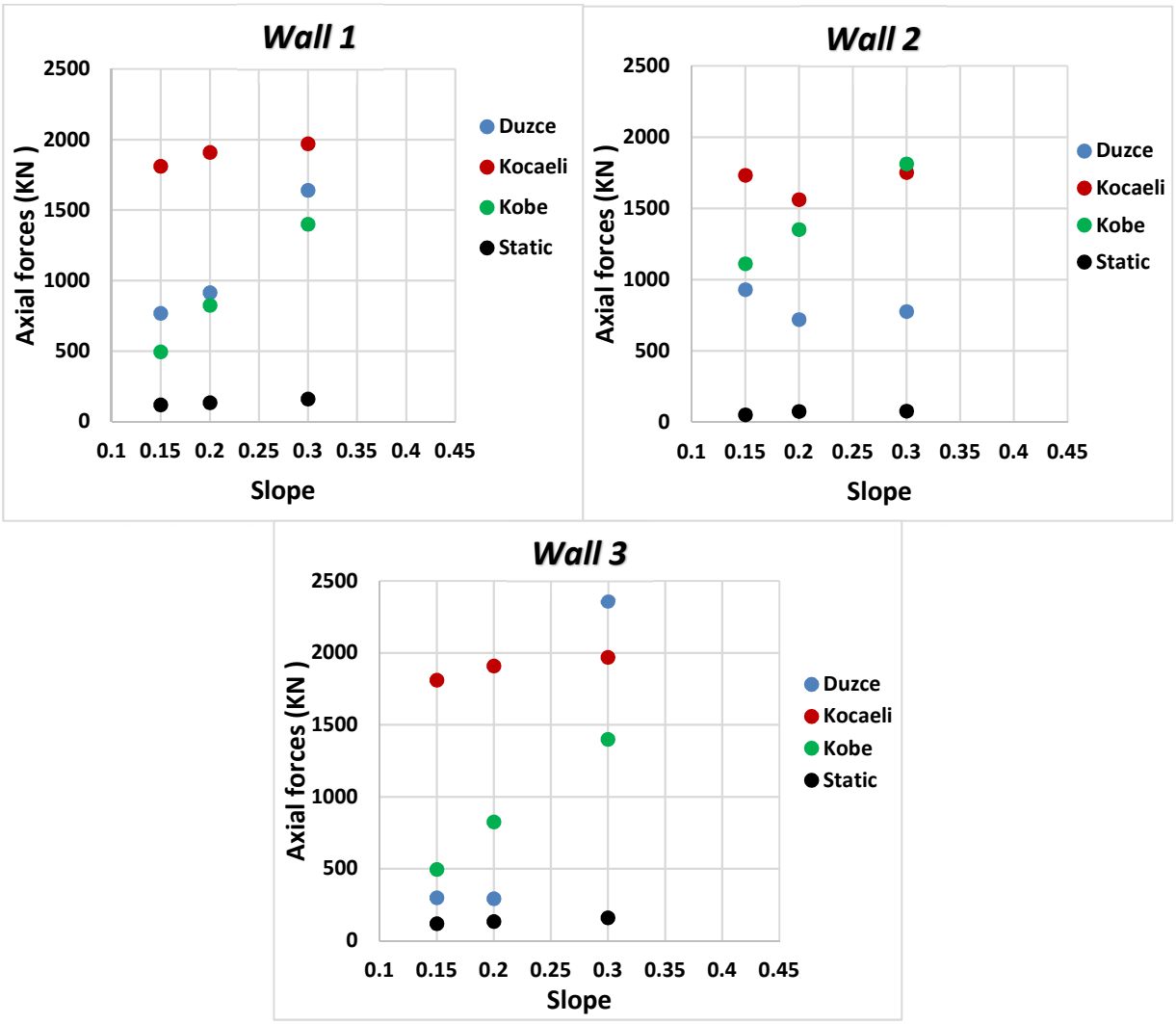


Figure 4.10. Axial force behavior with regard to the slope variation (**Cohesion=75 kPa**)

In static and dynamic cases as seen Figure 4.10, it can be observed that the axial force values were in an increasing tendency with the rising of slope in the Wall 1 and 3 recording the highest value of 160 kN in static case and as 2360 kN under Duzce Earthquake in the Wall 3 at the slope of 0.3.

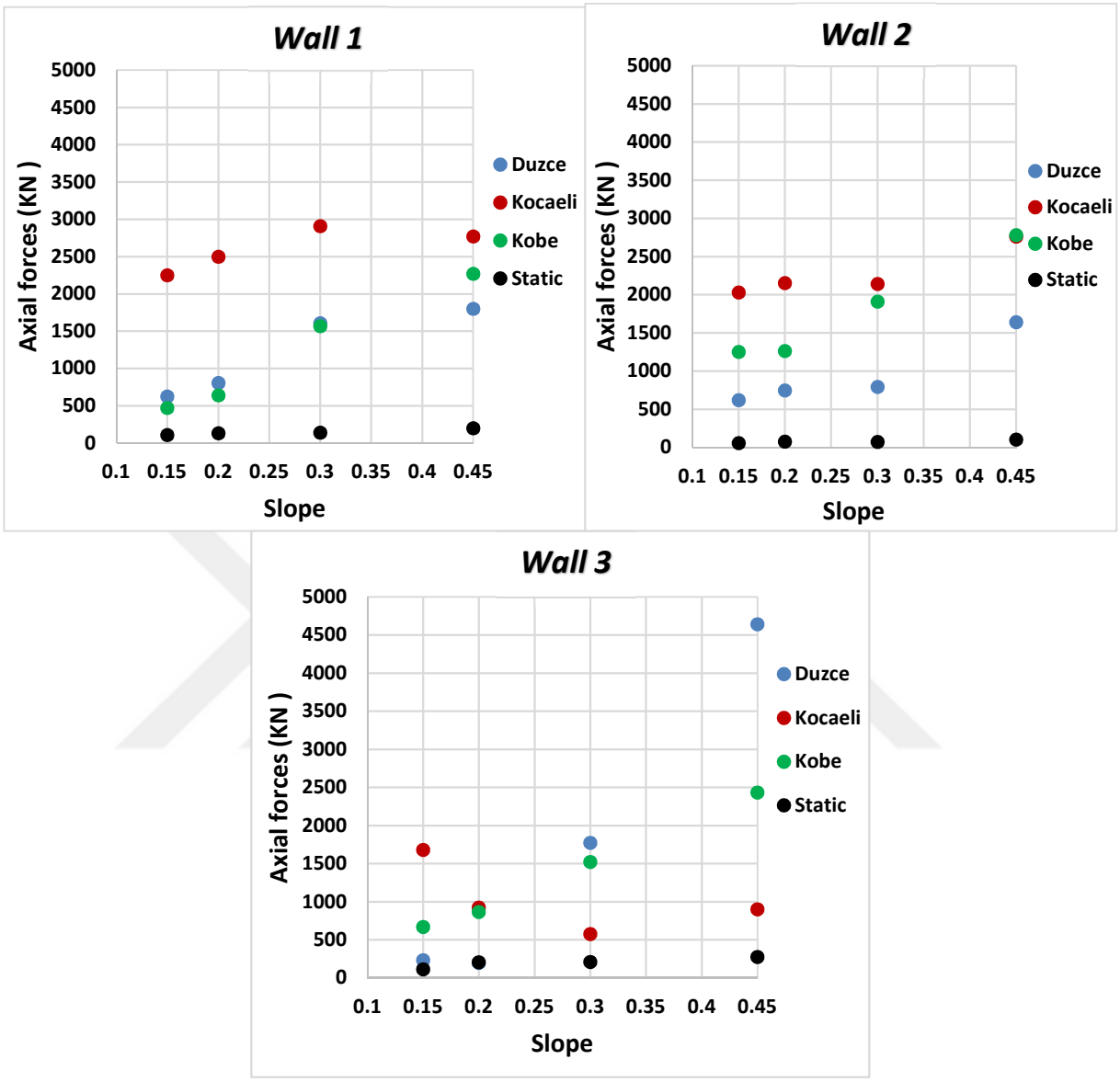


Figure 4.11. Axial force behavior with regard to the slope variation (**Cohesion=100 kPa**)

For the case of cohesion 100 kPa as shown in Figure 4.11, the biggest axial force value occurred was under Duzce Earthquake as 4460 kN in the wall 3. Wall 1 was affected more by Kocaeli Earthquake than the other motions in all the slopes.

The axial force values composed under Kobe and Duzce earthquakes were in an escalation with the rising of the slope ratio 0.15 to 0.45 for all the walls.

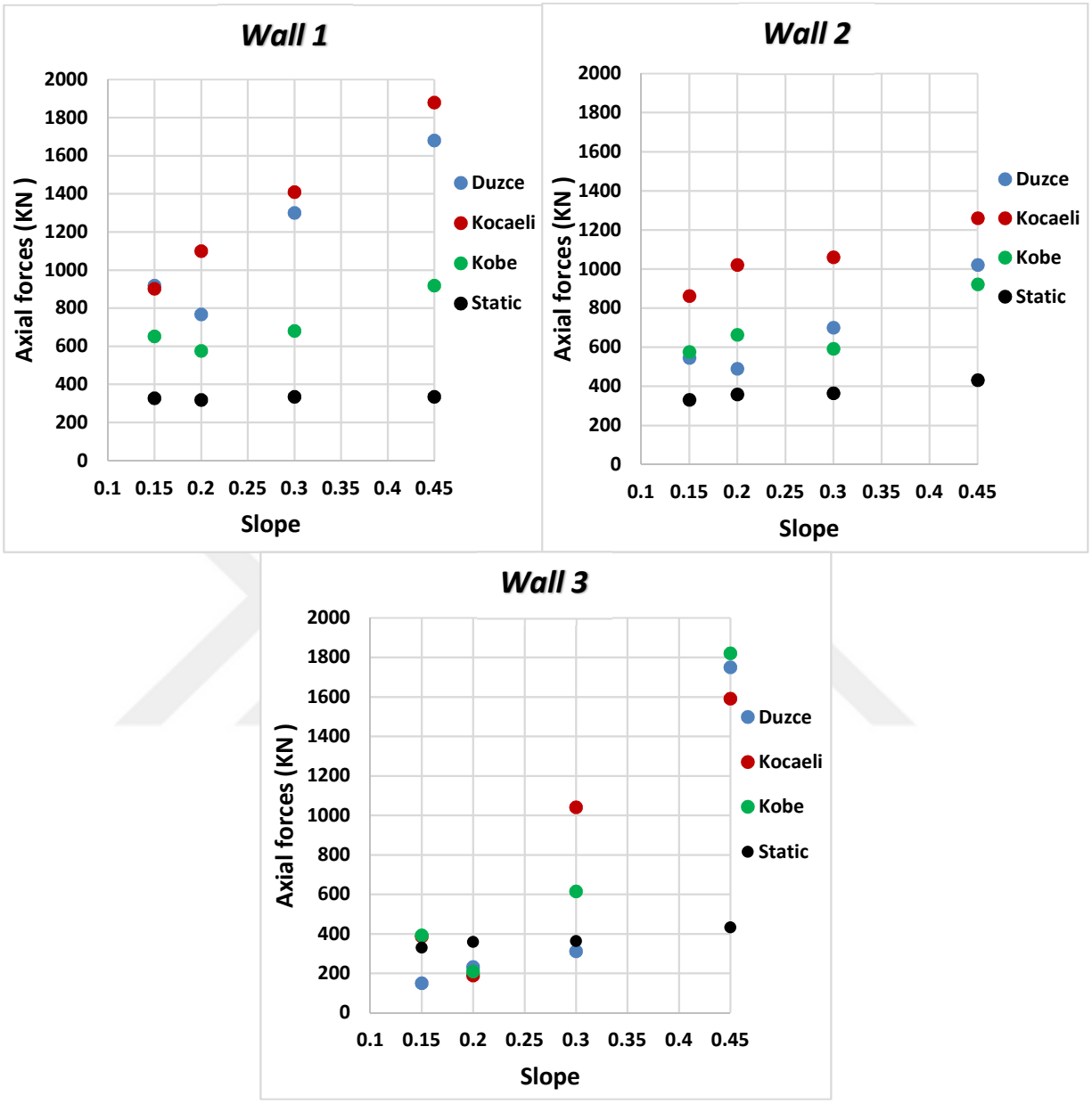


Figure 4.12. Axial force behavior with regard to the slope variation (**Cohesion=125 kPa**)

When the cohesion was increased to 125 Kpa, it was observed that the values of axial force in static state at slopes 0.15,0.2 and 0.3 was bigger than the axial forces which formed under Duzce at 0.15,0.3 and Duzce, Kocaeli and Kobe at 0.2 in the Wall 3. That is not surprising since earthquakes have big influence on shear forces.

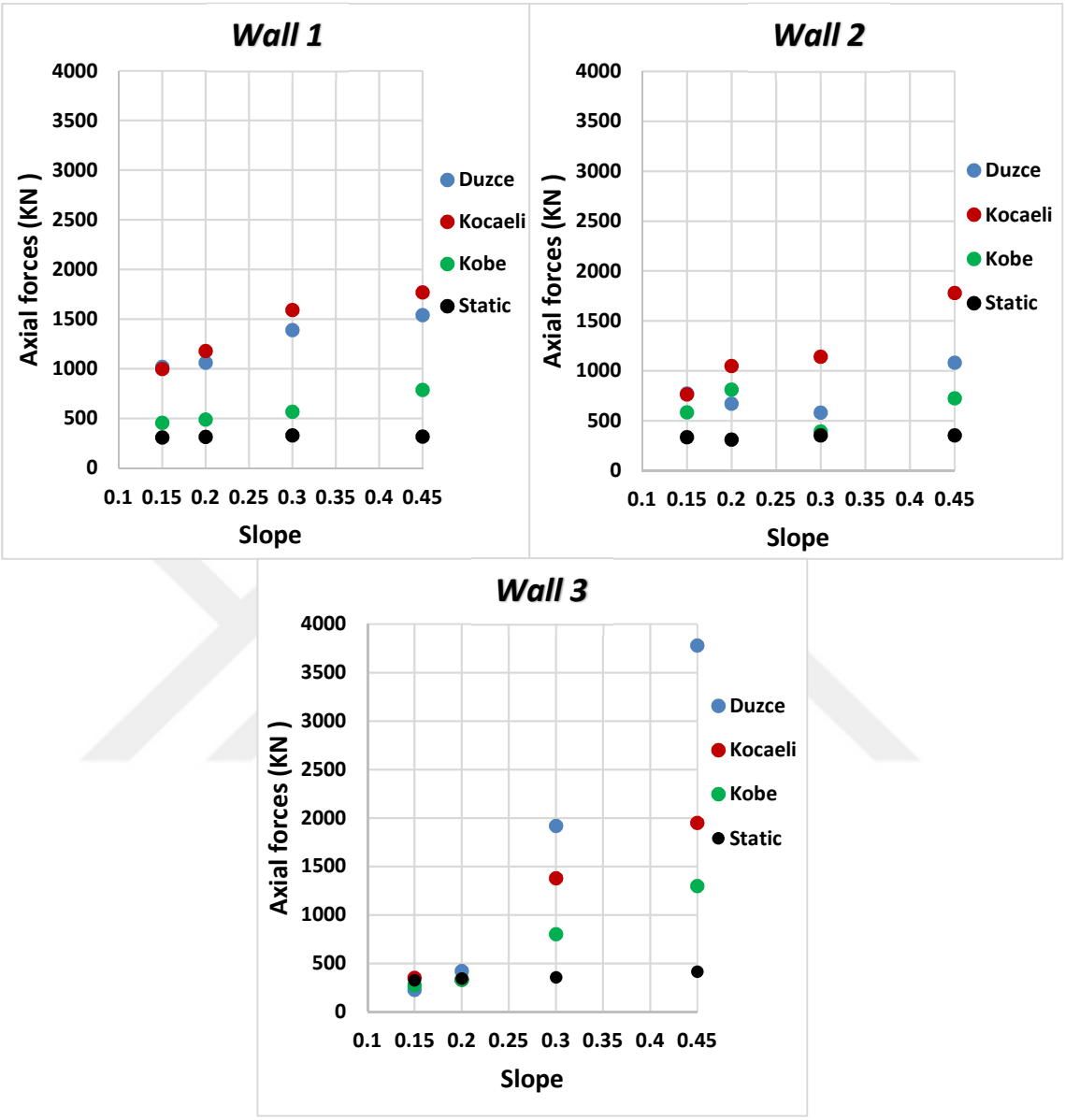


Figure 4.13. Axial force behavior with regard to the slope variation (**Cohesion=150 kPa**)

Figure 4.13 proves that the shear forces composed under static state in the Wall 3 were bigger than the values which formed under dynamic cases at 0.15, and those which formed under Kocaeli and Kobe Earthquakes at the slope of 0.2. Moreover, the rate of the increasing in term of axial force, was very big where the values were 227 kN at slope of 0.15 and 3780 kN at slope of 0.45. The variation of the dynamic loads is very crucial to estimate this kind of behavior.

4.1.4 Total Displacement Behavior

The results of the displacements will be discussed in this section. Since there is not much vertical displacement expected from the analysis, only total displacement behavior is considered for the displacement behavior. One more point is that since the total displacements are about zero for the static case dynamic case is studied solely and they are shown in Figure 4.14 to Figure 4.17.

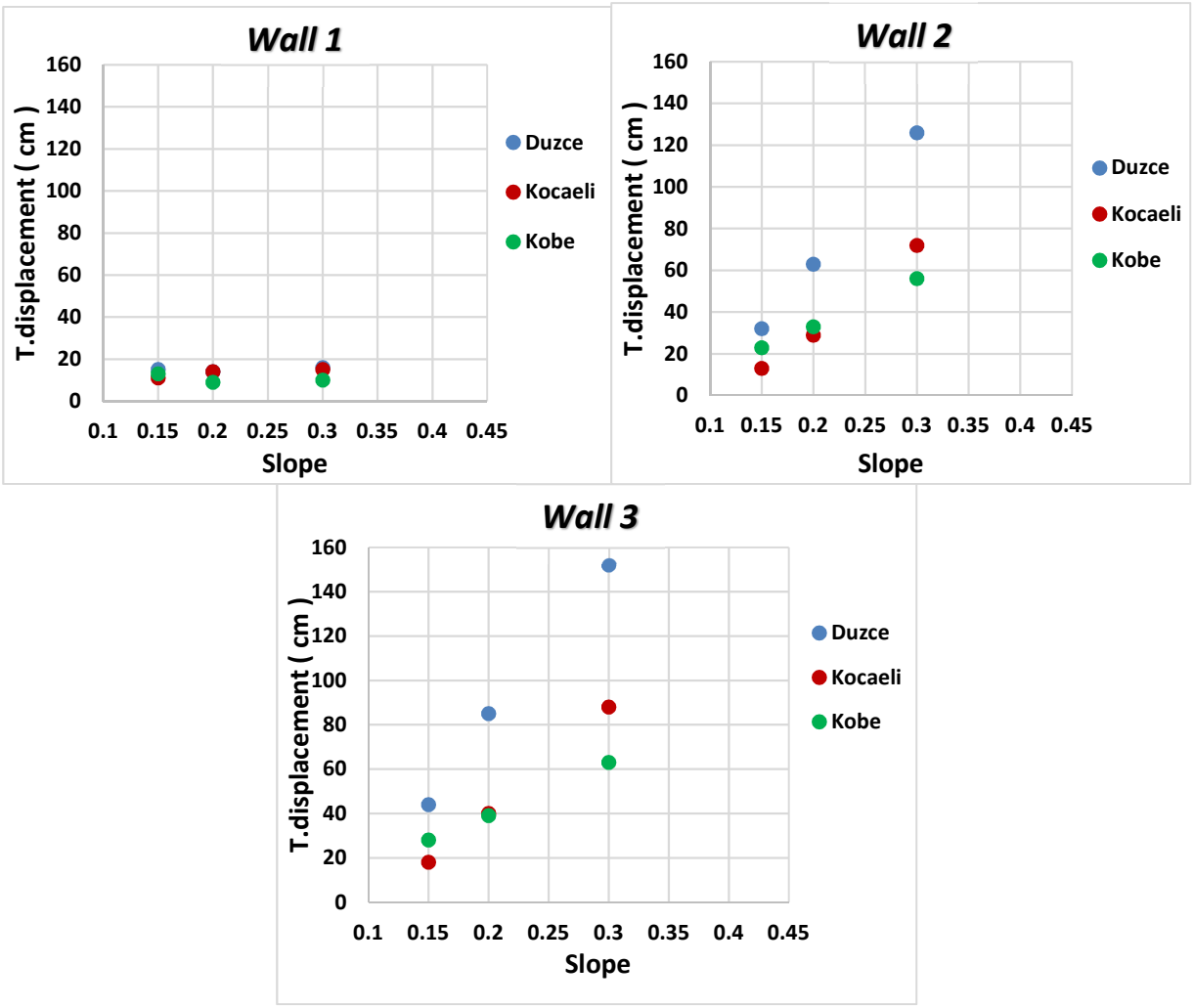


Figure 4.14. Total displacement behavior with regard to the slope variation (**Cohesion=75 kPa**)

Displacements which formed under Duzce Earthquake in the Wall 2 and 3 at all the slopes were bigger than the other earthquakes whereas the Wall 3 was affected in term of displacement more than the other walls having the highest value of displacement was 152 cm

as seen in Figure 4.14. In addition, it can be observed that the displacements composed under Kocaeli, Duzce and Kobe Earthquakes in the Wall 2 and 3 have an increasing trend when the slope ratio escalates.

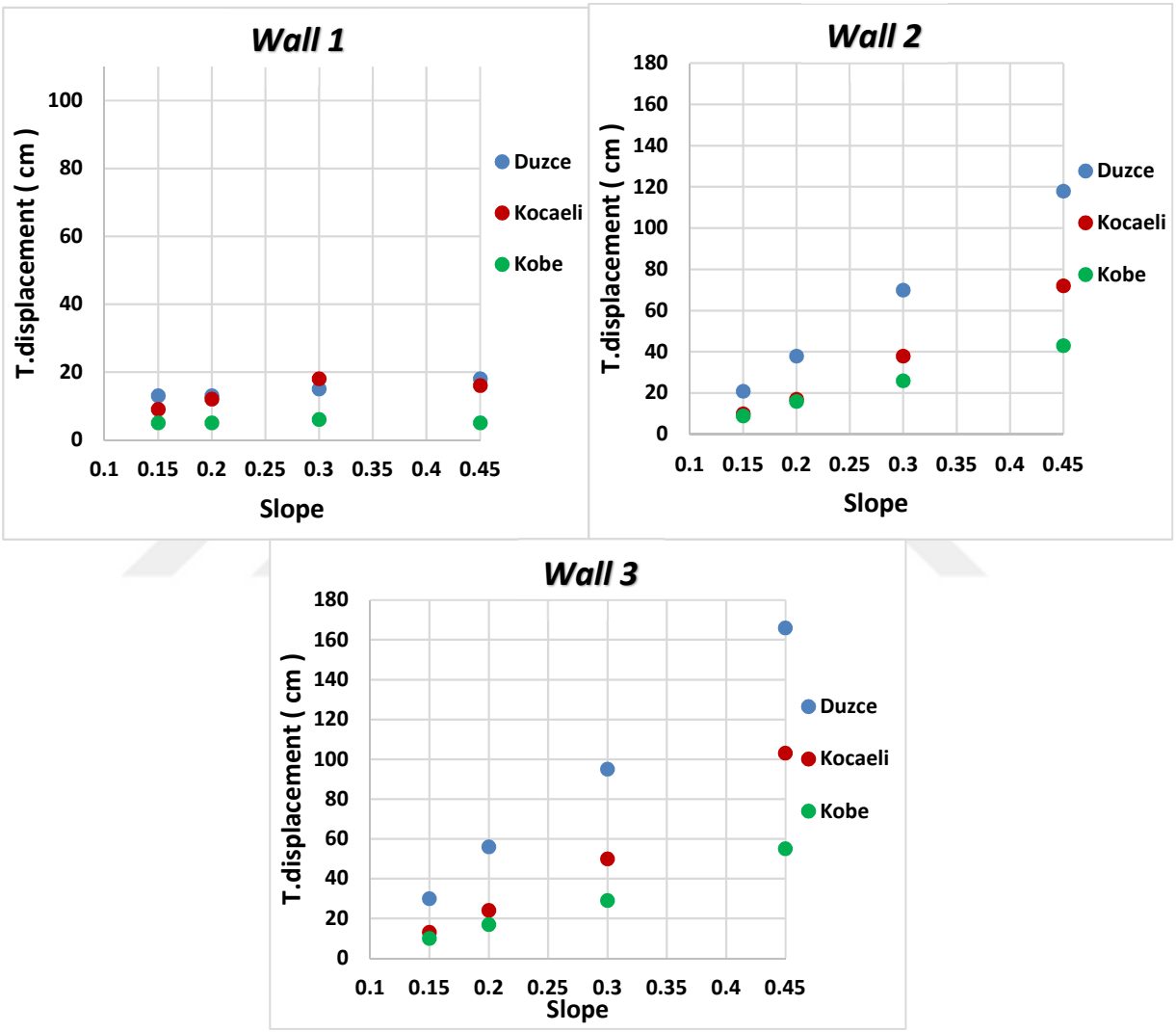


Figure 4.15. Total displacement behavior with regard to the slope variation (**Cohesion=100 kPa**)

In case when the cohesion increased from 75 to 100 kPa, all the walls were affected more by Kocaeli and Duzce excitations than Kobe Earthquake at all the slopes ratio as it is shown in Figure 4.15. The Wall 1 is not impacted too much in term of displacement where the biggest value was 18 cm whereas the displacement occurred by Duzce Earthquake was 118 cm in the Wall 2 and 166 cm in the Wall 3 at a slope of 0.45.

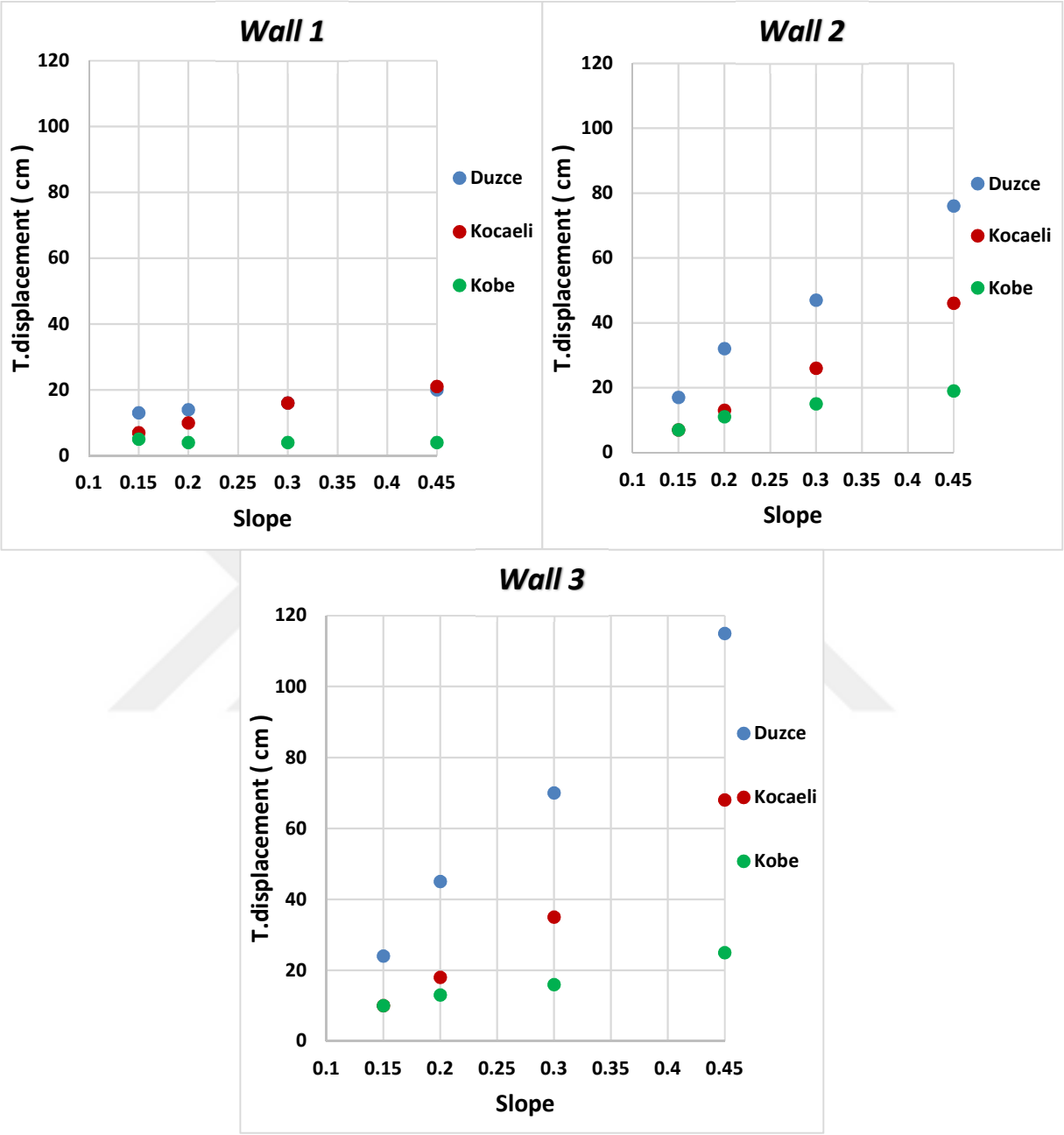


Figure 4.16. Total displacement behavior with regard to the slope variation (**Cohesion=125 kPa**)

At all the slopes, three walls were impacted by Duzce Earthquake more than the other earthquakes, where the biggest displacement of 115 cm has occurred in the third wall under Duzce Earthquake at the slope of 0.45 as presented in Figure 4.16. The displacements formed under these 3 earthquakes were in escalating path with the increasing slope ratio in the Wall 2 and Wall 3.

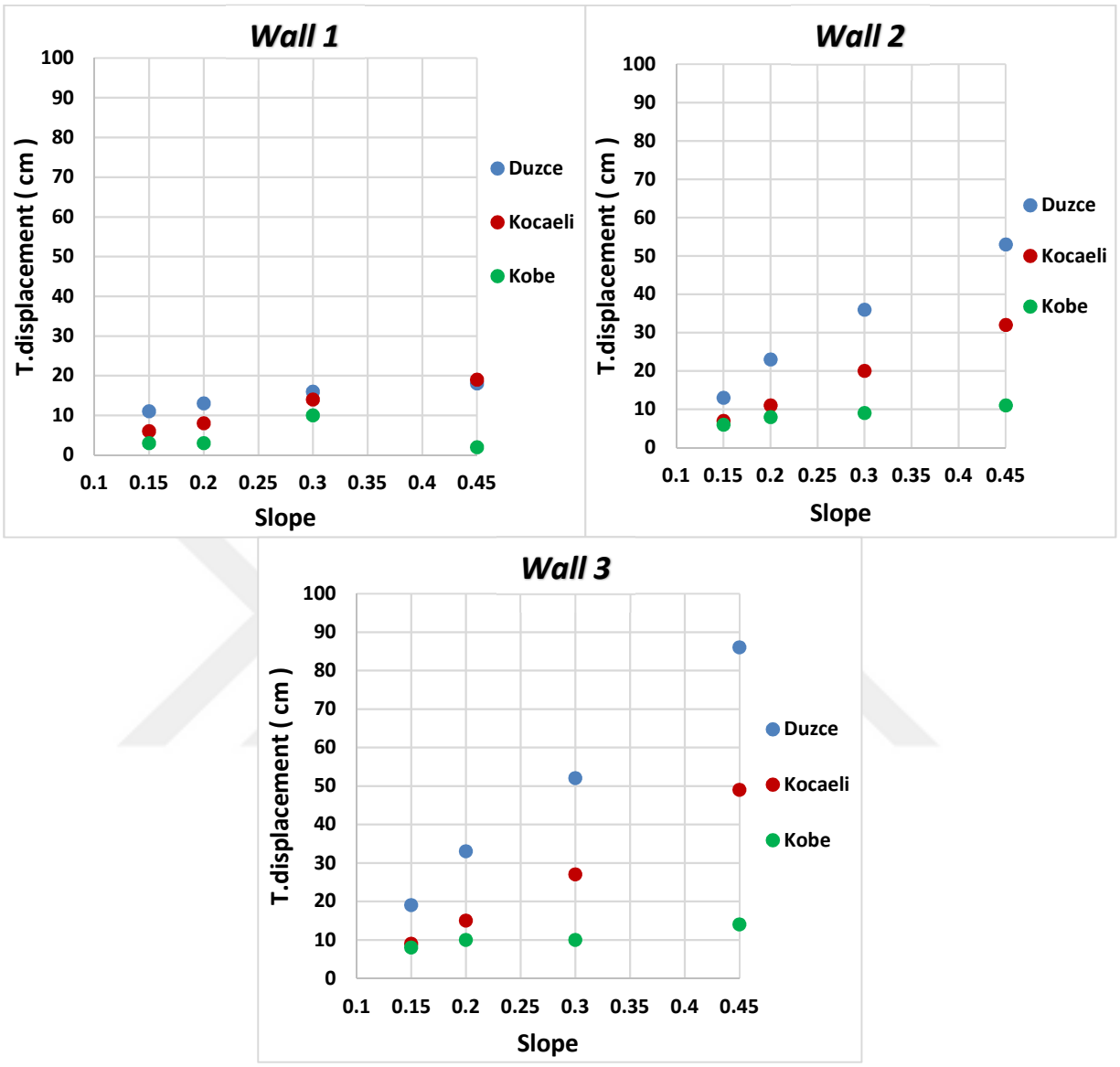


Figure 4.17. Total displacement behavior with regard to the slope variation (**Cohesion=150 kPa**)

Figure 4.17 shows a real reduction of the displacements happened in the Wall 1 under Kobe Earthquake where the values decreased to be 3 cm at slopes 0.15 and 0.2, and 2 cm at slope 0.45.

Additionally, the increased rate of the displacement between wall 1, 2 and 3 is more than the other earthquakes, where it was recorded as 18 cm in the wall 1 and 53 cm in the Wall 2 and 86 cm in the Wall 3 under Duzce Earthquake.

4.2 Effect of the Cohesion on the Lateral Forces and Moments

This section is about analyzing the outcomes of the moments, shear forces, axial forces and total displacement under Duzce, Kocaeli and Kobe earthquakes in static and dynamic states according to cohesions variation (75, 100, 125 and 150 kPa) with slope ratios of 0.15, 0.2, 0.3 and 0.45, respectively.

4.2.1 Lateral Moment Behavior

The results of moment of the Wall 1, 2, and 3 in static state and dynamic loading of Duzce, Kocaeli, Kobe Earthquakes are presented from Figure 4.18 to Figure 4.21 in terms of the cohesion variation with a constant slope ratio.

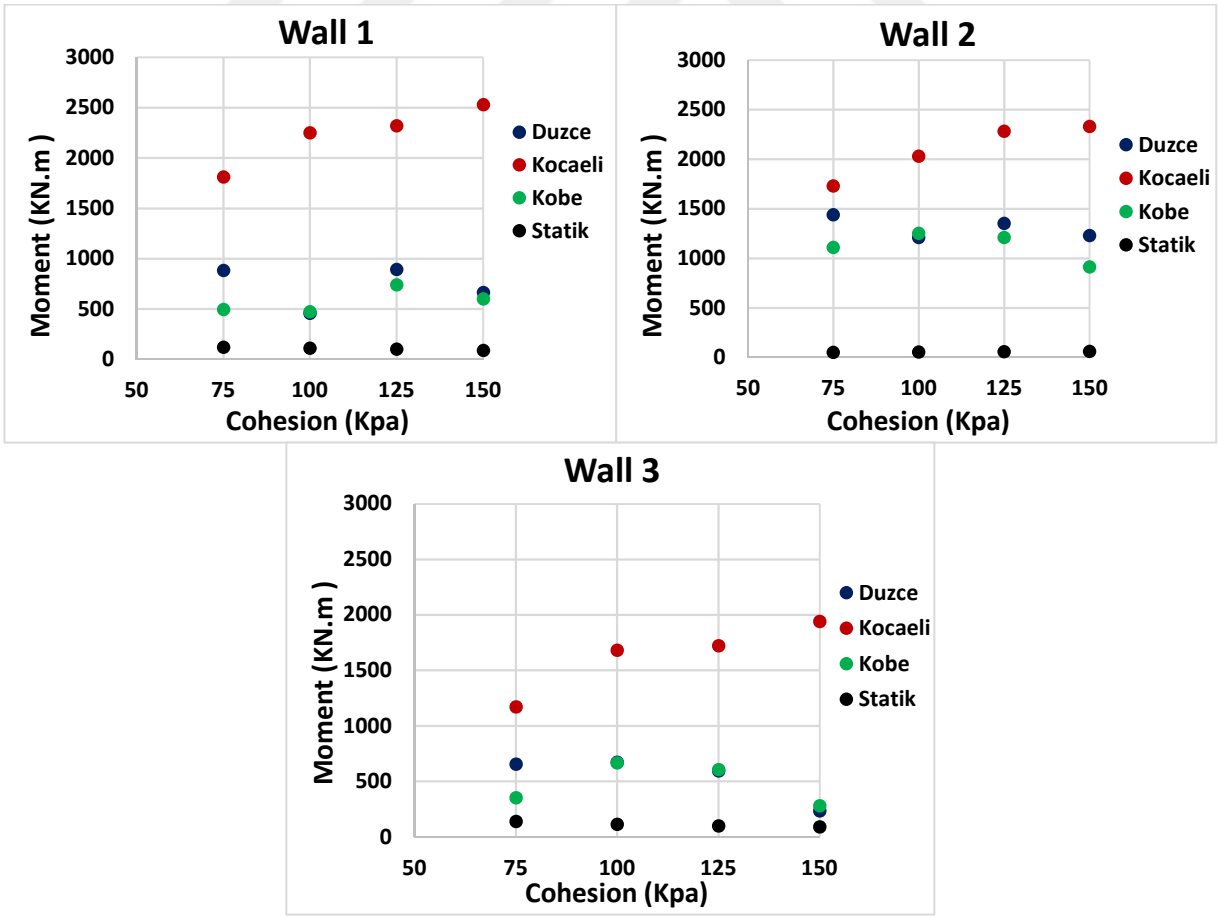


Figure 4.18. Moment behavior with regard to the cohesion variation (**Slope 0.15**)

It can be seen form the Figure 4.18 that when the undrained strength rises from 75 to 150 kPa, an increase of moment occurred in all the walls under Kocaeli Earthquake loading, where the biggest value recorded as 2530 kN.m on the Wall 1 in case of cohesion of 150 kPa. Values of moment in static state are smaller compared with dynamic state even the biggest moment value was 137 kN.m in the Wall 3.

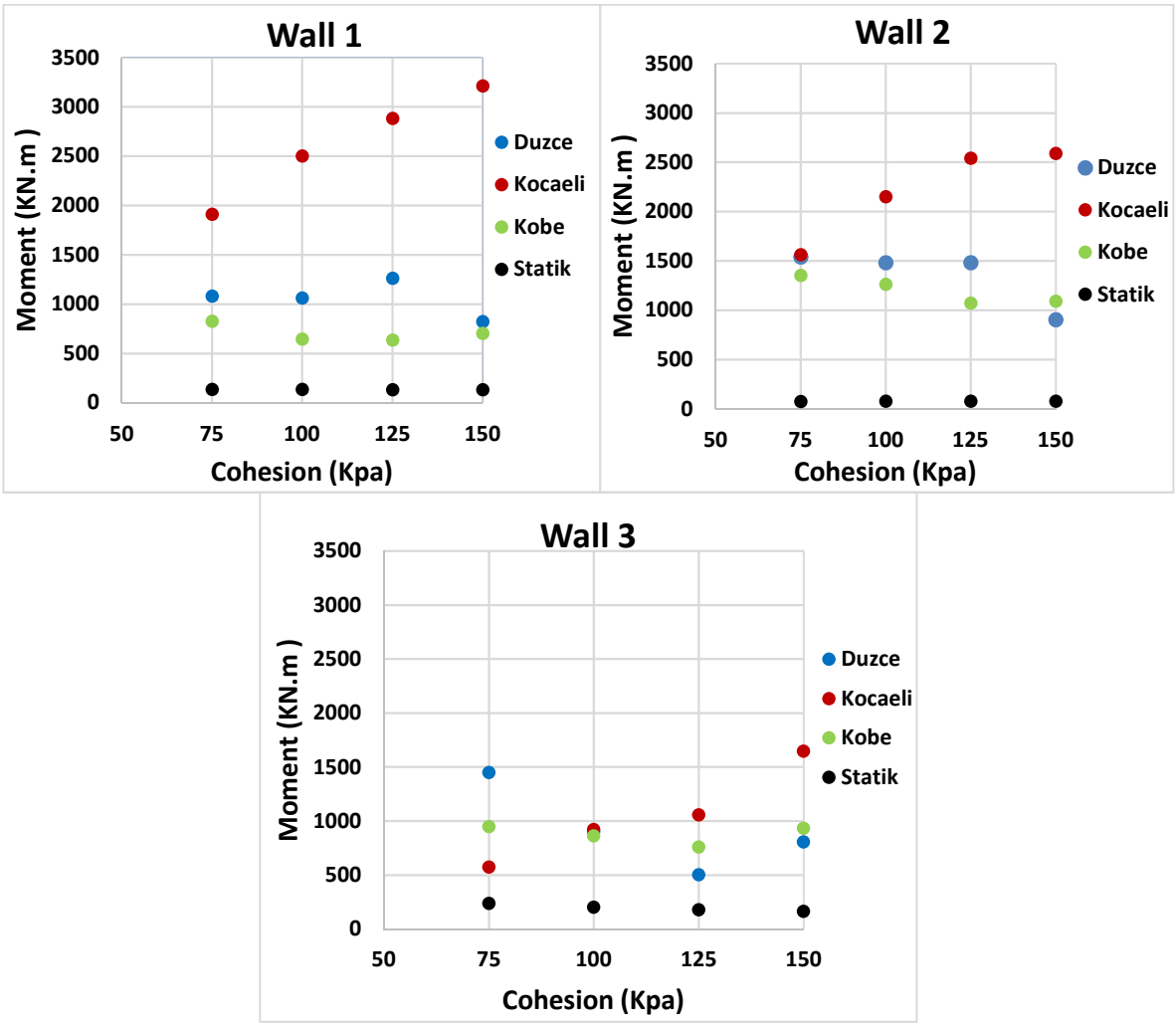


Figure 4.19. Moment behavior with regard to the cohesion variation (**Slope 0.2**)

Figure 4.19 presents that a decreasing tendency of moment under Duzce, Kobe and static state in Wall 2 and 3 as the cohesion increases when the slope ratio raises to 0.2. While the values of moments were on an increasing trend under Kocaeli earthquake in all the walls.

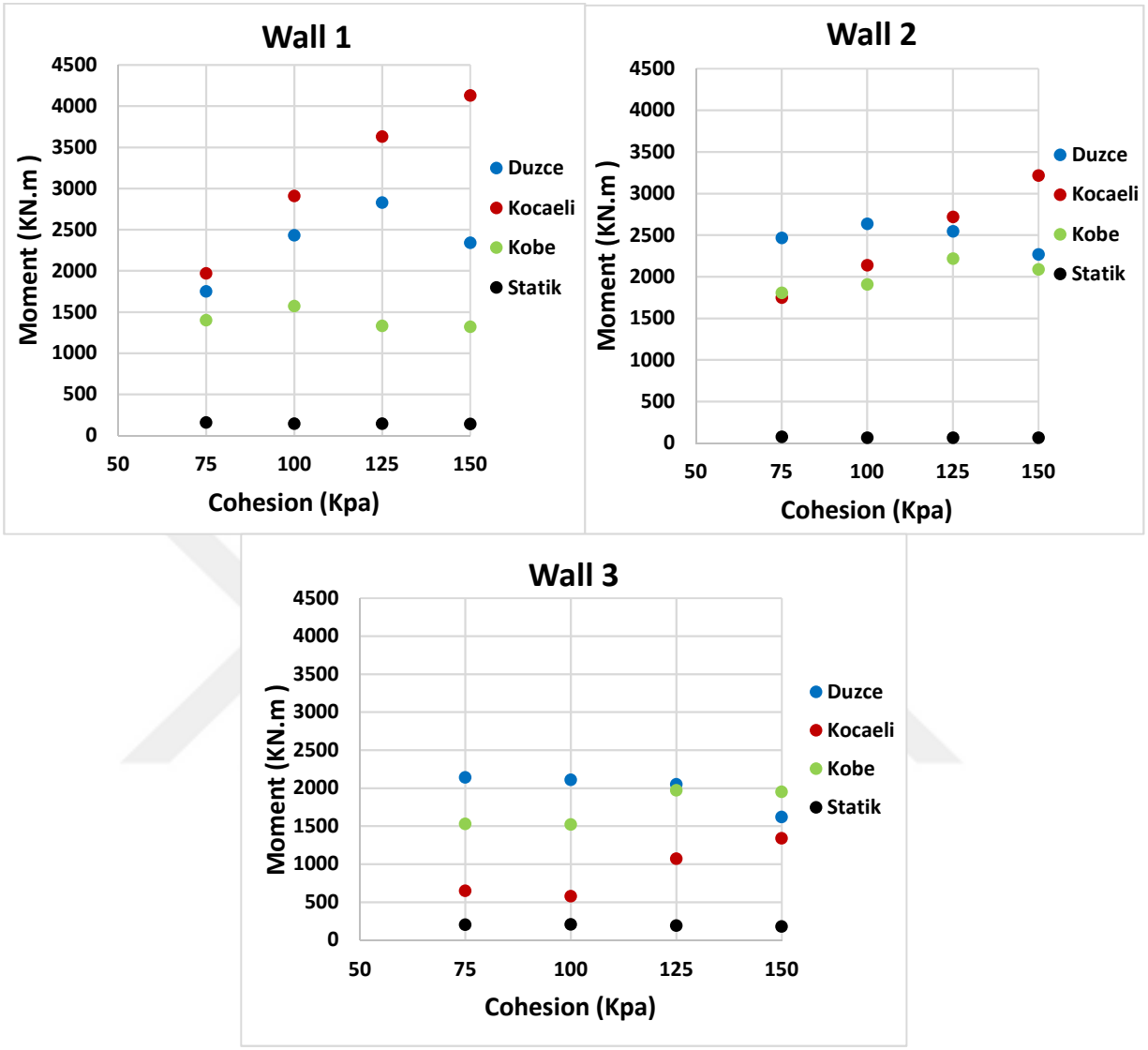


Figure 4.20. Moment behavior with regard to the cohesion variation (**Slope 0.3**)

In case of slope 0.3, it can be seen that the moment which was produced by Kocaeli Earthquake is the biggest as 4130 kN.m with regard to the others as shown in Figure 4.20. In addition, it is observed that the Wall 3 is not affected too much in terms of moments as much as the Wall 1 and 2 are, where there is an increasing of the moments values compared with the other walls, especially to those values which were composed under Kocaeli Earthquake loading.

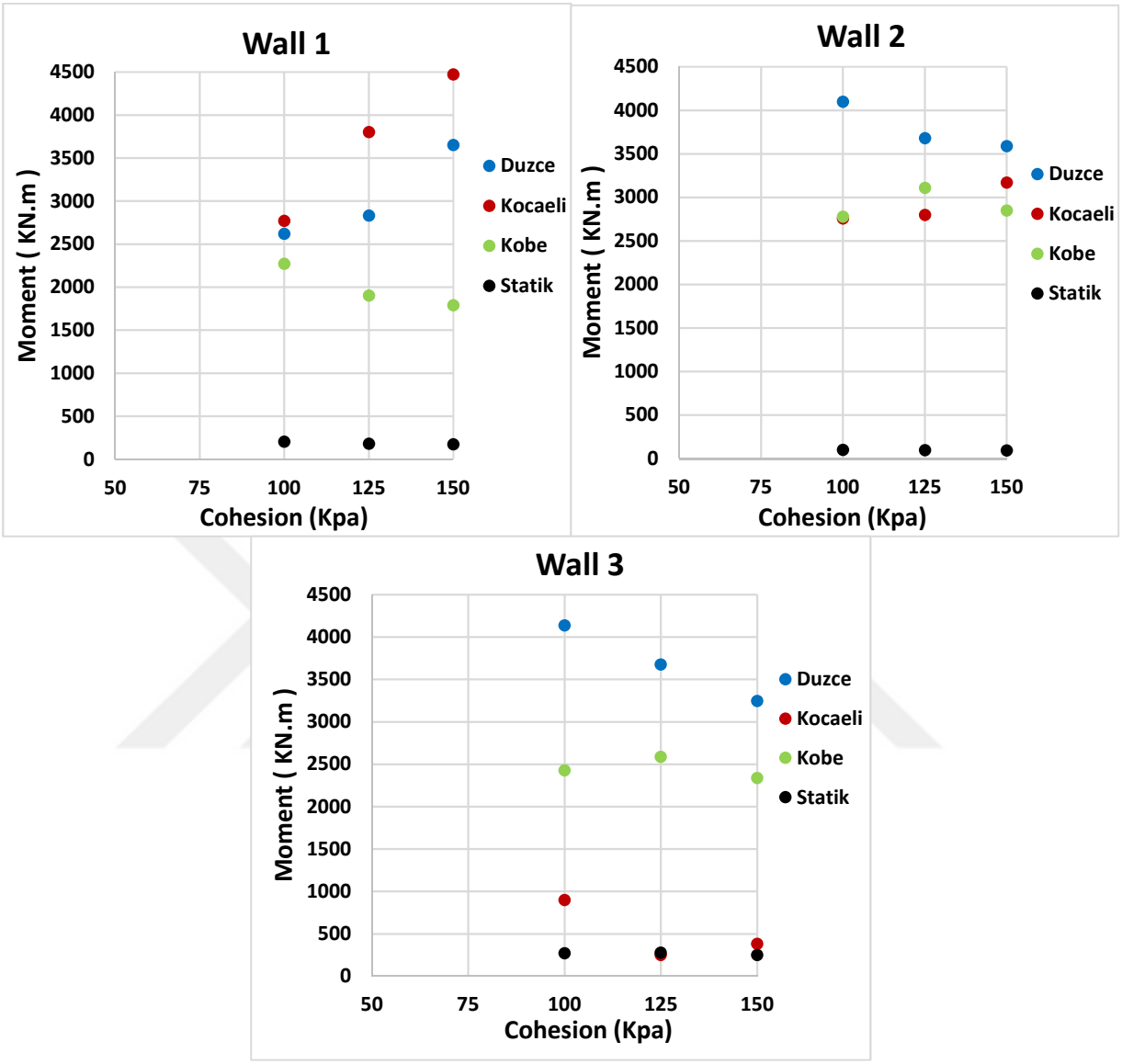


Figure 4.21. Moment behavior with regard to the cohesion variation (**Slope 0.45**)

Moving to the final case of 0.45 slope as in Figure 4.21, the maximum moment between all the slopes ratio occurred by Kocaeli earthquake in the Wall 1 at cohesion 150 Kpa (4470 kN.m). Another point here to mention is that the Wall 3 was not impacted by Kocaeli earthquake as in the Wall 1 and 2, where the moments significantly decreased to 253 kN.m when the cohesion was 125 Kpa. Considering that, this value is smaller than the moment which formed under static state (280 kN.m) as seen in the figure.

4.2.2 Shear Force Behavior

The shear force results has shown and done graphically in the following figures (from 4.22 to 4.25) in all the walls when the slopes are 0.15 -0.2 -0.3 -0.45 kPa in static state and dynamic state.

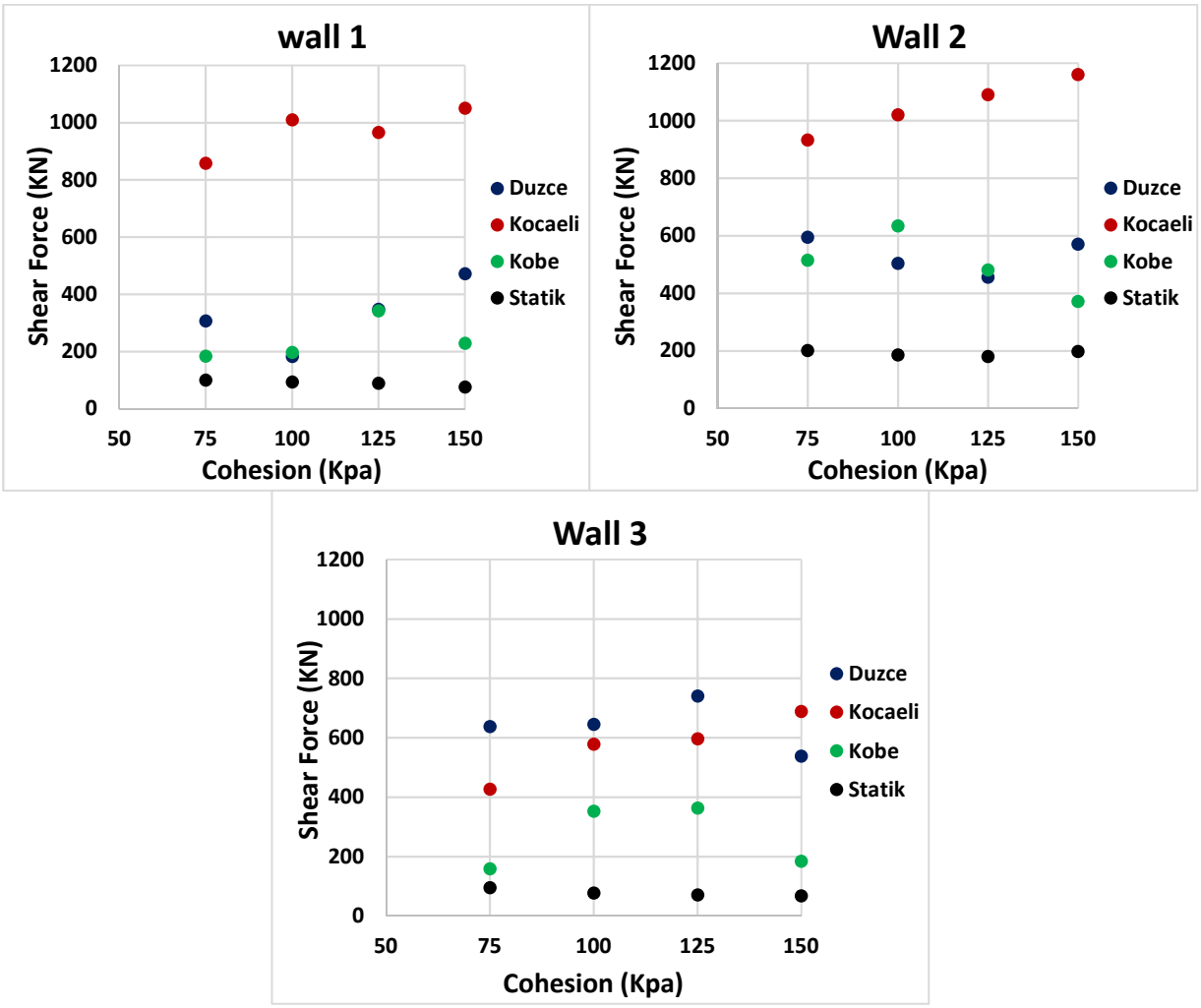


Figure 4.22. Shear force behavior with regard to the cohesion variation (**Slope 0.15**)

Figure 4.22 shows that the highest shear force values were formed respectively under Kocaeli and Duzce at cohesion 150 kPa in all three walls. In static case, a reduction was occurred to the value of shear force when the cohesion increased from 75 to 150 kPa, whereas the biggest value was in the Wall 2 at cohesion 75 Kpa.

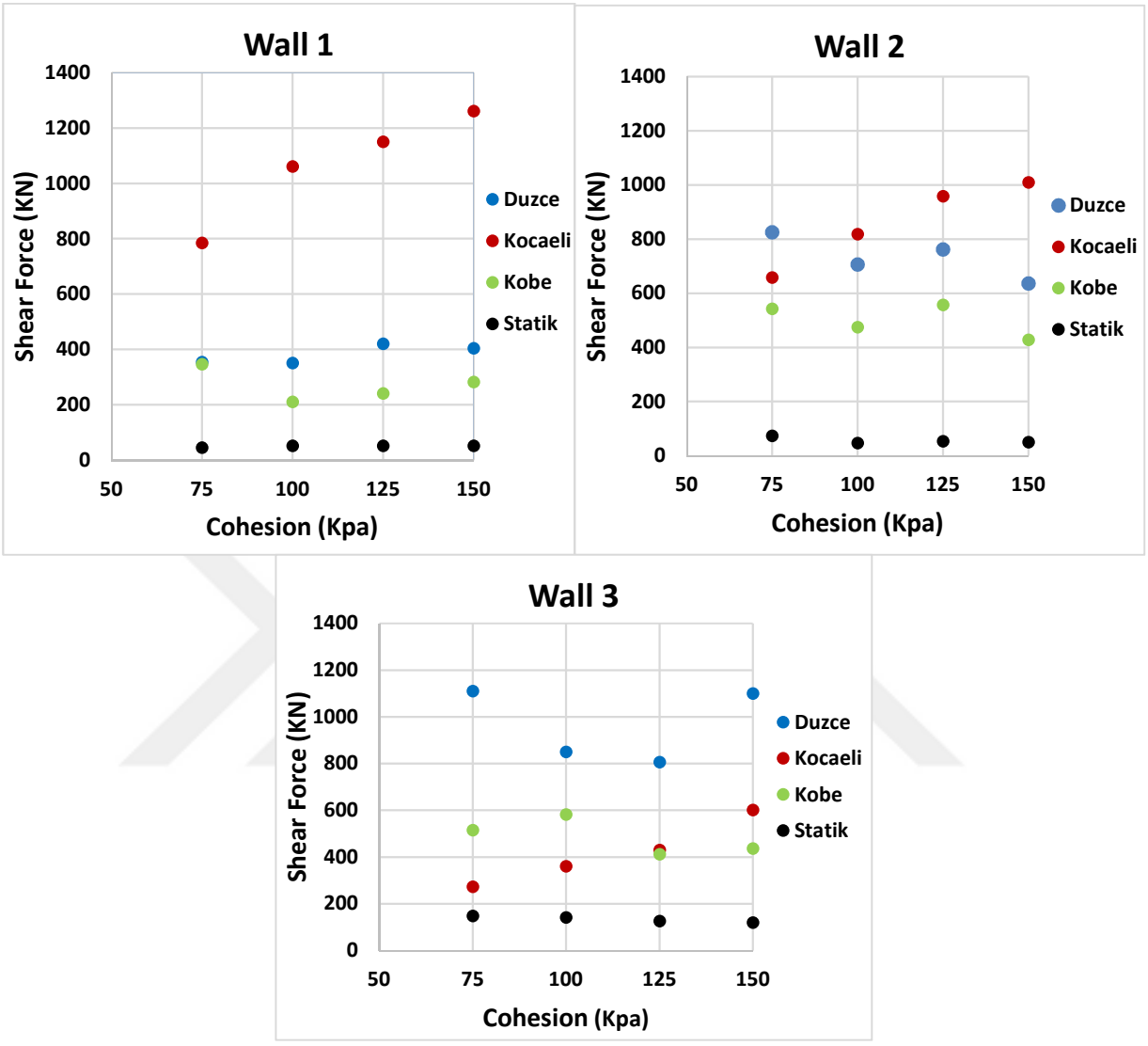


Figure 4.23. Shear force behavior with regard to the cohesion variation (**Slope 0.2**)

It can be seen from the Figure 4.23 that shear forces formed under static state are almost same in the three walls with a little increasement in the Wall 3. It was observed that only the values of shear force which composed under Kocaeli earthquake had an increasing trend when the cohesion rises in all the walls.

In all the cohesion cases, the highest shear force values had formed under Duzce Earthquake loading in the Wall 3 unlike in the Wall 1 and 2, which the highest values had composed under Kocaeli earthquake loading.

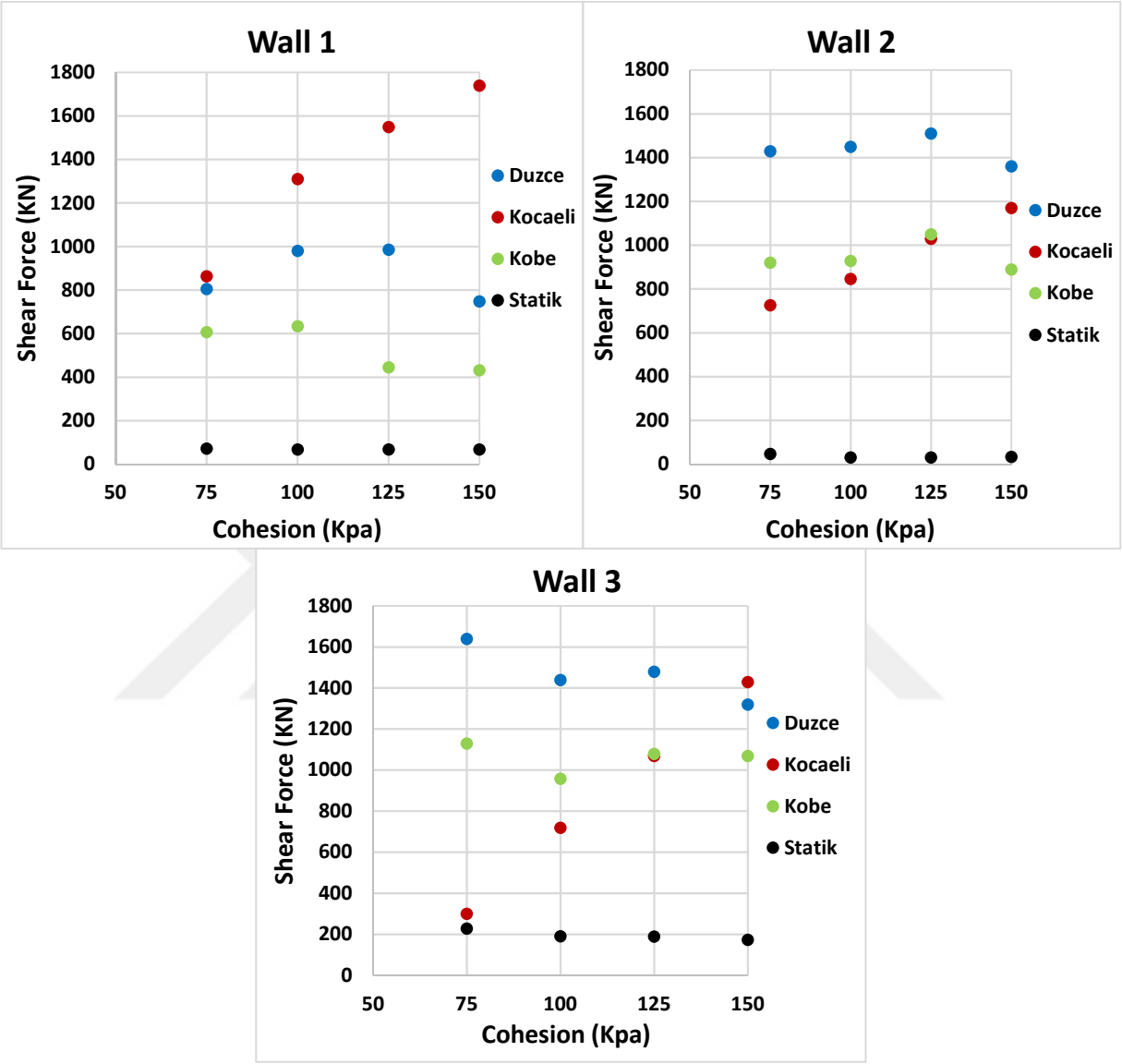


Figure 4.24. Shear force behavior with regard to the cohesion variation (**Slope 0.3**)

In case when the slope rises to 0.3, it was seen that the shear forces composed under Kobe Earthquakes, are in a gradually increasing form for all the walls at each cohesion value. An actual difference in the Wall 1 was noted between the shear forces value under Kocaeli and the other earthquakes especially at cohesion 100, 125 and 150 kPa. At cohesion 150, the values were 1740 kN by Kocaeli, 748 by Duzce and 432 by Kobe Earthquakes as presented in Figure 4.24.

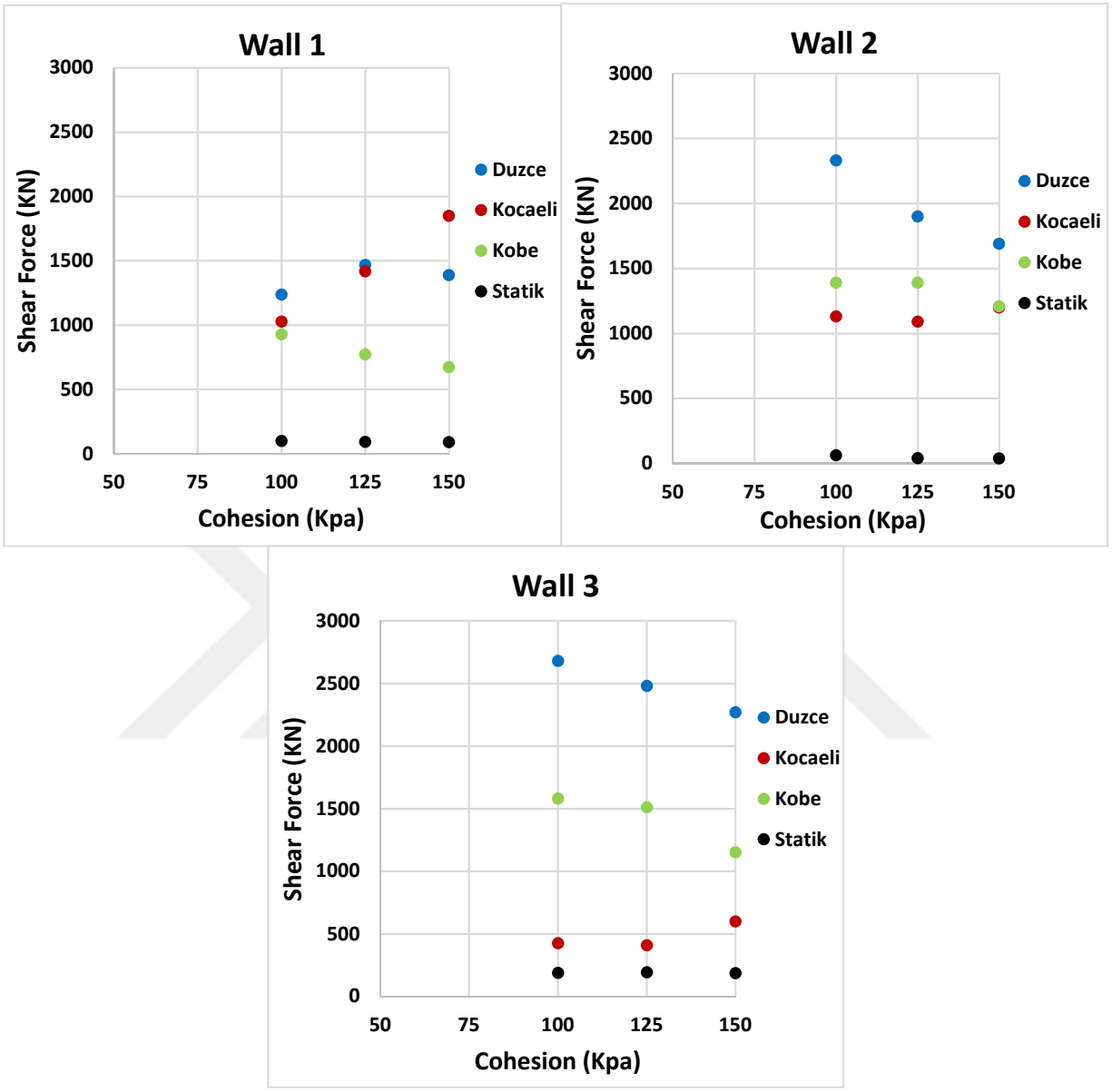


Figure 4.25. Shear force behavior with regard to the cohesion variation (**Slope 0.45**)

The maximum shear force that occurred between the slopes had happened on the slope 0.45 in the Wall 1 at cohesion 100 kPa under Duzce shaking as 2680 kPa. In additional, when the cohesion was in escalating tendency, shear forces formed by Kobe and Duzce earthquakes were in a reduction in the Wall 2 and 3.

4.2.3 Axial Force Behavior

In this part axial forces noted as a result of the analysis for the variation of cohesion at different slope ratio under static and dynamic loads as presented in Figure 4.26 to 4.29.

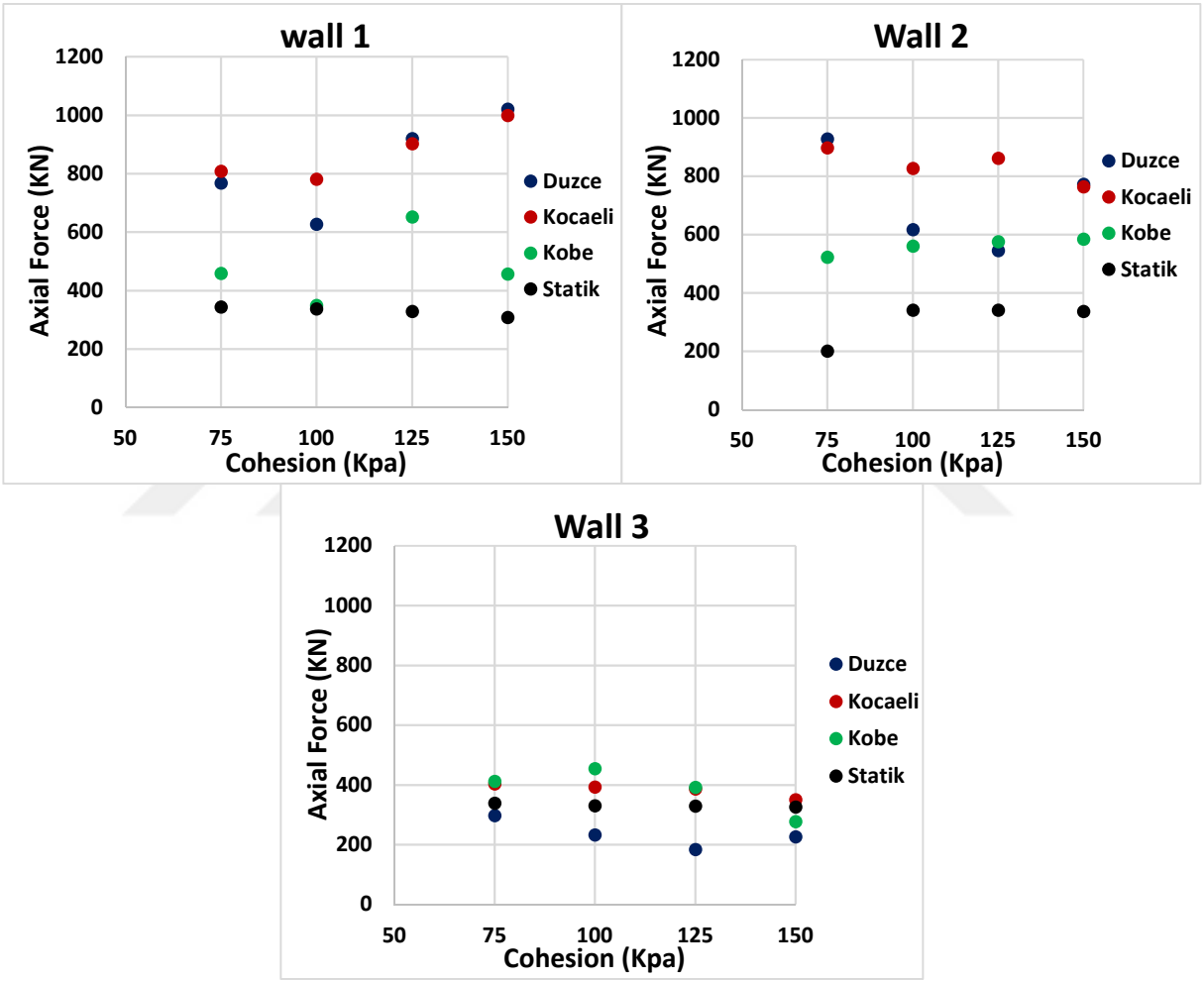


Figure 4.26. Axial force behavior with regard to the cohesion variation (**Slope 0.15**)

Wall 1 and 2 were impacted in term of axial force under dynamic cases more than the Wall 3, where the biggest axial force value had formed by Kobe Earthquake as 455 KN. Additionally, the axial force values that composed under static state in the Wall 3 were bigger than Duzce at all the cohesions at slope 0.15 as it observed in Figure 4.26.

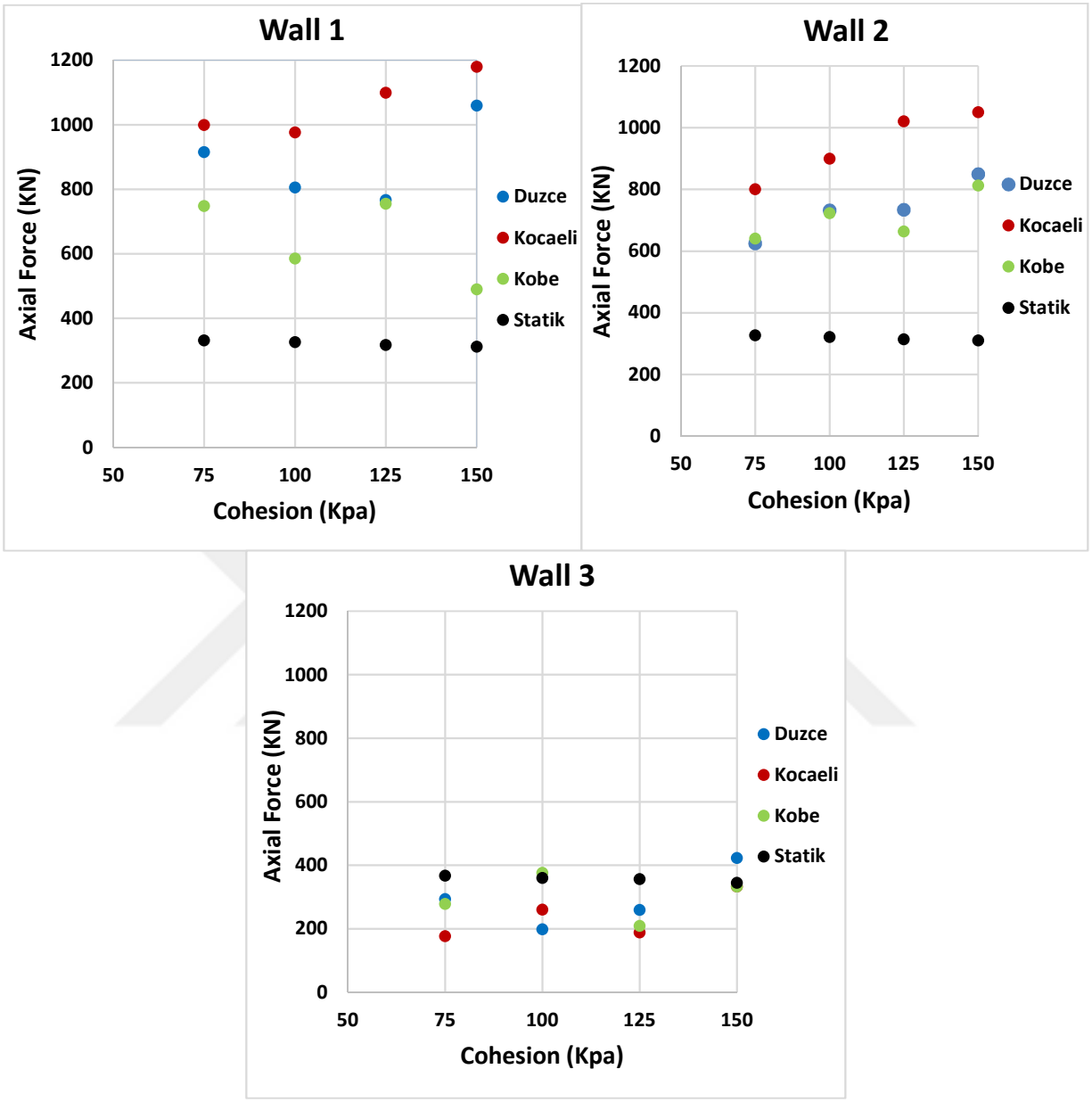


Figure 4.27. Axial force behavior with regard to the cohesion variation (**Slope 0.2**)

On slope of 0.2, it can be said that axial forces in dynamic case were lowered gradually from the Wall 1 to Wall 3 at each cohesion, to be smaller than those which are composed under static case in the Wall 3 whereas these value in static case are approximately constant in all the walls as observed in Figure 4.27.

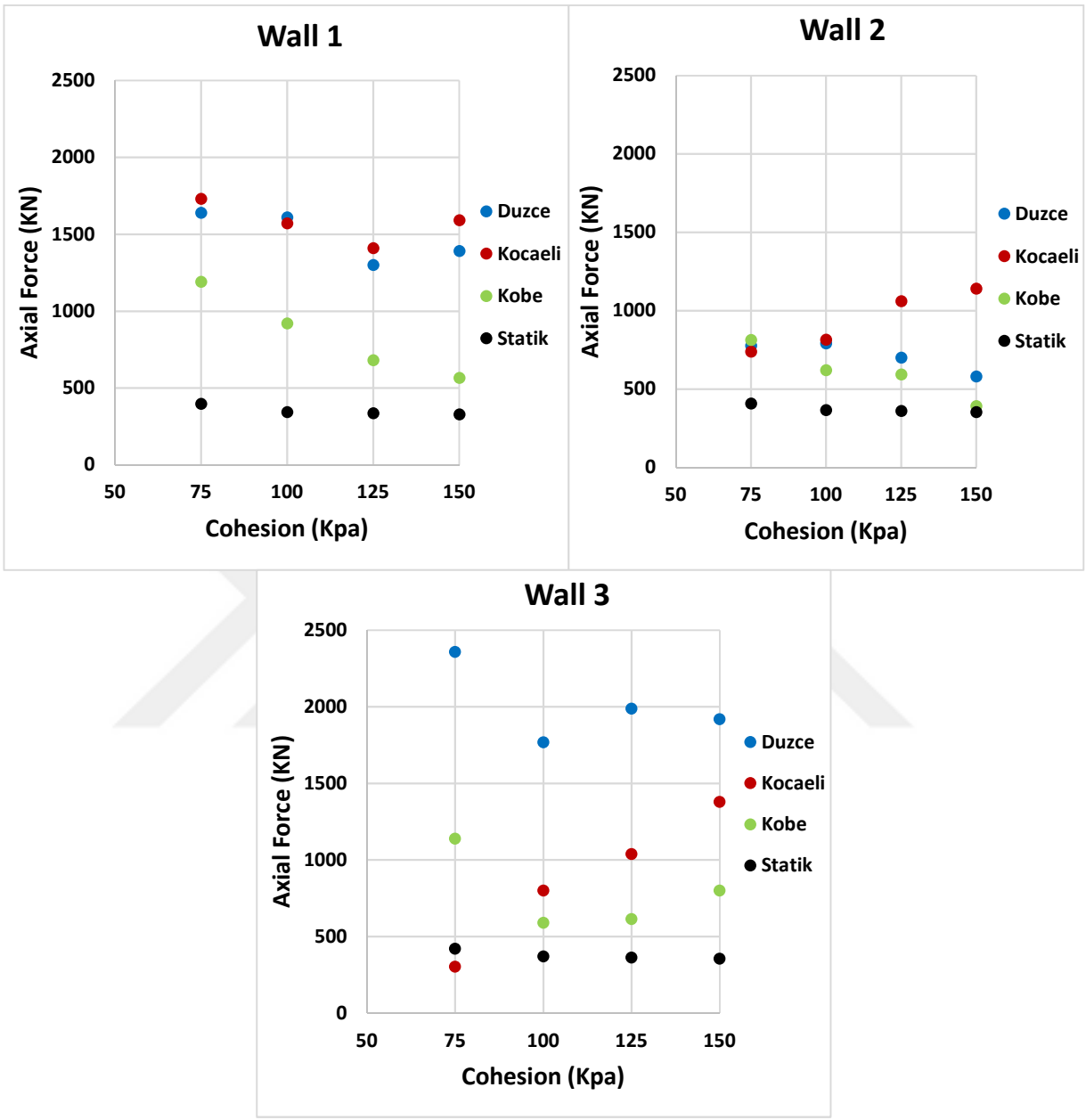


Figure 4.28. Axial force behavior with regard to the cohesion variation (**Slope 0.3**)

Figure 4.28 presents a descending trend of the axial force values in the Wall 1 under all the earthquakes loading with the increasing of cohesion. Duzce earthquake affected more in the Wall 3 in term of axial force, where there is an actual difference between the values under Duzce and the other earthquakes.

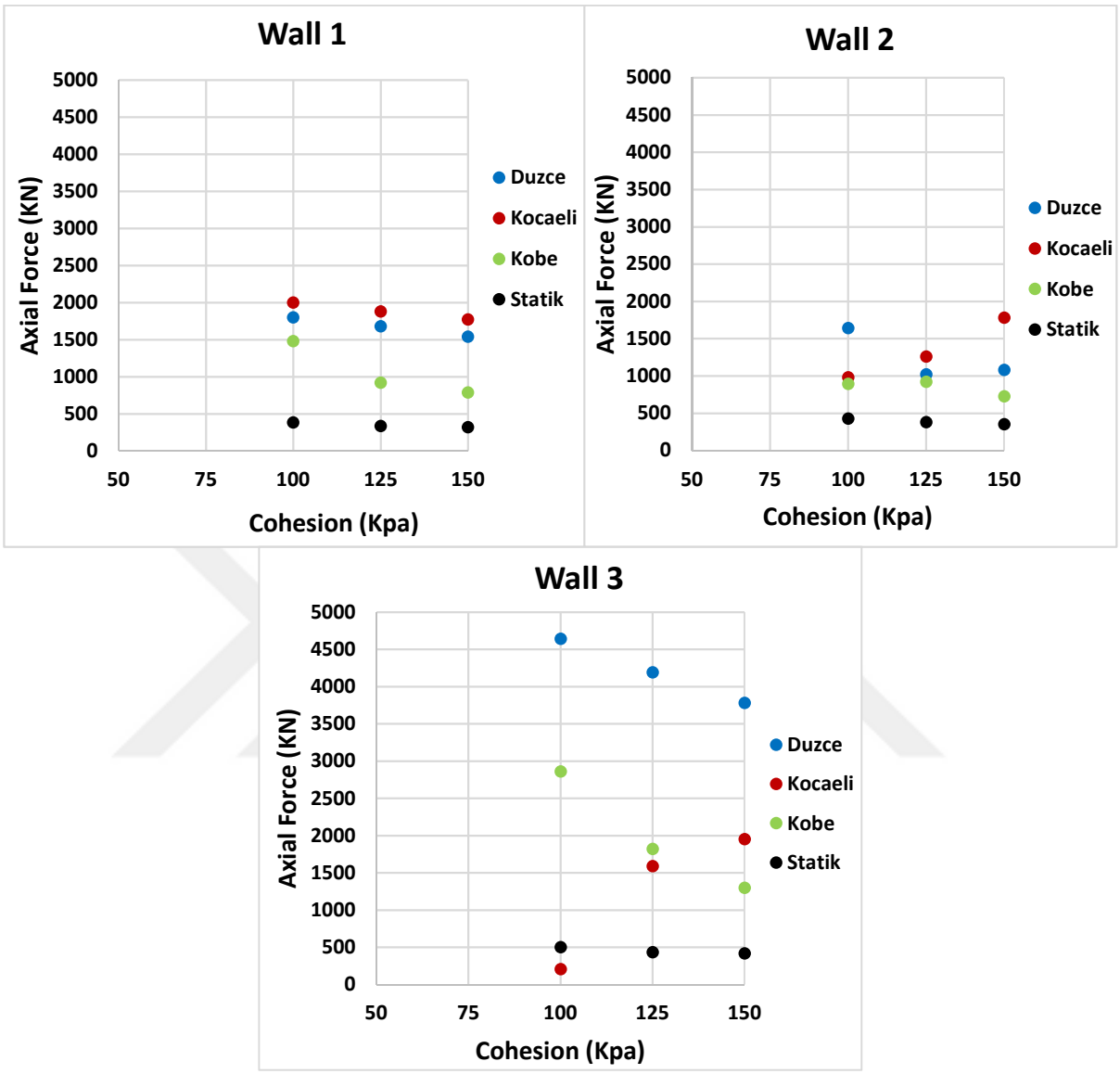


Figure 4.29. Axial force behavior with regard to the cohesion variation (**Slope 0.45**)

Maximum and minimum axial force values had recorded in slope 0.45whereas these values had occurred when the cohesion was 100 kPa by Duzce and Kocaeli Earthquake loading in the Wall 3 respectively as 4640 kN, and 208 kN.

Another point here to underline is that the axial force values was in descending trend as the cohesion increases under Duzce shaking in all the walls.

4.2.4 Total Displacement Behavior

Results of the total displacement will be discussed in this part and as mentioned before, due to the values of vertical and horizontal displacements being around zero, only total displacement behavior is considered for the displacement behavior.

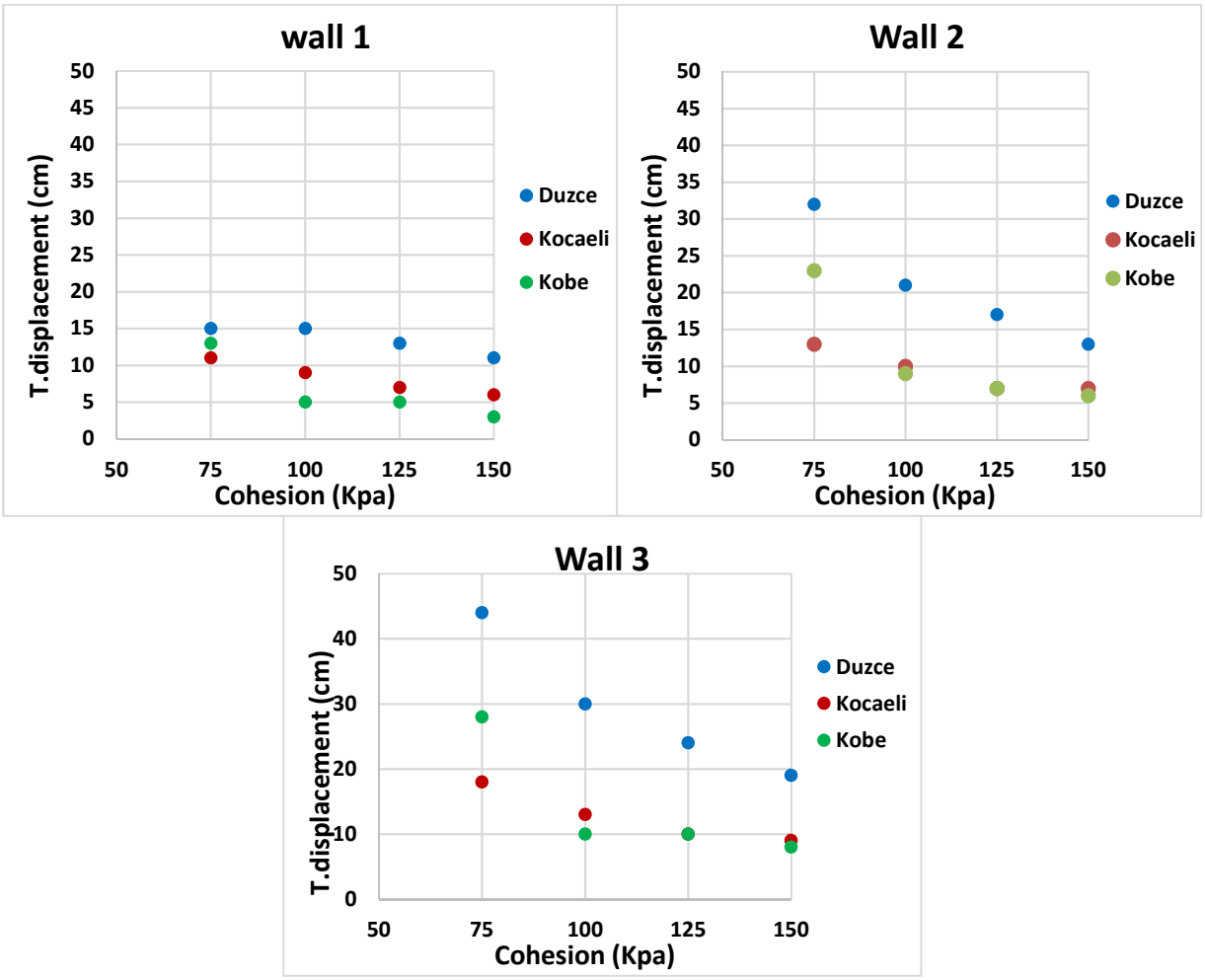


Figure 4.30. Total displacement behavior with regard to the cohesion variation (**Slope 0.15**)

In case of 0.15 slope, it observed that all the walls had impacted in term of displacement under Duzce Earthquake much more than the other earthquakes at all the cohesion cases. Besides, a real increasing tendency of the total displacement in the dynamic state as the cohesion increases in the Wall 1,2 and 3 as it is seen in Figure 4.30.

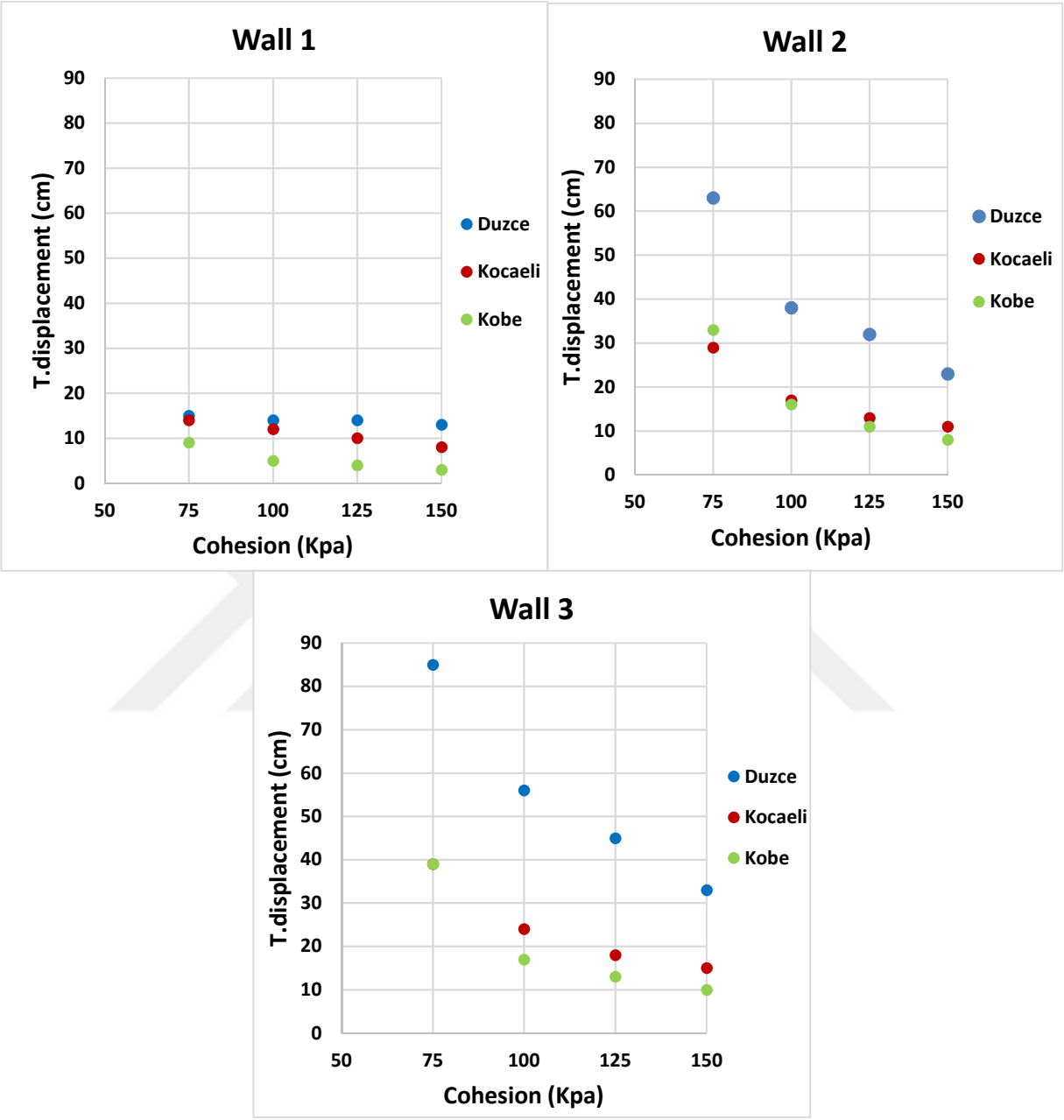


Figure 4.31. Total displacement behavior with regard to the cohesion variation (**slope 0.2**)

By raising of the slope to 0.2, the total displacement values in the Walls 2 and 3 were increased respectively to be 63 cm and 85 cm at the cohesion of 75 kPa. Additionally, it should be noticed that the values were in a decreasing tendency with the rising of cohesion as it is shown in Figure 4.31.

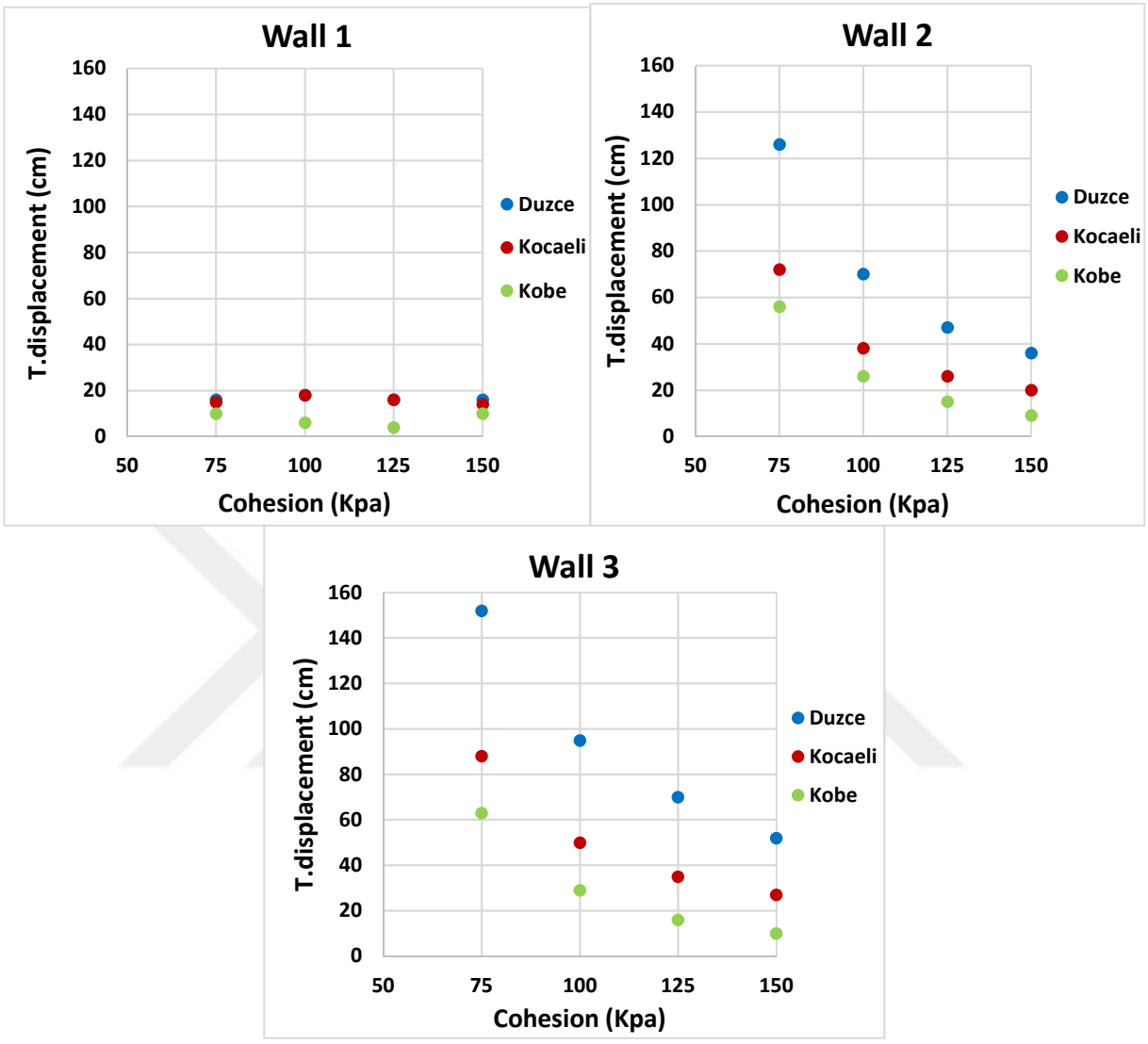


Figure 4.32. Total displacement behavior with regard to the cohesion variation (**slope 0.3**)

A real increasing of the displacement was seen on the slope of 0.3 in the Walls 1 and 2, where the highest values recorded were at the cohesion of 75 kPa by Duzce Earthquake as 126 cm in the Wall 2, and 152 cm in the Wall 3 as presented in Figure 4.32.

Wall 1 is not affected too much in terms of the total displacement compared with the Wall 2 and 3 whereas the highest value occurred was by Kocaeli earthquake as 18 cm.

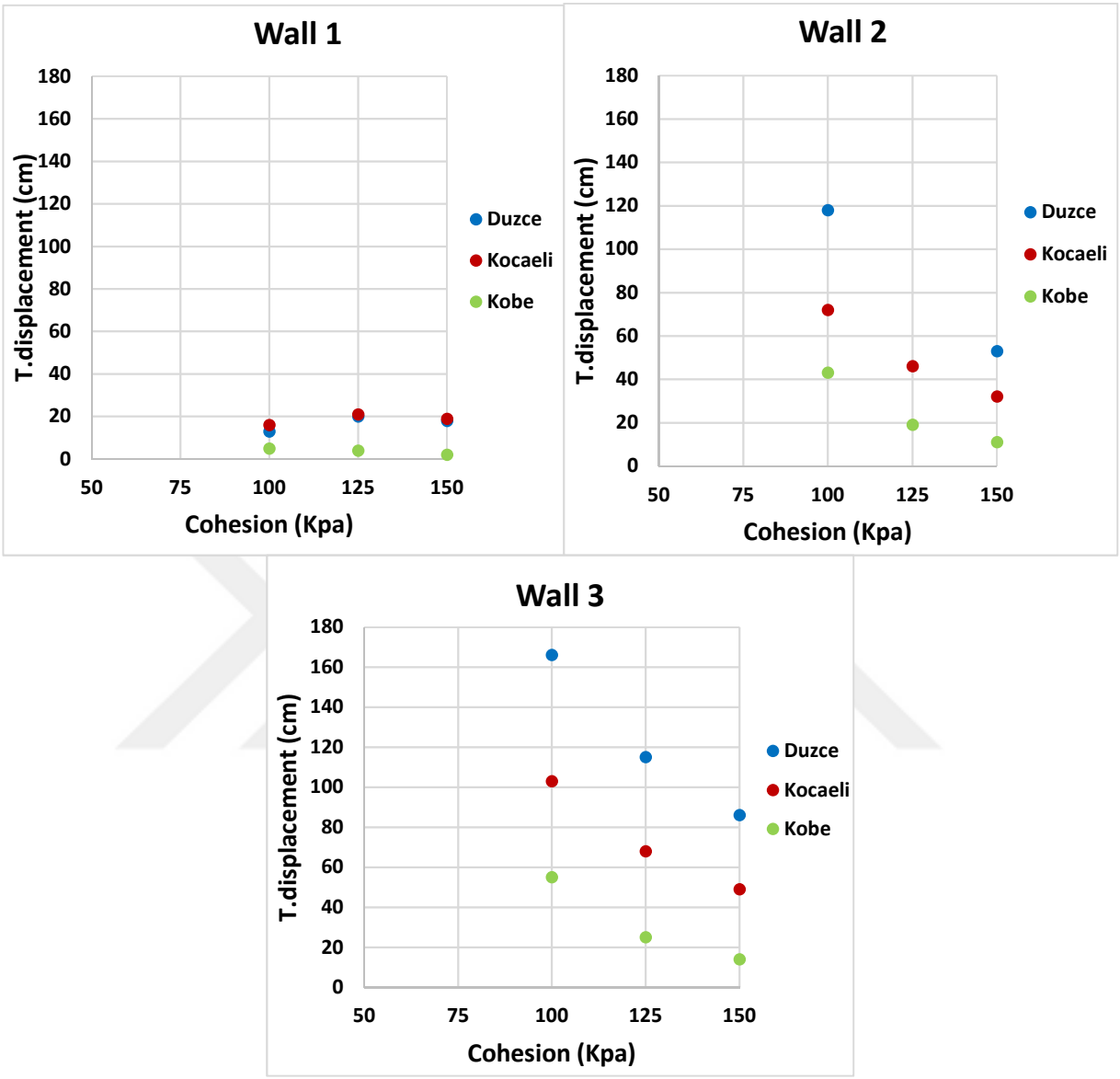


Figure 4.33. Total displacement behavior with regard to the cohesion variation (**slope 0.45**)

Figure 4.33 shows that the maximum total displacement occurred on the slope of 0.45 under Duzce Earthquake loading at the cohesion of 100 Kpa where the maximum value was in the Wall 3 as 166 cm. Also, it can be noticed that the highest values in term of total displacement had composed under Duzce Earthquake at all the cohesions.

Finally, a gradual reduction of the displacements was observed when the cohesion was increased from 100 to 150 kPa in the Wall 2 and 3.

4.3 FEM analysis of Anchored Pile Walls

Due to the big deformations which had occurred in the case of 0.45 slope and 100 kPa of cohesion, where the total displacement recorded 160 cm, it was required to support the walls with anchors to improve the structure and reduce the deformations occurred. In this section, the re-run analysis of the most critical case will be explained.

4.3.1 Deterministic Analysis of an Anchored Pile Walls

The high deformation levels were recorded for the models especially at the slope of 0.45 therefore the system was updated with 2 anchors at each wall as seen in Figure 4.34. Node to node anchor was used to model the anchor. A force of 200 kN/m was applied on the anchor element and elastic geogrid element was used to model the grout body with the normal stiffness of 10^5 kN/m.

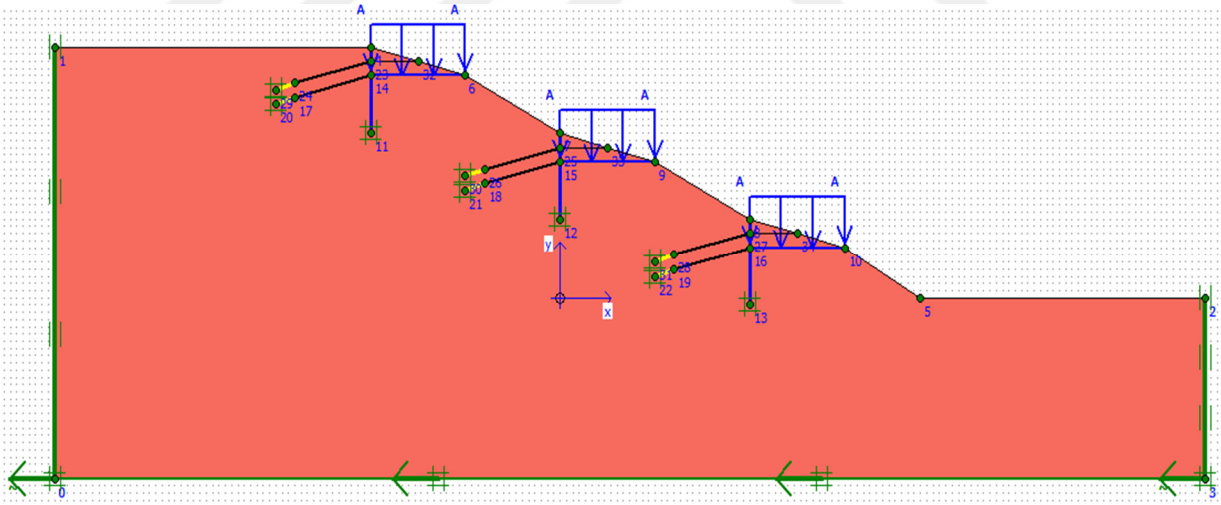


Figure 4.34. Anchored pile wall model in PLAXIS

A screenshot of the model properties for the anchor and the grouting is presented in Figure 4.35. Both of the material model was set to work as an elastic behavior.

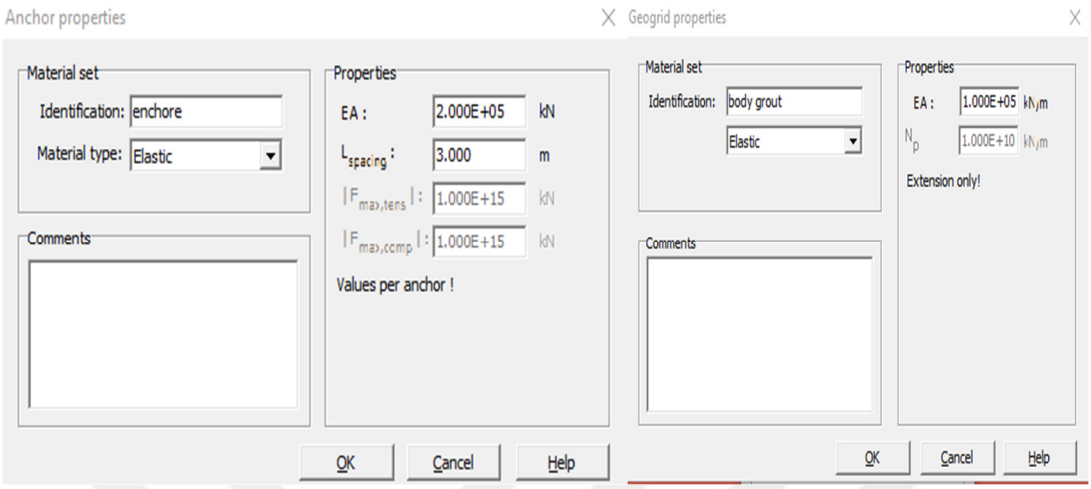


Figure 4.35. Anchor and Geogrid properties

4.3.2 Comparison Between Unanchored and Anchored Pile Walls

A comparison was done from the outcomes of moment, shear, axial forces, and displacements between unanchored and anchored pile walls that were studied to observe how the anchors could reduce the deformations and improve the ground behavior.

Unanchored pile walls **Anchored pile walls**

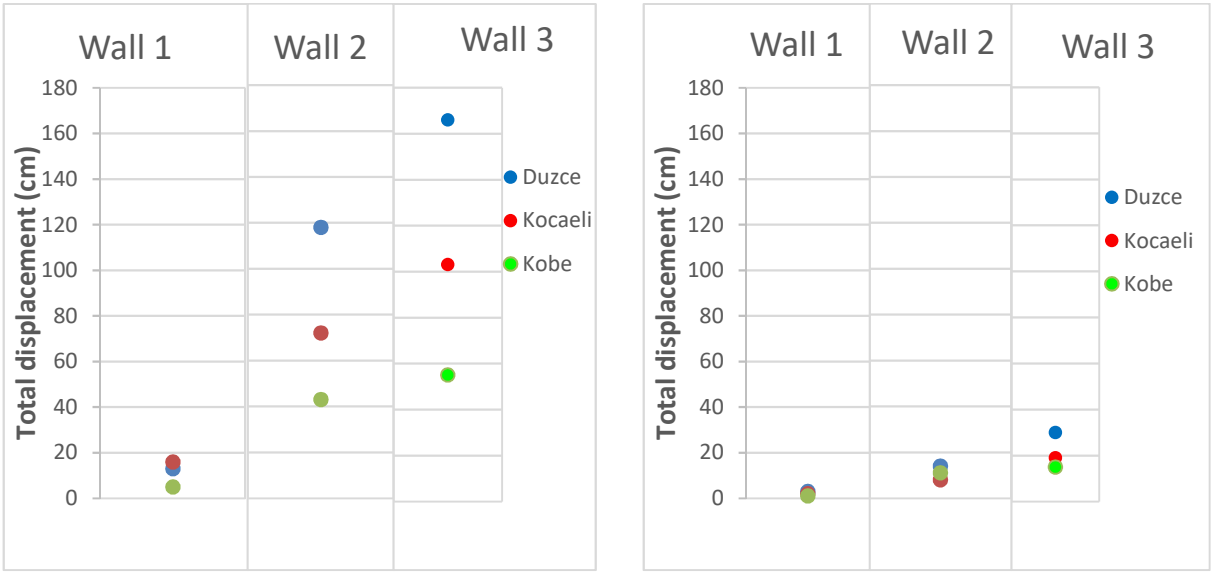


Figure 4.36. difference of total displacement between Unanchored and Anchored Piles

A big reduction of the displacement had occurred when the walls were anchored by 2 anchors as it is seen in Figure 4.36. The displacements were decreased under all the earthquakes, specifically, where the values under Duzce Earthquake decreased from 16 cm to 3 cm in the Wall 1, 118 cm to 14 cm in Wall 2, and 166 cm to 30 cm in Wall 3.

Difference of the results in terms of the moment, shear and axial forces between unanchored and anchored pile walls are presented in Figure 4.37. There is not a certain tendency in an increase or decrease in the comparison of two different models in any different parameter.

As in detail, it can be seen that the values of moments were decreased under Duzce and Kocaeli Earthquake in anchored walls of the Wall 1, while it was increased under Kobe shaking. In term of shear force, under all the earthquakes the values were approximately constant with a little increasing under Kocaeli and Kobe earthquakes when the walls were anchored. Values of axial forces were stable under Kocaeli excitation, but they were decreased under Duzce and Kobe Earthquakes.

The outcomes in the anchored Wall 2 show that there is an increasing tendency of the moment and shear forces which formed by all three earthquakes, with a little difference in the axial forces. Shear force results for the Kocaeli Earthquake are about the same although some differences were observed for the others.

Lastly, it was clearly observed that the results of moment, shear and axial forces which formed under Duzce earthquake were reduced too much comparing with the unanchored wall in the Wall 3.

Unanchored pile walls **Anchored Pile walls**

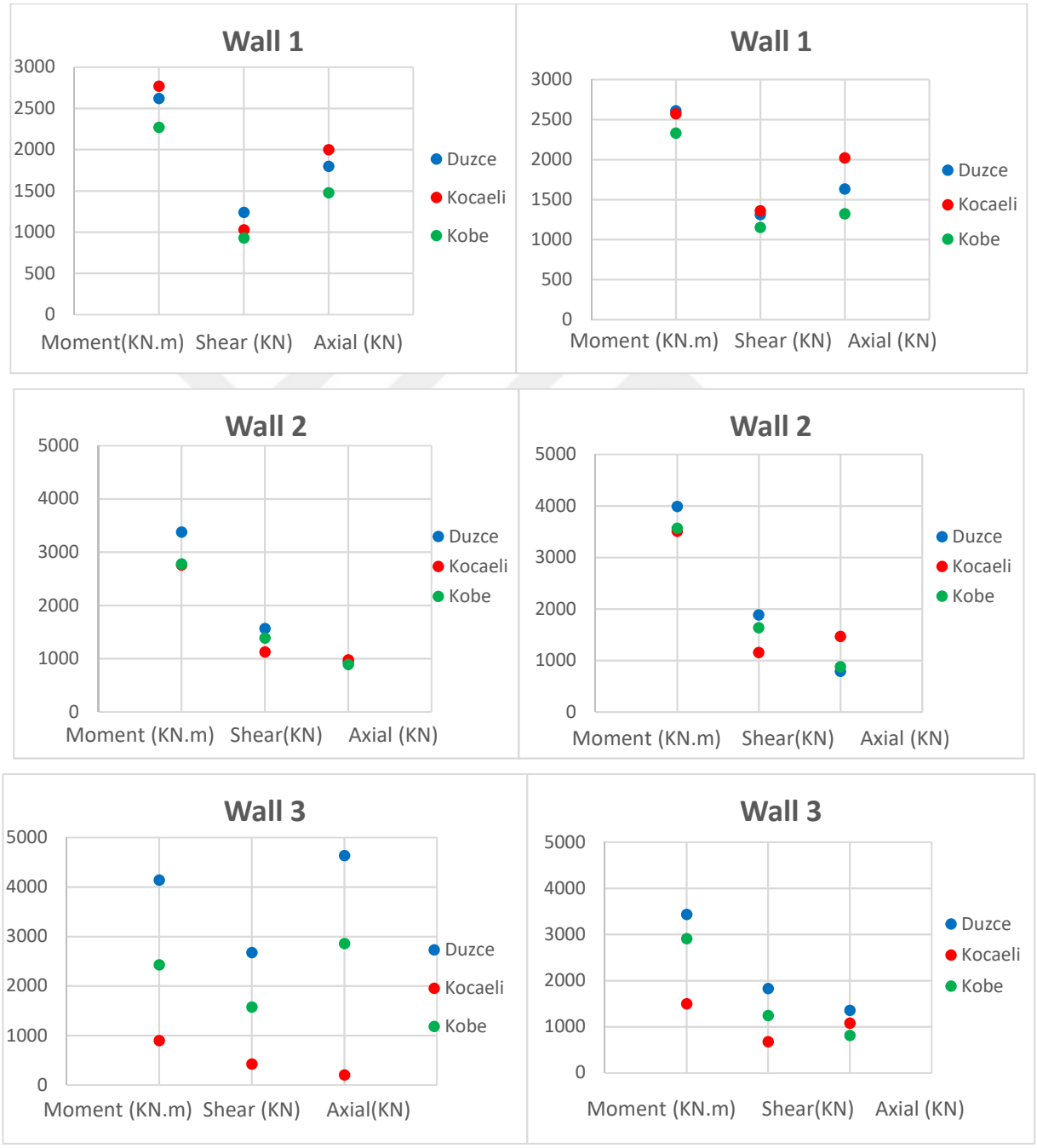


Figure 4.37. Difference of moment, shear, and axial forces between unanchored and anchored pile walls

4.4 Calculation of the Reinforcement Capacity of Pile Wall

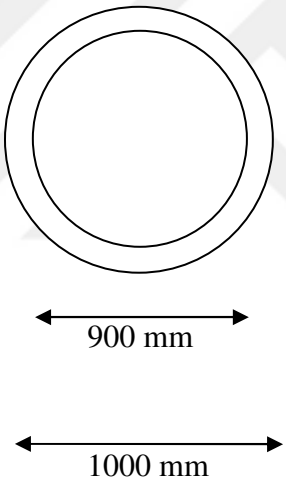
A hand calculation of the reinforcement of the wall for the most critical case was done to assess the bearing capacity of the wall and check it if the cross-section will be enough to carry the loads.

- Concrete class: C30/37 ; S420 (**TS 500**)

  F_{cd}= 30/1.5= 20 f_{yd}= 420/1.15 = 365

Concrete cover = 5 cm

- M_d= 4470 KN.m
- N_d= 3000 KN



d/h = 900/1000= 0.9

(**Turkish Building Code Number 3.3.2.1**) $0.01 \leq \rho \leq 0.04$

A_c= 3.14x1000²/4 = 785000 mm²

If ρ_{max} = 0.04 then $A_{st,max}$= 0.04x785000= 31400 mm²

If ϕ=36 then $n = \frac{31400}{3.14 \cdot 36^2/4} = 31$

Solution with Ugur Ersoy Charts:

m=f_{yd}/f_{cd} = 365/20 =18.25 Pxm =0.04x18.25= **0.73**

$e=M_d/N_d = 4470/3000 = 1.49$ $e/h = 1.49/1 =$ **1.49**

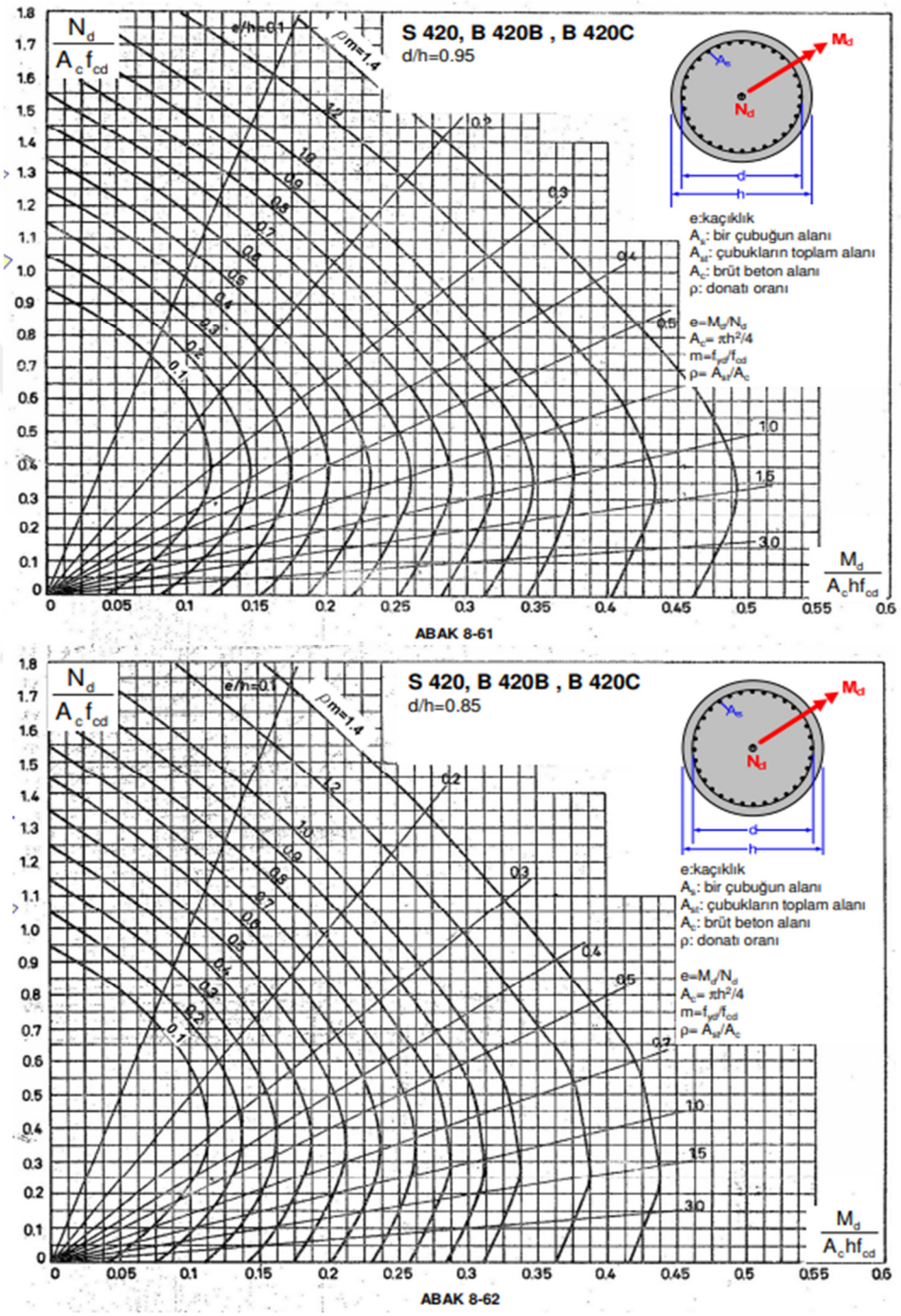


Figure 4.38. Charts from Ugur Ersoy Reinforce Concrete

d/h= 0.9 the average of $\frac{Nr}{Ac \cdot fcd} = (0.21 + 0.19) / 2 = 0.2$

and of $\frac{Mr}{Ac \cdot h \cdot fcd} =$ (0.29 + 0.28)/2 = 0.285

- ✓ Nr = 0.2x785000x20 = 3140 KN > 3000 KN

- ✓ Mr = 0.285x785000x1000x20 = 4474 KN.m ≈ 4470 KN.m

The final outcome of the rod was selected as **30 ϕ 36**. The main purpose of this calculation was to show the capacity of the cross section to see if the area was enough to put his much steel inside.

5. CONCLUSIONS AND SUGGESTIONS

Chapter 5 focuses on the results of the most critical cases (i.e. maximum values of the forces and moments) and then will target to the discussion part.

5.1 Change in Moments

In this section, the change of maximum moments which formed under the three earthquakes will be discussed according to the cohesions and the slopes variations.

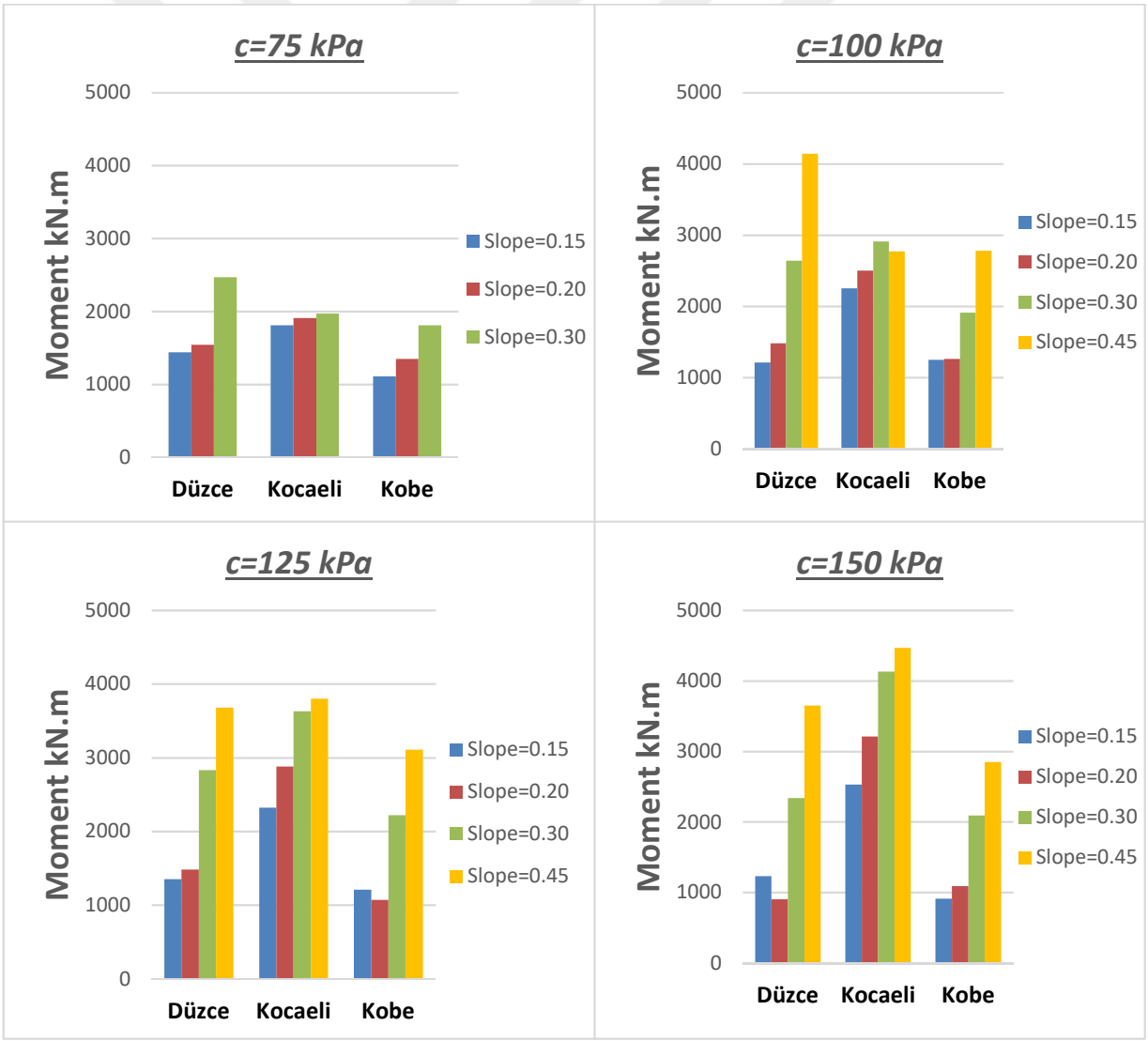


Figure 5.1. Variations of maximum moments according to the cohesion

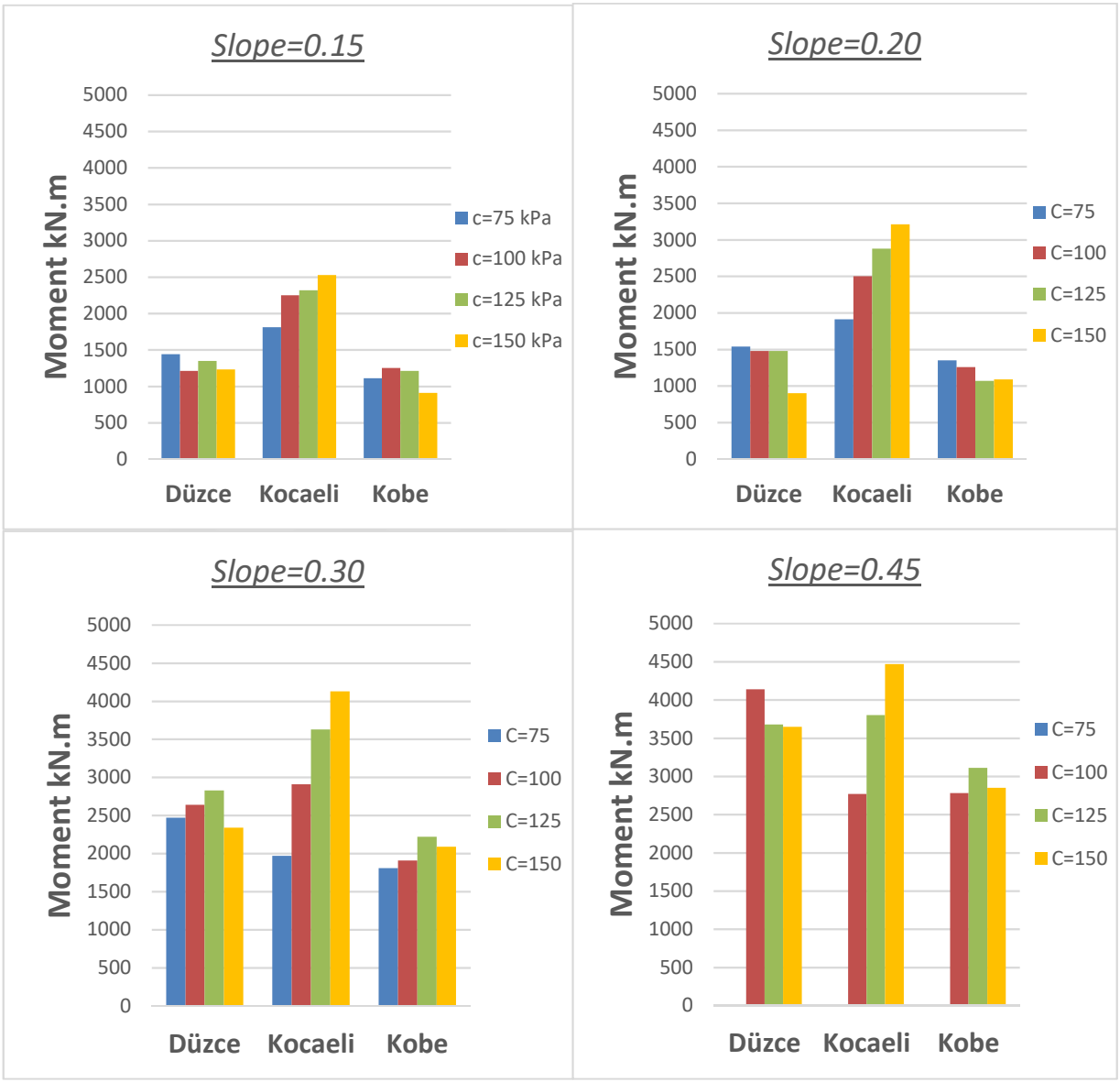


Figure 5.2. variations of maximum moments according to the slopes

It can be seen form the Figure 5.1 and Figure 5.2 that the lowest moments have occurred in the case that the cohesion was 75 kPa at slope of 0.15, and they increased respectively with the raising of the cohesions and slopes. In the case of cohesion 150 kPa, the highest of the maximum moments was composed under Kocaeli earthquake as 4470 kN.m at the slope of 0.45, and the minimum value was recorded as 911 kN.m that was formed under

Duzce Earthquake at slope of 0.15. The important point to underline here is that even with the same peak ground acceleration of three different motions have different effects on the behavior of a pile wall. Of course, the increase in slope ratio would affect the moments in a negative sense but the undrained strength alone is not the main characteristic to estimate the behavioral differences. For instance, the Kobe Earthquake produced a moment of 800 kN.m whereas it was recorded as around 2500 kN.m for Kocaeli shaking for the same soil profile as seen on the top left of the Figure 5.2. Therefore, the soil profile having an undrained shear strength of 150 kPa does not necessarily mean to bear more stresses and moments. It is an obvious outcome that the frequency content of a motion is a key parameter to estimate the dynamic behavior of a soil or structure.

5.2 Change in Shear forces

Discussion of the change in the maximum of shear forces under Duzce, Kocaeli and Kobe earthquakes were summarized similar to the previous section and presented in Figure 5.3 and Figure 5.4.

It has been observed from the Figure 5.3 that the shear forces had not much change at the slope of 0.15 even with the increase of cohesion. However, they started increasing with the risen of the slopes at other cohesion levels. There is a big difference between the values of the shear force among the slopes where under all the earthquakes loading, and in all the cohesion cases the highest values of the shear forces were recorded at the slope of 0.45 as 2640 kN. Duzce happened to be the most shear force producer compared to other two at any cohesion and slope values as seen both figures.

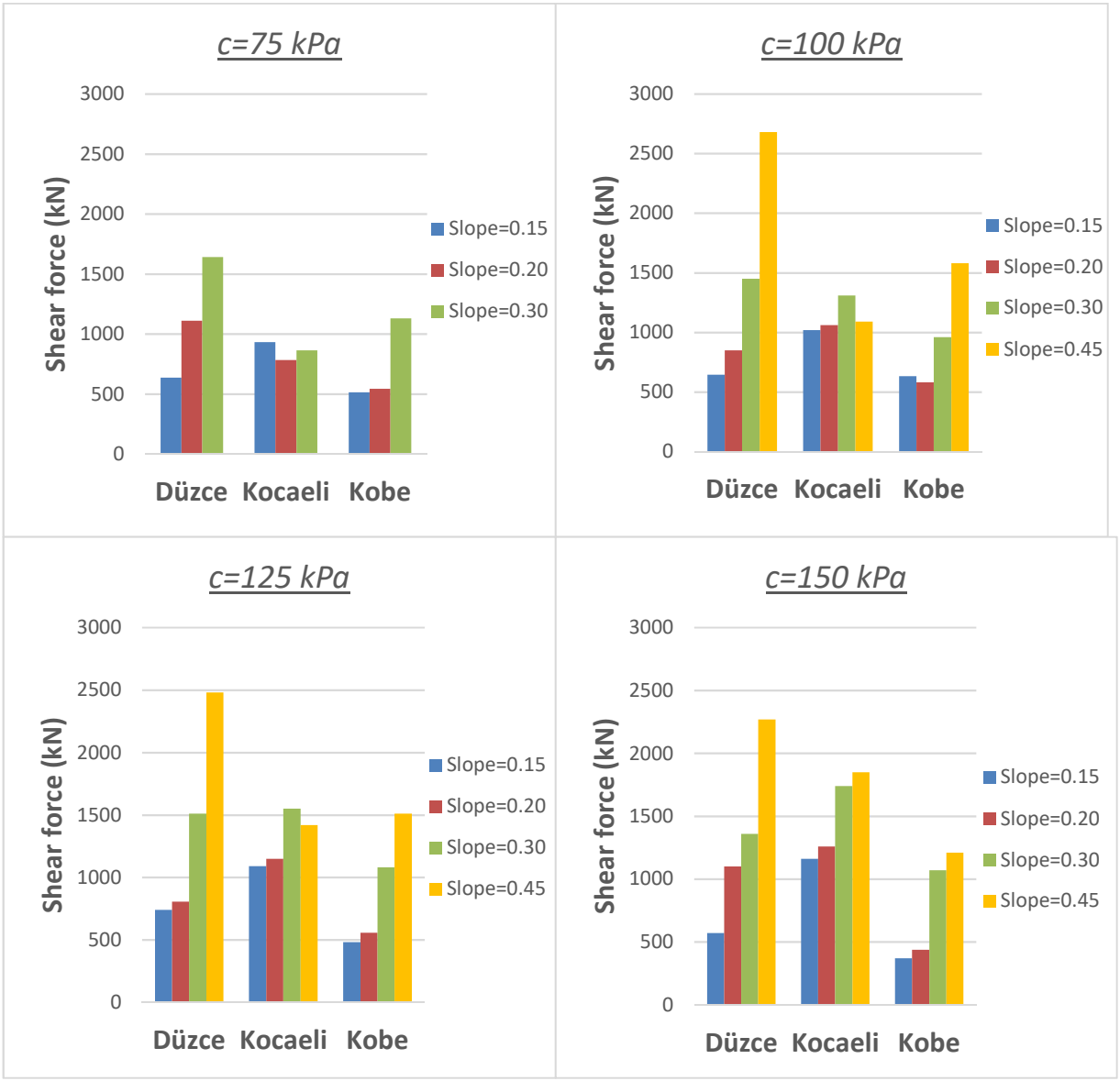


Figure 5.3. Variations of maximum shear forces according to the cohesion

The most expected situation was to get the highest shear forces at the slope of 0.45 and it is obviously what we get from the finite element analysis. The frequency content again displays an important role with the different behavior of shear forces with regarded to the change in motion as seen on the right bottom of the Figure 5.4.

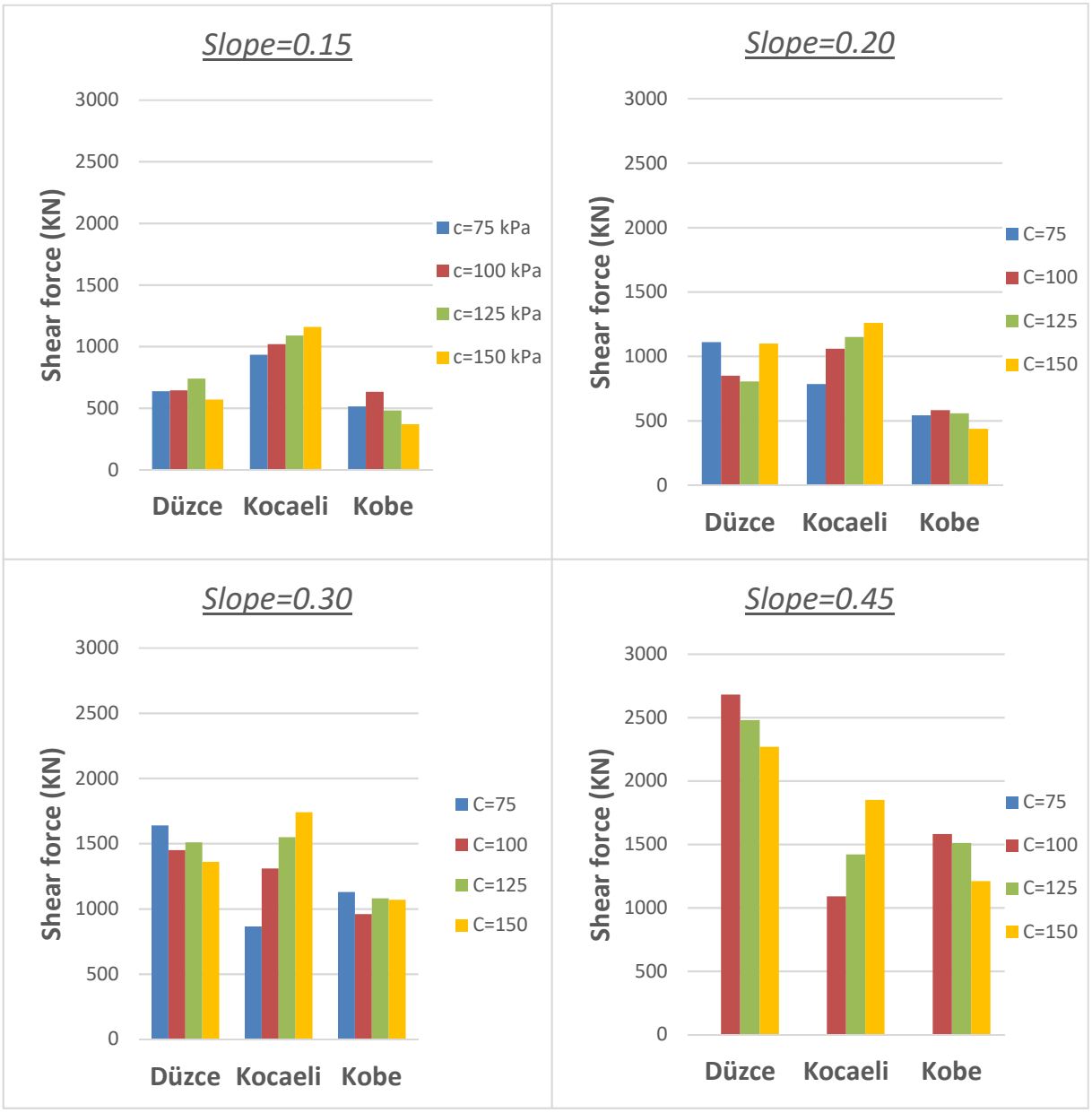


Figure 5.4. Variations of maximum shear forces according to the slopes

5.3 Change in Axial forces

The difference of maximum axial forces which formed under the three earthquakes has been discussed corresponding to the cohesions and the slopes ratios variations and they are presented in Figure 5.5 and Figure 5.6.

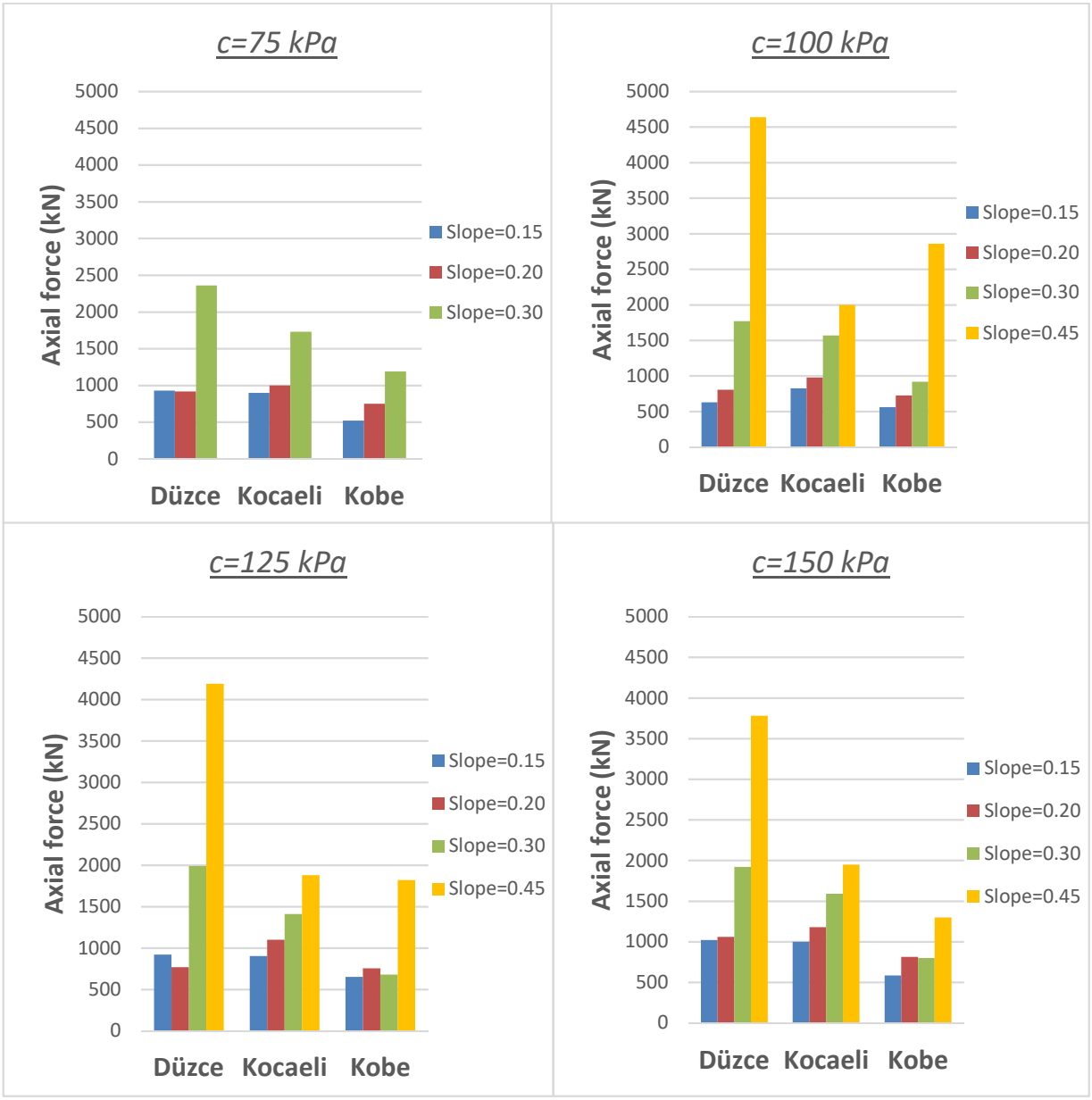


Figure 5.5. Variations of maximum axial forces according to the cohesion

Figure 5.5 shows the variations of the axial forces for different slope and undrained strength levels. The most critical values observed at the slope of 0.45 where the values achieved a great hike under all the earthquakes, and especially by Duzce excitation where the axial forces reached to 4640 kN.

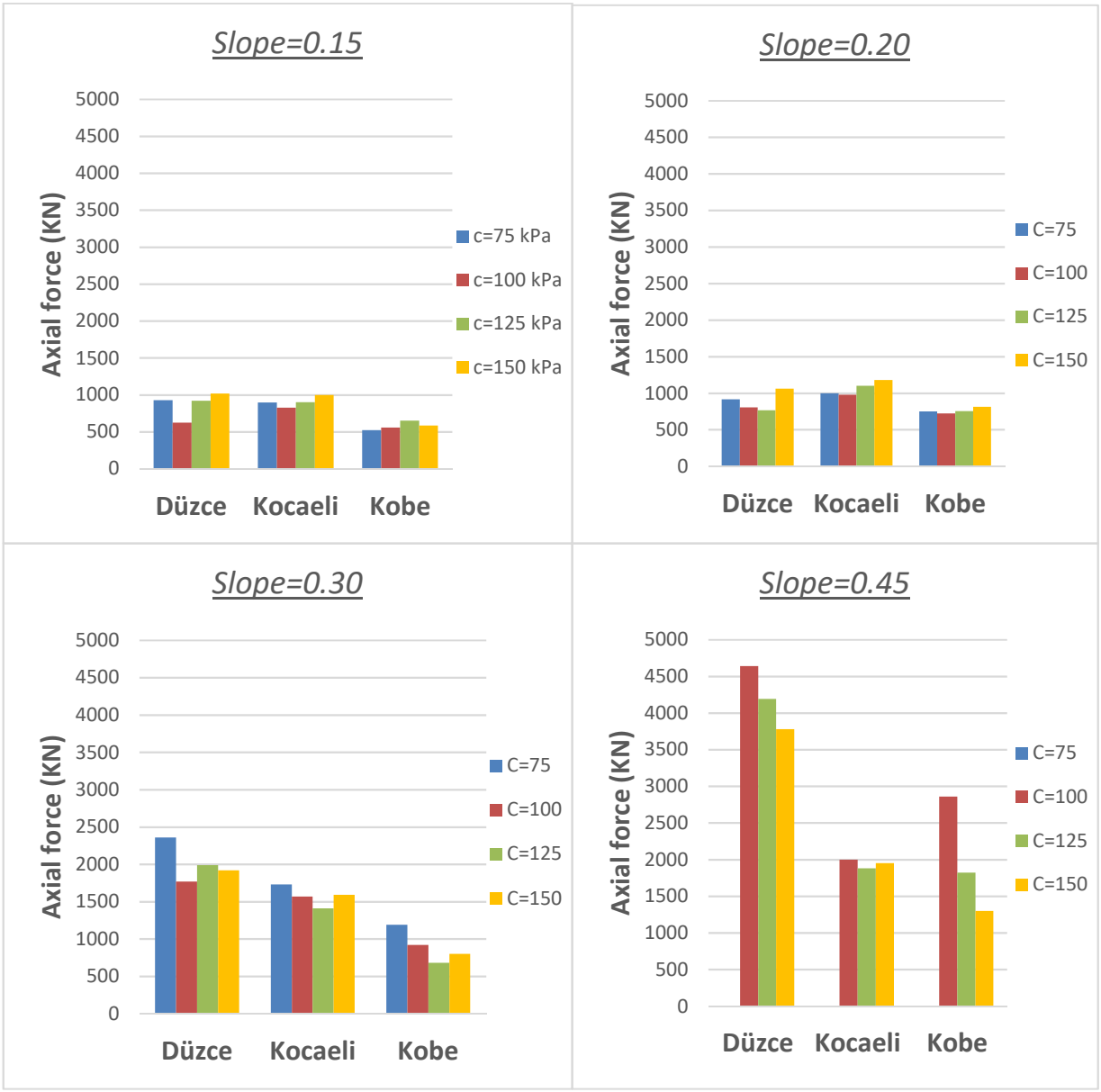


Figure 5.6. variations of maximum axial forces according the Slopes

Regarding the slope variation, the axial forces were almost constant with a little variation at slopes 0.15 and 0.2. For the other two slope ratios, as the cohesion increases the axial forces seem to decrease for all three motions, Duzce being the highest one whereas the other two change their positions for the slope of 0.3 and 0.45.

5.4 Discussion on the Effect of the Peak Ground Acceleration

As mentioned before, site specific peak ground acceleration was determined as 0.46 from the new Turkish Building Code (2019). Just to sake of the evaluating the difference of the maximum acceleration, Duzce Earthquake data was selected since the most critical values were observed with this shaking and it was scaled to the 0.3g. A comparison were done in the case of when the cohesion was 100 and at the slope of 0.45 in terms of moment, shear, axial forces, and displacements under different accelerations 0.3g and 0.46g, correspondingly that have the same frequency content.

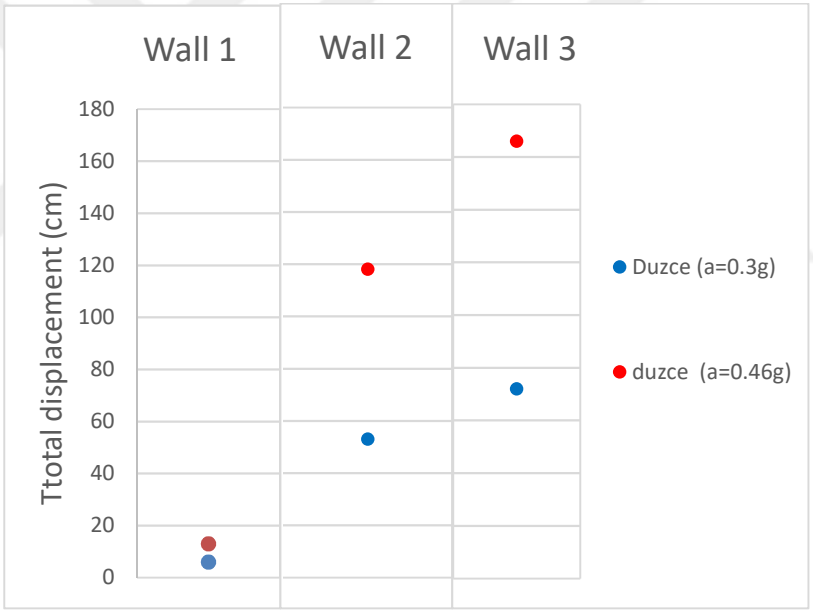


Figure 5.7. Comparison of total displacement under Duzce (PGA=0.3g) and (PGA=0.46g)

Figure 5.7 shows the total displacement behavior for two different scaled motions and the results were not unexpected. Although the Wall 1 has similar deformation levels for both cases, the difference becomes obvious for the Wall 2 and Wall 3 being more than double in terms of total displacement. The comparison of the forces and moments are presented in Figure 5.8.

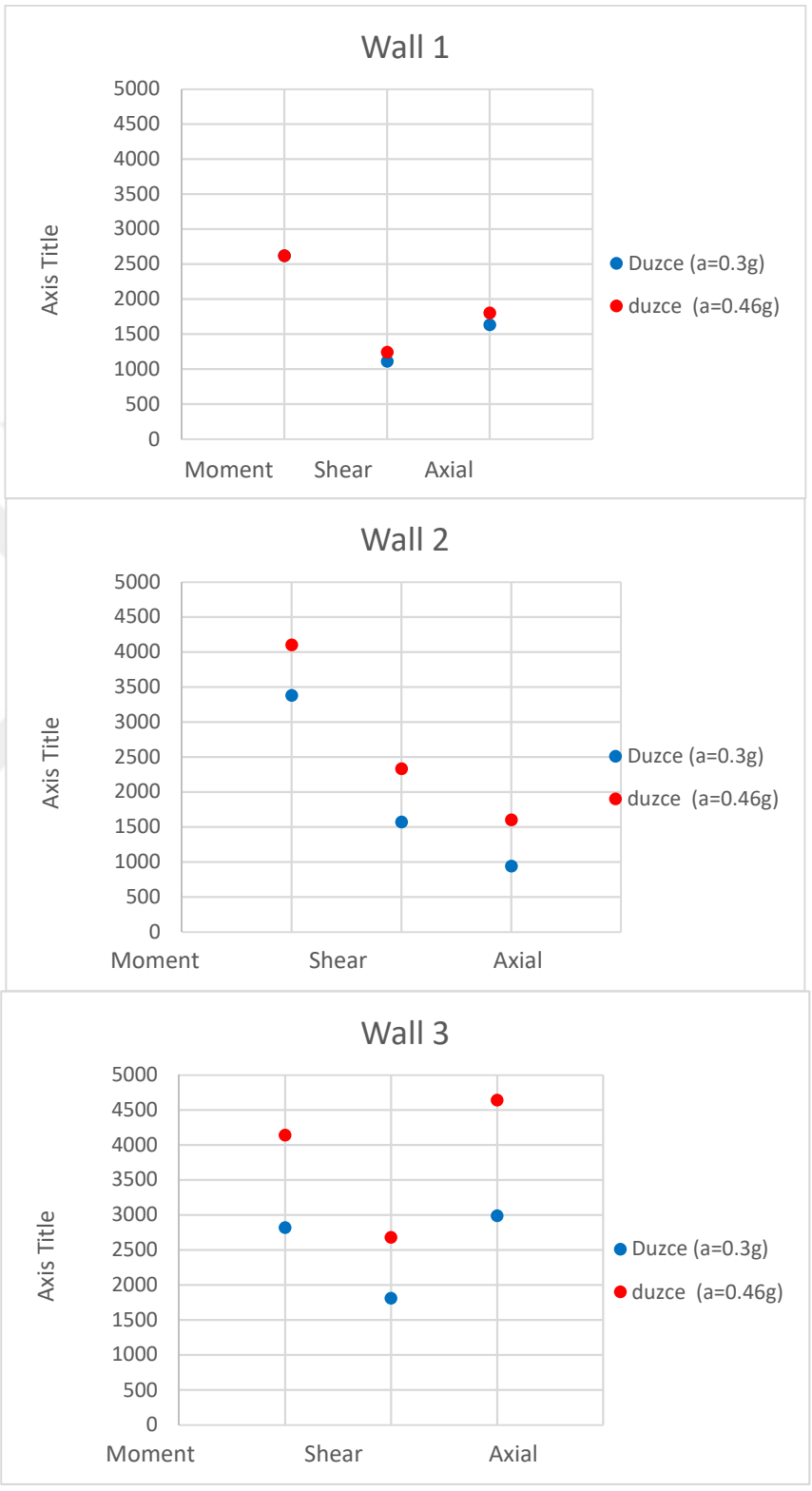


Figure 5.8. Comparison of moment, shear, axial forces under Duzce (PGA=0.3g) and (PGA=0.46g)

The outcome difference is clear that when the acceleration of Duzce earthquake was 0.46g, the total displacements and all the forces in the Wall 1, 2 and 3 were bigger than when it was 0.3g, with a slight difference of the increase rate in Wall 1 where the values of all the results are approximately similar but the case starts to raise in the Wall 2 and Wall 3.

In summary, the seismic behavior of the pile walls that hold a slope soil is one of the most important aspect of the geotechnical applications. The soil behavior under cyclic loading obviously varies with the change in characteristics of the excitation such as duration and frequency content. Another important point is that the undrained strength of soil which was modeled as in variation of cohesion does not give concrete expectations such as the cohesion increases the total displacement would decrease, etc. The soil-structure behavior and the stress transmission and distribution that the Mohr Coulomb Model play an important role to estimate the behavior of the pile walls in terms of moment, shear force, axial force, and total displacement. It is clear that analysis are time consuming but the behavior change is crucial with the variety of the based motions therefore it should not be underestimated.

REFERENCES

Chowdhury 2010 , Robin Geotechnical Slope Analysis, Faculty of Engineering, University of Wollongong, Wollongong, Australia page 21-27

Duncan, J.M. and Wright, S.G. (2005) Soil Strength and Slope Stabilty. John Wiley & Sons, Inc., pp. 199

Broms, B.B. and Wong, K.S. (1991) Landslides in Fang, H., ed., Foundation Engineering Handbook: New York, Van Nostrand Reinhold, pp. 410-446.

Hrennikoff, A. (1941). "Solution of problems of elasticity by the framework method". Journal of applied mechanics 8.4: 169–175.

Chowdhury 2010 , Robin Geotechnical Slope Analysis, Faculty of Engineering, University of Wollongong, Wollongong, Australia page 240-255

Assist., M. D. (n.d.). An Overview on Methods for Slope Stability Analysis . International Journal of Engineering Research & Technology (IJERT.

Broere, R. B. (January 2004). PLAXIS 2D - Version 8. Delft University of Technology & PLAXIS b.v., The Netherlands : D. Waterman.

H. Khabbaz1, B. F. (n.d.). Finite Element Methods against Limit Equilibrium Approaches for Slope Stability Analysis.

Indra Noer Hamdhan1. (n.d.). Slope Stability Analysis with the Finite Element Method. Lecturer, Department of Civil Engineering, National Institute of Technology, Bandung, Indonesia.

J.krahn, D. F. (n.d.). Comparison of slope stability methods of analysis. Canadian Geotechnical Journal, 1977, Vol.14, No.3 :pp.429-439

Lu-wang, L. j.-l. (2013). stability analysis of some new types of retaining wall with FEM. information technology journal.

REFERENCES (continued)

Burman, S. P. Acharya. (February 2015) Comparative study of slope stability analysis using traditional limit equilibrium method and finite element method. Kharagpur, India: Road, Housing & Urban Development Research Center.

Matthewsa, C., Farooka, Z., & Helmb:, P. SLOPE STABILITY ANALYSIS – LIMIT EQUILIBRIUM OR THE FINITE ELEMENT METHOD? (Technical Paper - Ground Engineering - May 2014. pp 22-28).

Nielsen, H. B. (1992). Basics of Retaining Wall Book, A Design Guide for Earth Retaining Structures 10 Edition . Page 49-58

Sikder, A. J. (March 2004). Design basis and economic aspects of different types of retaining walls . Journal of Civil Engineering (IEB), 32 (1) (2004) 17-34.

(Grift ths, D. V. & Lane, P. A. (1999).Slope stability analysis by Fnite elements. Volume 49 Issue 3, June 1999, pp. 387-403

Bishop, A.W., (1955), "The Use of the Slip Circle in the Stability Analysis of Slopes", geotechnical, Vol. 5, pp 7 - 17.

Fellenius, W., (1936), "Calculation of the Stability of Earth Dams", Trans. 2nd Cong. on Large Dams, Vol 4, p 445.

Janbu, N., (1973), "Slope Stability Computations", Embankment Dam Engineering, Ed. by Hirshfeld and Poulos, John Wiley & Sons, New York. p. 47-86

Matthews, C., Farook, Z. & Helm, P.R. (2014). Slope stability analysis – limit equilibrium or the finite element method? Technical Paper. Ground Engineering. May. pp. 22-28

J. Khan and M. Sikder Design basis and economic aspects of different types of retainingwalls/

Journal of Civil Engineering (IEB), 32 (1) (2004) 17-34

Elias, V; Christopher, B.R.; Berg, R.R. 2001. Mechanically Stabilized Earth Walls and Reinforced Soil Slopes Design and Construction Guidelines. U.S. Department of Transportation Federal Highway Administration (FHWA). Washington, DC. 394 p.

REFERENCES (continued)

RBJ Brinkgreve, WM Swolfs, E Engin, D Waterman, A Chesaru, PG Bonnier, V Galavi Journal User manual, Plaxis bv, 2010

Radu Crahmaliuc March 10th, 2020 , 75 Years of the Finite Element Method Book

Duncan, J.M. (1996). State of the Art: Limit Equilibrium and Finite-Element Analysis of Slopes. Journal of Geotechnical Engineering, 122(7):577-596.

Terzaghi - 1996 Soil Mechanics in Engineering Practice, 3rd Edition -, Ralph B. Peck, Gholamreza Mesri

D. G. Fredlund H. Rahardjo M. D. Fredlund Unsaturated Soil Mechanics in Engineering Practice Journal of Geotechnical and Geoenvironmental Engineering, March 01, 2006

Rowshon Jadid, 2016 Pullout Resistance of Concrete Anchor Block Embedded in Cohesionless Soil Geomechanics and Engineering, Vol. 12, No. 4 (2017) 675-688

Clayton, C.R.I., 2014. "Earth Pressures and Earth Retaining Structures Book", Third Edition, CRC Press, London, and New York.

Alex Jacob1, A. A. (2018). Slope stability analysis using numerical modelling. International Research Journal of Engineering and Technology (IRJET). Volume: 05 Issue: 04

Ali Fawaz, Elias Farah, Fadi Hagechehade. Slope Stability Analysis Using Numerical Modelling. American Journal of Civil Engineering. Vol. 2, No. 3, 2014, pp. 60-67.

Azzam, W.R (2014). Finite element analysis of skirted foundation adjacent to sand slope under earthquake loading. HBRC Journal. Volume 11, Issue 2, Pages 231-239

F. Tschuchnigg, H. S. (2015). Slope stability analysis by means of finite element limit analysis and finite element strength reduction techniques. a Computational Geotechnics Group, Institute for Soil Mechanics and Foundation Engineering, Graz University of Technology, Austria

REFERENCES

Fei SONG, R.-Y. C.-Q. (2017). Stability Analysis of Reinforced Slope Based on Limit Equilibrium Method. ISSN 1330-3651 (Print), ISSN 1848-6339

Gupta, S. R. (2016). Analysis of a Nailed Soil Slope Using Limit Equilibrium and Finite Element Methods. Springer International Publishing Switzerland 2016

I Hermanto, U C Sari , M N Sholeh, . (2020). The stability analysis study of conventional retaining walls variation design in vertical slope. Journal of Physics: Conference Series. The 8th Engineering International Conference 2019.

Ugur Ersoy Turkish Building Code Reinforced Concrete , Ankara, 1980 Middle East Technical University